ESD-TR-67-602

SECOND QUARTERLY TECHNICAL REPORT - LASA EXPERIMENTAL SIGNAL PROCESSING SYSTEM

MAY 1967

DIRECTORATE OF PLANNING AND TECHNOLOGY
ELECTRONIC SYSTEMS DIVISION
AIR FORCE SYSTEMS COMMAND
UNITED STATES AIR FORCE
L. G. Hanscom Field, Bedford, Massachusetts

Sponsored by: Advanced Research Projects Agency
Washington, D. C.

ARPA Order No. 800

(Prepared under Contract No. F19628-67-C-0198 by International Business Machines Corp., 18100 Frederick Pike, Gaithersburg, Maryland 20760)

OTHER NOTICES

Do not return this copy. Retain or destroy.

SECOND QUARTERLY TECHNICAL REPORT - LASA EXPERIMENTAL SIGNAL PROCESSING SYSTEM

MAY 1967

DIRECTORATE OF PLANNING AND TECHNOLOGY
ELECTRONIC SYSTEMS DIVISION
AIR FORCE SYSTEMS COMMAND
UNITED STATES AIR FORCE
L. G. Hanscom Field, Bedford, Massachusetts

Sponsored by: Advanced Research Projects Agency
Washington, D. C.

ARPA Order No. 800

(Prepared under Contract No. F19628-67-C-0198 by International Business Machines Corp., 18100 Frederick Pike, Gaithersburg, Maryland 20760)

FOREWORD

This research is supported by the Advanced Research Projects Agency. The Electronics Systems Division technical project officer for Contract No. F19628-67-C-0198 is Major Cleve P. Malone, USAF (ESLE). This report covers the period from 1 February 1967 through 30 April 1967.

This technical report has been reviewed and is approved.

Paul W. Ridenour, Lt. Col., USAF
Chief, Development Engineering Division
Directorate of Planning and Technology

ABSTRACT

This Second Quarterly Technical Report for the LASA Experimental Signal Processing System discusses the effort expended during the second quarter to provide the hardware and software to support research and development directed toward the study of seismic signal processing; and it delineates work tasks planned for the next quarter. This document also presents detailed information related to configurations, array monitor and control, data compression, scaling, display, and array design.

CONTENTS

ILLUSTRATIONS

TABLES

Section 1

INTRODUCTION

The work reported herein was performed under the "LASA Experimental Signal Processing System," Contract Number F19628-67-C-0198, and is a continuation of the "Large Aperture Seismic Array Signal Processing Study,"[1] Contract Number SD-296, and the "Large Aperture Seismic Array Signal Processing Communications and Simulation Study,"[2,3,4] Contract Number AF19(628)-5948.

The purpose of this contract is to design, develop and implement the LASA Experimental Signal Processing System (ESPS), including the hardware and software, to provide an experimental capability to

a. Evaluate performance of the system in accordance with system requirements.

b. Demonstrate the capability to meet basic LASA signal processing objectives.

c. Conduct research to develop means of improving and extending the capability of the system.

d. Perform seismic and signal processing experiments of interest.

In addition to the above, activities to support the future integration of the system will:

a. Specify the requirements to interface with, control and monitor the LASA array.

b. Specify the requirements for a facility to house the system in Montana.

During this second reporting period, effort was principally directed to three areas:

1. Completion of plans and occupancy of the Seismic Array Analysis Center (SAAC), Van Ness Centre, Suite 450, 4301 Connecticut Avenue, Washington, D. C. 20008.

2. Installation and utilization of the Detection and Event Processors and peripheral equipment as System/360 Model 40 G and H general-purpose computers, respectively.

3. Initiation of array-processing synthesis, analysis and design for Array II.

Section 2

RESULTS AND SUMMARY OF WORK ACCOMPLISHED

The three subsections which follow correspond to the functional disciplines.

2.1 SYSTEM ACTIVITIES

Studies during this quarter addressed the composite detection system and developed a comprehensive array-processing synthesis procedure responsive to both seismic missions of event detection and location. Analysis of array geometry, communications, process errors, and implicit computer burden considered the inherent data character; these analyses are presented in the appendixes.

Since large seismic arrays produce extensive raw data, message encoding is a critical system constituent. Delta modulation, sample rate reduction, and floating-point word formats have been examined to establish data compression techniques appropriate to array data acquisition and communication (see Appendix C). We recommend use of a base 4 modified floating-point encoding of short period seismic data sampled at 10 Hz. This study considered system performance implications, subarray equipment compatibility, and the objective to efficiently use commercially available modular communication facilities.

The resulting communication rate is thereby reduced to approximately 35 percent of current requirements without significantly impairing system performance. Actual seismic histories were employed to evaluate several trace reconstruction algorithms, and the observed errors were commensurate with classical error-bound estimates. The introduced noise power and deviation bounds are negligible when reconstruction is derived from four or more data

points, which verifies the signal integrity at this reduced sampling rate. Instrument rescaling and analog filter tuning adjustments are latent modifications which can further improve system performance.

Detection process parameters have been reviewed, and an initial scaling has been formulated which is compatible with operational developments, evaluation, and data analysis support. Sampling rate, data quantum, saturation level, and estimated statistical characteristics of the composite noise inherent in both the raw data and the fixed-point digital process have been evaluated at the nodes of each stage (see Appendix D). Numerical error contributions are insignificant thereby substantiating the detection architecture. Filter response deviations due to coefficient quantization are presented, and a slight pass band ripple is evident for conventionally rounded values. The encountered characteristics are adequate, and since the detection filter can be subsequently upgraded when statistically significant spectral estimate ensembles are available, no secondary filter adjustments were considered necessary at this time.

Experimental display modification to support a strip chart recorder proved feasible and is described in Appendix E. This extension implements a rapid multichannel hard-copy background capability of medium accuracy which facilitates process documentation and provides an efficient method for gross data editing.

Transformations between the frequency and time domains are often desired to efficiently analyze signals and characterize processes. Array instrument calibration, phase velocity estimation, reverberation suppression, and special event processing are operational functions which may conceivably require the application of the Cooley-Tukey (Fast Fourier) algorithm. An analysis of the errors encountered when implementing this process with 16-bit fixed-point arithmetic was conducted and simulations performed. When proper intermediate scaling precautions are exercised, the concept appears feasible. Estimates of implementing this operation as a microcoded algorithm have now been generated, and an execution time of 100 milliseconds as opposed to 920 milliseconds in fixed-point and 1080 milliseconds in floating-point, coded

in assembly language, are required to transform a 256 complex number array on an IBM 360/2040. As the Event Processor architecture evolves, significance of this advancement to the system will be evaluated to determine the desirability of implementing the transformation as an addition to the microcode repertoire.

The comprehensive array synthesis presented in Appendix F illustrates a methodical procedure which is pertinent to overall system objectives, provides tradeoff flexibility, and identifies crucial variables which require measurements to establish experimental verification. This establishes the necessary objectives of a precursor data measurement program and provides the structure for subsequent array designs.

2.2 PROGRAMMING

Programming effort during this quarter centered on

1. Microprogramming
2. Detection Processing
3. Supervisor/Monitor
4. Program Conversion.

Accomplishments in each of these areas is presented in the following subsections.

2.2.1 Microprogramming

Microprogramming activity centered around two areas: continued testing and the new RIT threshold computation.

Following installation of the 2040G at SAAC, microcode testing was continued. After completion of these tests, debug work on the detection controller revealed a number of data-dependent errors; these were corrected as they appeared with no loss in execution speed.

The improved RIT threshold computation operation (previously reported upon[5]) was installed in both machines. Testing of this addition revealed no operational errors.

2.2.2 Detection Processing

Detection processing activity was centered in two areas: data acquisition and the detection controller.

2.2.2.1 Data Acquisition

The initial version of this program[5] was modified to take advantage of the real-time input format. The program, operating in an off-line mode, accepts as input LASA data tapes and generates a seismometer level tape in the same format as the real-time seismometer input format. This data tape will serve as the primary input to the Detection Processor. The editing and reformatting function will also provide a record of the type and number of errors (modem, parity and illegal values) on an individual seismometer, subarray and array basis.

2.2.2.2 Detection Controller

Work was aimed at expanding the version written for microcode testing. Initial operating parameters were defined as were input and output formats. A version of the controller was completed and initial experimentation was begun.

The operating parameters are previously reported.[4] These parameters were used to assess the operating posture of the controller. Input data consisted primarily of a special data tape which contained six known events. A pseudo-noise tape was also created and used to obtain an initial noise estimate for insertion into the noise averaging section. The type of outputs generated are also previously reported.[4]

Testing of the controller pointed up some errors in the microcodes, and these in turn resulted in some reprogramming effort. In particular, core storage allocation and arrangement were the major areas of redefinition.

Initial experimentation consisted of running the detection controller to generate intermediate data tapes of subarray beams and LASA beams. These tapes were plotted and the plots used to locate errors in the controller. The listed output of detected arrivals was also an aid in error detection.

2.2.3 Supervisor/Monitor

Upon arrival of the IBM System/360 Model 2040G at SAAC, significant effort was expended in systems generation and maintenance functions. The operating system in use is a modified version of the IBM Disk Operating System (DOS) under which the ESPS programming development will proceed. Supervisor/monitor activity for the Detection and Event Processors is discussed in the following sections.

2.2.3.1 Detection Subsystem

Performance Test Tool. A means of measuring the detection processing capability under conditions of minimum overhead was designed and coded. The object was to operate independently of DOS so as to maximize the available computing time. This allowed a measure of the upper bound of computing capability. Also, by comparison with a detection processing program which used DOS, a measure of the overhead incurred in the latter arrangement would be available. This would aid in the planning of the eventual real-time detection monitor. This test tool was made available so it could be combined with the detection processing program.

Prototype Detection Monitor. Work progressed in the development of the detection monitor. The first version will be capable of taking simulated real-time inputs asynchronously with detection processing. This requires a multi-programming capability. The modifications to the DOS needed to make this possible were identified.

2.2.3.2 Event Subsystem

The Disk Operating System does not fully support the implementation of programs using the 1627 plotter, the experimental display, channel-to-channel, and the 2250 display. The provision of a general-purpose capability tailored to the SAAC configuration was given the most emphasis during this quarter. Specifications were made for the needed supervisor modifications to support the plotter and the experimental display on the 2040H.

The first objective in developing the experimental Event Processor monitor includes as a fundamental requirement the ability to execute programs automatically. Whereas in a general-purpose operating system, the load on the system is controlled by a computer operator, in an automatic system a job is executed by signals set and detected internally. For example, event processing will be triggered by an interrupt via the channel-to-channel from the Detection Processor subsystem. The modifications to DOS needed to build this capability were investigated during this quarter.

The capability represented by the prototype system would be extended in further versions to provide the automatic job scheduling capability to build a system responsive to its external environment.

2.2.4 Program Conversion

The programs developed for the IBM 7090 during previous studies were converted to the IBM System/360 to run under the IBM Disk Operating System. In general, this conversion process was easily accomplished since the majority of the programs were written in FORTRAN. The major changes made to the FORTRAN programs involved array sizes and logical statements.

Two programs, the LASA tape edit and the read routine, were rewritten. The LASA tape edit program, written in Assembly Language for the IBM 7090, finds its System/360 counterpart in the data acquisition program discussed above. The read routine provides the capability for the FORTRAN-oriented data analysis programs to process the data tapes prepared by the data acquisition program. It is an input routine which accepts the real-time formatted tapes, and unpacks and places in floating-point form the seismometer channels on these tapes.

The conversion process offered the opportunity to increase the capability of several programs. In particular, program capability in the signal and noise power calculations and correlation areas was extended. The power programs were provided with a sliding integration window capability as opposed to the fixed window of the IBM 7090 version. In addition, power averages for 25, 19,

16 and 13 seismometers, and 21, 17, 13 and 9 subarrays were included in the calculations.

The correlation program was modified to correlate pairs of data channels, provide intermediate correlation coefficients for all pairs, and record the output information as a function of distance between the sensors in each pair. The output format includes a running sum of the correlation coefficients for all pairs considered in the processing from which an average correlation coefficient as a function of distance between elements can be obtained.

Minor modifications were made to several other programs to provide greater flexibility and efficiency in their execution capability.

2.3 OPERATIONS

Effort during this quarter was expended in the following operational areas:

1. SAAC
2. Maintenance Plan
3. System Procedures
4. Experimental Display
5. ESPS General Specification
6. ESPS Acceptance Test Plan
7. Interface Monitor and Control Specification.

The activity in each of these areas is discussed in the following sections.

2.3.1 SAAC

The Seismic Array Analysis Center (SAAC) was occupied by IBM LASA Project personnel on March 20, 1967. Prior to this, specific office layouts and the computer room layout were prepared and approved; and coordination of the computer installation commenced.

Installation of the initial SAAC machine system (described in Appendix A) was completed, and the GSA acceptance requirements were met during March 1967.

As program debug efforts began, critical examination was given to system utilization and performance. As a result and in view of current overall project needs, several changes were made to adapt the hardware system to a more efficient configuration for software development. These changes include:

a. System interconnections will be implemented on an as-required basis to minimize software interaction.

b. Additional unit-record equipment (line printer, reader/punch) was ordered to provide general-purpose capabilities on the System/360 2040G (Detection Processor) during the programming debug phase.

c. The conflicts arising from use of a shared disk control unit, when the two processors are operating independently, results in inefficient processor utilization. Since this will be a common operational mode during system development, an additional disk control unit and drive were ordered.

d. Plans were formed to establish the System/360 Model 2044H as a stand-alone computing system with the capability to be integrated as an interconnected processor at a later date.

The Detection Processor was used for approximately 200 hours for this quarter, with the major amount of this time being used for debugging programs and for data analysis.

2.3.2 Maintenance Plan

During the reporting period, attention was given to developing a maintenance approach for the system hardware tailored to the configuration being used and the overall system performance requirements.

Basic maintenance concepts are valid in the usual situation where the processor can be reconfigured to maintenance subsystems allowing the prime function of detection processing to proceed uninterrupted. An unusual case results when "machine state failures" (those which occur when a precise programming system environment has been established) occur between the interconnected processors and their associated shared control units. Several techniques have evolved in other systems of the same general type and these are being studied to determine the best approach.

2.3.3 System Procedures

Two undesirable situations were identified as a result of investigating the fail soft technique to be employed in the on-line, real-time system. These were:

a. Dominant control unit — the last control unit of a series of control units provides the termination for the channel/control unit signals. When power to this unit is removed, or is lost, a floating condition occurs on these lines which can render a processor inoperative. Due to the interconnected configuration in the system, this condition is intolerable. The designed solution will eliminate the requirement for power-up on the terminating control unit.

b. Power on/off transients — during the power on/off sequences of control units, undesirable noise signals occur on the interface control and signal lines. As a result, error conditions can be generated which would adversely affect system operation. As in item a., the presence of the system interconnections makes this an unacceptable situation. A design to isolate any unit which is transitioning power from interface control and signal lines until transition has been completed is in progress. The required equipment changes have been requested for installation as soon as the field change packages are available.

2.3.4 Experimental Display

The logic design and fabrication of the hardware for the on-line experimental display system has been completed. The system is now under unit test. Design reviews have been conducted and the necessary documentation for software generation has been provided.

2.3.5 ESPS General Specification

A preliminary version of the ESPS General Specification was written and distributed for project review. This specification establishes performance, design, development and test requirements for the LASA Experimental Signal Processing System. Equipment selection and program design necessary to provide a system capable of supporting research and development in techniques of seismic signal processing are presented.

This document provides the inputs which form the basis for developing further system documentation such as Programming Specifications and the Acceptance Test Plan. In turn, these documents will provide the criteria for design, performance and test of the system, and system components.

2.3.6 ESPS Acceptance Test Plan

The initial draft of the Acceptance Test Plan was completed and distributed for project review during this reporting period. This document presents the tests, equipment, program, and subsystems necessary to demonstrate the capability of the system to meet the specified requirements.

Included in this document are system descriptions, test requirements, concept of testing, test methods and test support requirements. Information supplied by this plan will be used as a guide in developing the quality assurance portion of the programming specifications. This portion of the programming specification will establish the details governing each of the tests to be conducted.

2.3.7 Interface Monitor and Control

The interface monitor and control requirements (Appendix B) were completed during this reporting period. The preliminary version of the Array Interface, Monitor, and Control Functional Specification was drafted and has been submitted for project review prior to final editing and release.

Section 3

PLANS

The following activities are planned for next quarter. Discussions correspond to the functional disciplines. Each task is presented with sufficient perspective to identify its interrelation and contributions to the project.

3.1 SYSTEM ACTIVITIES

Threshold parameters will be studied to characterize the noise rejection and signal identification capabilities of the implemented detection criterion. An initial set of parameters will be selected to complete the microcode definition for data analysis.

A dynamic array geometry model will be developed to establish the optimum gain array configuration within a circular constraint for specific homogeneous noise fields. This model will support a performance/cost tradeoff, and can potentially extend the art of prudent array design. Noise field models are an essential input to this activity, and the capability to derive such empirical characterizations will be actively pursued.

Comprehensive data analysis activities will be structured to efficiently provide additional base data for phase data anomaly characterization and to extend the knowledge of both the signal parameters and the inherent noise field. Subsequent process evaluation objectives will be considered to minimize the composite data and computer requirements.

Automatic phase delay estimation techniques will be pursued in an effort to develop a precise analytical capability amenable to the efficient acquisition of statistically significant anomalous observations from the available bulk raw data. Samples obtained from the presently defined regions or sectors will be used to evaluate the anomaly characterization prior to being incorporated into the library data.

Phase delay retrieval and signal wavefront analysis segments of the event process structure will be detailed to permit the initiation of precursor encoding for technique evaluation. Initial linkage requirements will thus be identified, and will serve as departure datums for the evaluation of the event process.

A standardized orthogonal polynomial representation will be adopted for the teleseismic range. Error characteristics will be examined for several event arrival phases to determine if single precision computation is adequate. Geographic coordinate estimation will be examined to identify the necessary program structure.

Beam pattern shaping will be examined to determine if such techniques are effective in combating coherent noise originating in the proximity of desired signals. If feasible, this would significantly extend the special event processing capability to enhance specific signals in the presence of simultaneous wave arrivals.

3.2 PROGRAMMING

Plans for the next quarter include activities in both the Detection and Event Processor functions.

3.2.1 Detection Processor

The detection controller routine will be modified so that it will accept as input the edited and reformatted tapes produced by the data acquisition program. An additional version of this routine will be produced and will contain the required modifications to allow its use in data analysis activity.

The first model of the detection monitor will be generated and tested by simulation of the detection controller and simulation of a real-time interface using the event processor and channel-to-channel capability. Following the successful testing of this model it will be combined with the detection controller and will form the first model of the Detection Processor program.

3.2.2 Event Processor

The required modifications and additions to the Disk Operating System will be generated and will provide the required support for the special peripheral input/output devices attached to the Event Processor (2040H). This support includes the 1627 plotter, experimental display, channel-to-channel, and the 2250 visual display unit. This activity will provide a general-purpose operating system tailored to the SAAC configuration.

Generation of a multiprogramming capability will provide efficient and flexible use of the machine configuration. The presence of two computers with one printer, one plotter and one card punch necessitates the spooling of output from tape to these devices.

The IBM Disk Operating System with multiprogramming permits the concurrent operation of three independent jobs. To facilitate the spooling of output, we will provide utility programs which will operate full-time in two of these partitions, while the third partition will have full-stacked job capability.

Experimental program development will be effected to aid in developing Event Processor functions. This program will include activity in the time delay, beam selection, arrival identification, and event location areas.

To facilitiate the use of the 1627 plotter, a set of basic plotter routines will be developed. A partial plotter routine program package is available, and the required modifications and extensions to this package will be made to provide the plotter capability required at SAAC.

The programs required to present waveforms and beams on the experimental display will be developed and tested when this display is integrated with the 2040H processor. The definition and design of the program specifications for the 2250 visual display unit will be addressed, and implementation of these functions will be in progress.

3.3 OPERATIONS

Plans for the next quarter include acitivity in SAAC expansion, equipment, and data item reporting.

Tentative office layout plans have been drafted to expand SAAC approximately 2800 square feet. These plans include the addition of a seminar room, several offices, a small library and document control area. Other modifications of office space will result in changing the location of the reception area and the possible addition of one or two more offices by conversion of one conference room. Plans for rearrangement of the computer rooms and tape storage area are in progress. These plans will consider alternative configurations of the interface system equipment. Operation of SAAC has demonstrated the need for more storage space for data processing supplies and magnetic tapes as well as desk space for operation of the tape library.

The installation of the LASA intermediate computing system is scheduled for completion at the start of the fourth quarter. Heavy activity is expected in integrating the supervisor software routines required to support the various system interconnections. With both the System/360 40G and System/360 40H fully operational during the next quarter, an expected partial second shift will be operating to fully use the 176 hours of machine time allowed in the basic monthly rental. A large shipment of tapes will be ordered for processing through our edit programs. In the future, tape ordering will be on a continuing basis in order to develop an adequate base for system experimentation and test.

The LASA experimental display system modified for on-line operation is scheduled for hardware integration with the LASA computing system during the third quarter. Primary emphasis will be placed on the beam and waveform functions so that the program debug effort can be started. The strip chart recorder functions will be integrated when test software is available.

Immediate plans call for project review of the General Specification and Acceptance Test Plan so that the next level of system documentation may in turn be initiated.

Section 4

REFERENCES

1. "Large Aperture Seismic Array Signal Processing Study," IBM Final Report Contract No. SD-296, 15 July 1965.

2. "LASA Signal Processing, Simulation, and Communications Study," IBM First Quarterly Technical Report Contract No. AF 19(628) - 5948, ESD-TR-66-463, Vol. I, May 1966.

3. "LASA Signal Processing, Simulation, and Communications Study," IBM Second Quarterly Technical Report ESD-TR-66-515, September 1966.

4. "LASA Signal Processing, Simulation, and Communications Study," IBM Final Report Contract No. AF 19(628) - 5948, ESD-TR-66-635, March 1967.

5. "LASA Experimental Signal Processing System," IBM First Quarterly Technical Report Contract No. F 19628-67-C-0198, ESD-TR-67-458, February 1967.

6. Lincoln Laboratories, "LASA Magnetic Tape Format," Lincoln Labs Memorandum, 17 November 1966.

7. "Bell System Data Communication Technical Reference Manual," Wideband Data Stations X303A10, X303A20, X303A30 Types, Interface Specification, October 1964 (Preliminary).

8. A. Papoulis, "Error Analysis in Sampling Theory," Proceedings of the IEEE, July 1967.

9. D.C. Stickler, "An Upper Bound on Aliasing Error," Proceedings of the IEEE, March 1967.

10. H. Freeman, "Discrete Time Systems," John Wiley and Sons, 1965.

11. W.B. Davenport, Jr., and W.L. Root, "An Introduction to The Theory of Random Signals and Noise," McGraw-Hill, New York, 1958.

Appendix A

MACHINE CONFIGURATIONS

The initial and second SAAC machine configurations are presented in figures A-1 and A-2 respectively.

During March 1967 the IBM System/360 Model 40G (Detection Processor) was received and installed, and on March 20, 1967, it was released to the LASA Project for utilization. In April 1967, the IBM System/360 Model 40H (Event Processor) was received and installed. It is expected that it will be accepted for use in May 1967.

Figure A-2 presents the SAAC machine configuration as it will exist during the next quarter. The cross-hatching indicates units to be added to the system during the quarter.

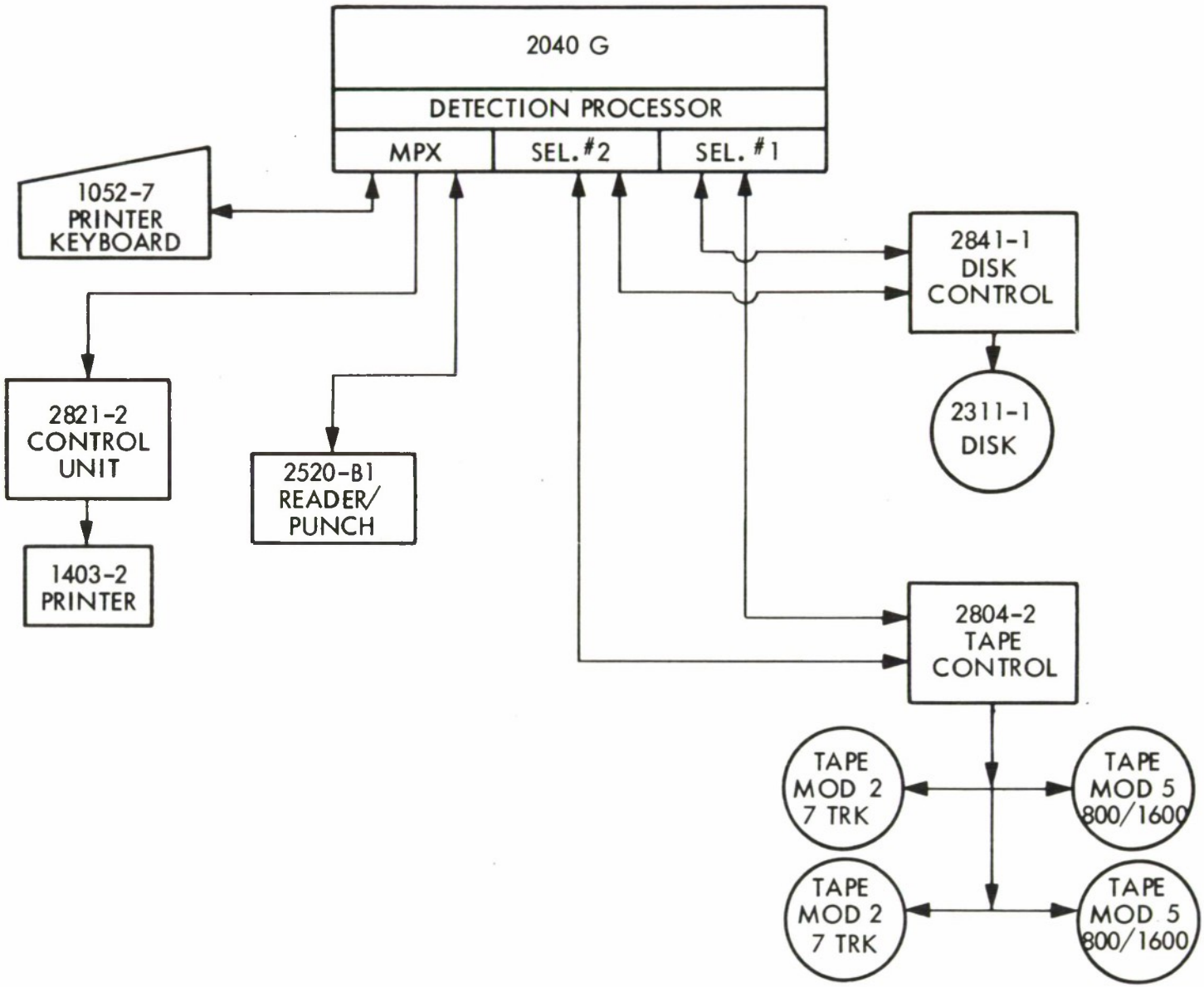

Figure A-1. Initial Configuration

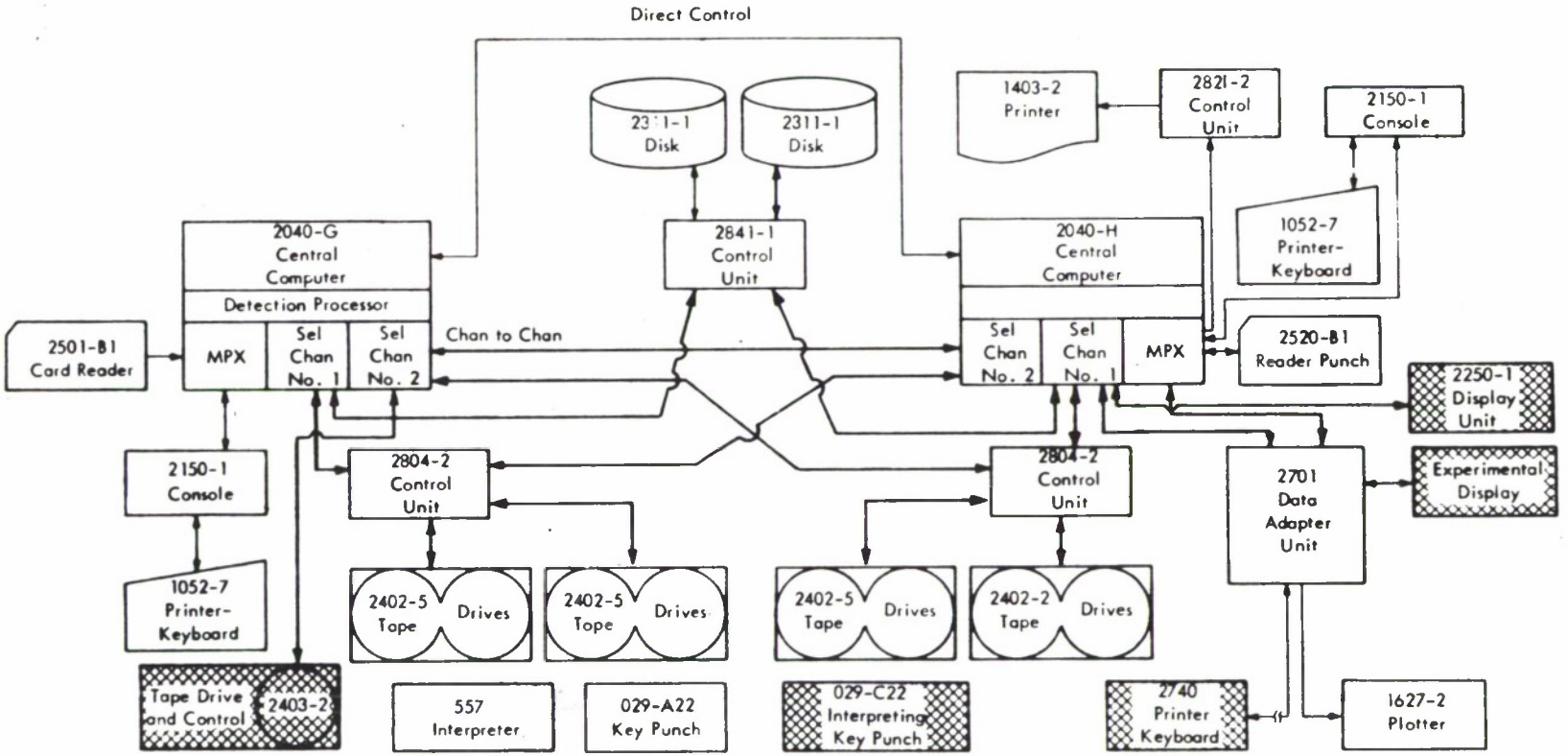

Figure A-2. Second Configuration

Appendix B

ARRAY MONITOR AND CONTROL REQUIREMENTS

B.1 INTRODUCTION

An operator's console and a maintenance console shall be provided to facilitate monitoring the seismometer outputs, as well as the computer processing, to make printed records of the signals being processed, and to initiate commands to the processor or array to perform diagnostic tests for maintenance purposes or to calibrate the array seismometers. Operation of the console displays and keyboard entries shall be in conjunction with computer programs which control the transfer of data between the computer and the console.

B.2 GENERAL DESCRIPTION

B.2.1 Array Monitoring

The rectified output of each seismometer shall be integrated over a specified time interval. Selected seismometer outputs may be monitored by displaying the signal received on a cathode ray tube waveform display. Six to eight such signals may be displayed simultaneously for comparison, and any particular signal shall be selectable to be displayed continuously for detailed examination. In addition to the waveform display, a capability must exist for making a printed record of the signals on a strip chart recorder or similar analog recording device for later study or for examination at a point remote from the processing center.

Array alarm conditions shall be continuously monitored to provide indication of power failure, etc. Since the operation of the array will be dependent upon the performance of the two way communication link between the array and the processing center, it will be necessary to monitor the communication equipment and to provide indicators to the operator, as well as to the processor, in the event of a communication link failure. The error detection bits of data received, modem AGC warning, and loss of synchronism of message frame must be monitored.

B.2.2 Monitor Computer Processing

Computer processing will be monitored on a waveform display and/or a beam display. These displays will make it possible to view a large quantity of output data as a single image and to obtain information on absolute as well as relative values.

The computer equipment shall be monitored and status indicated.

B.2.3 Array Control Commands

A number of test facilities have been designed into the subarray equipment and will be placed in operation by commands from the computer or consoles. These facilities are necessary for maintenance of the array, as well as calibration of the array seismometers, and provide a means of sampling special sensing equipment at the subarrays. A designated six-bit field of the message transmitted to each subarray shall contain the command codes. These command codes will be transmitted to any one selected subarray at a time and must not interfere with normal operation of the other subarrays. The formation of the commands and the selection of the subarray and subarray data must be performed under program control or by manual entry keys on the consoles. The command code received at the subarray shall be transmitted back to the Data Center for verification.

B.2.4 Output Display for Maintenance of Array and Communication Link

One waveform display will be used for monitoring the array and processor and a second waveform will be used for maintenance purposes. A strip chart recorder will provide a permanent record of the output from any seismometer. Most of the diagnostic routines will be performed automatically, under program control, with their results summarized and a printed console log presented on the output printer. When desirable, the spectral response of a selected channel may be displayed on the waveform display with acceptable limits superimposed. Or, the numeric evaluation of the spectral response, as well as numeric parameters or status indicator, may be displayed.

B.3 OPERATIONAL CHARACTERISTICS

B.3.1 Digital to Analog Conversion

Eight digital to analog conversion units shall be provided to give eight independent analog output channels. These channels will accept digital information in binary form (13 bits plus sign and provide analog output voltage of $\pm$ 10 volts with an accuracy of $\pm$ 0.1 percent) and a minimum conversion rate of 1000 words per second. The outputs shall be compatible with the strip chart recorder inputs.

B.3.2 Strip Recorder

An eight channel strip recorder must be provided for recording analog signals. The inputs to the recorder are to be compatible with the analog output channels provided so that digital data may be used to monitor analog signals during on-line processing. The strip chart recorder will be a Sanborn Model 7708A, with 8801A preamplifiers or equivalent.

B.3.3 Waveform Display

The waveform displays will be used to collect and display signals taken from any seismometer and/or test points determined by subarray control

commands. All seismometer and test point data will be collected and stored in a processor which will, upon receipt of manual requests, format selected portions of the collected data into messages that will fit the requirements of a waveform display.

B.3.3.1 Display

Eight traces, with up to 500 sample points per trace, will be displayed on a CRT. The abscissa will represent time and the ordinate will represent linear signal strength (amplitude) of each sample point. A vertical line cursor may be superimposed on the waveform display. Each waveform may be processed independently. Provision shall be made for vertical magnification of the waveforms. Display flicker will be kept to a minimum by matching its repetition rate to a specific phosphor. The rate should be not less than 30 Hz.

The phosphor should be selected so that smear, under normal computer room lighting conditions, will not be apparent.

B.3.4 Beam Display

The Beam Display will be used to display signals which have been taken from the LASA array seismometers, formed into a beam (measure of seismic energy level at a specific inverse phase velocity location), and converted into a word that will display the beam's intensity level. A large number of beams will be formed and displayed on the CRT. Thus, the seismic activity at a large number of contiguous inverse phase velocity locations will be displayed at the same time.

An external processor will collect and store seismic data, form the beams, and format them into messages that will fit the requirements of a beam display.

B.3.4.1 Display

A 32 by 32 matrix of beams will be displayed on the CRT. Each matrix element will be the position of a beam assigned to a specific inverse velocity space location.

Each beam's relative intensity (energy) level will be indicated by the spot intensity (CRT beam current) at the XY coordinate point assigned to it. Thus, light output at a beam's coordinate will be a function of the beam's seismic energy level. The functional relationship may be linear, logarithmic, or floated logarithmic.

Beam size must be adjustable so that beams do not overlap and at the same time are spaced no more than 15 percent of the beam width apart.

Display flicker must be kept to a minimum by matching its repetition rate to the selected phosphor. The rate should be no less than 30 Hz.

The phosphor should be selected so that smear, under normal computer room lighting conditions, will not be apparent.

Update rate (fresh data) can occur at a maximum rate of 10 Hz.

B.3.4.2 Manual Inputs

Manual Inputs (MI) are required to instruct the external processor on what kinds of display data it should format and store in the display storage element.

An MI keyboard overlay providing the following functions is required:

a. Select the beams that will be displayed.

b. Expand the display around some specific beam.

c. Freeze a selected pattern at some point in time.

d. Play back some previous pattern.

e. Select the functional relationship between beam seismic energy and display brightness.

f. Select and display a specific seismometer output at some specific trace location.

g. Expand a selected trace a specified number of times.

h. Display a cursor mark on a selected trace or beam; shift the cursor in conjunction with an MI entry control, relative to other beams or traces.

i. Format maintenance instructions that can be used to control maintenance activity at the array.

j. Enter a seven bit pedestal for selecting threshold level.

B.3.4.3 X-Y Plotter and TWX Facility

The equipment must include an X-Y plotter and the facility to operate a remote teletype terminal.

B.3.5 Array Calibration and Maintenance Facilities

B.3 5.1 Calibration

Calibration of the seismometers shall be accomplished, a subarray at a time, by transmitting a command under computer control to the subarray which places a sine wave of known frequency or a pseudo-random waveform of known amplitude on each sensor calibration coil. The data received from each seismometer of the array is the sum of the known test waveform and any ambient vibrations occurring at that time, and is analyzed by the computer to determine the calibration of the individual seismometer as to amplitude and frequency of response.

B.3.5.2 Maintenance

a. Manual—The maintenance console shall be provided with eight channels of digital to analog conversion, eight channels of strip chart recording, and a six to eight trace waveform display which can be utilized to observe and record various array output waveforms. Under manual control, by the setting of switches, any subarray shall be selectable and any word of the message received from that subarray shall be selectable for presentation as a waveform display or made available at any one of the eight digital to analog output channels. Each D/A output channel may be connected to a strip chart recorder channel. Keys shall be provided to designate a six bit command to initiate its transmission to a selected subarray to effect the various tests available in the subarray equipment.[6]

b. Computer Controlled Maintenance—By diagnostic programming, any subarray shall be selectable to receive any of the test commands. The data received from the subarray may be recorded on the strip recorder as an analog waveform, may be displayed on a waveform scope, or an analysis may be made as to amplitude and frequency by the computer to ascertain the validity of the seismometer outputs. The significant results are then recorded by the log-out printer.

Under program control the American Telephone & Telegraph Co. type X303A-10 [5] modems at the computer will be connected to provide a loop test capability, utilizing computer generated data transmission as the source of the messages.

Additional loop test capabilities shall be provided at the subarray level, with a computer generated test command resulting in generation of subarray test signals.

Appendix C

SEISMIC DATA COMPRESSION

C.1 INTRODUCTION

Present LASA instrumentation consists of analog sensors with corresponding amplifiers capable of operating throughout a 72 dB dynamic range. Precision analog communications are feasible for short distances, but digital techniques are more favorable when traversing long distances with a significant composite data rate. This has led to a subarray concept, where an ensemble of analog signals from local sensors are collected at a central instrumentation vault, band limited, sampled, multiplexed, digitized, and subsequently transmitted to the LASA communications terminal. A fourteen bit fixed point conversion is consistent with the analog instrumentation performance characteristics and establishes the present fundamental data rate of 280 baud per instrument when samples are acquired at a 20 Hz rate. Since the LASA contains 525 seismometers, a 147 kilobaud (Kb) communications capability is required to acquire directly the short period instrument data. Secondary instrumentation and overhead for synchronization and error control has extended this burden to 201.6 Kb. This is presently implemented as twenty-one 19.2 Kb channels which impose a 403.2 Kb facility requirement.

The potential advantages of processing at a remote location creates interest in extending the LASA communications network. Continued utilization of the 403.2 Kb composite channel is obviously impractical, and even the base data rate of 147 Kb constitutes a major communication cost. A survey of data compression techniques is appropriate to establish the feasibility of remote processing and to derive more efficient data acquisition techniques for large arrays.

C.2 DELTA MODULATION

In many applications, a significant data reduction has been achieved by employing delta modulation; i.e., transmitting the signal change encountered during the sample interval. Characteristics of this technique are presented by Figure C-1, which illustrates the word length reduction potential when the required sampling rate is excessive for the predominant signal components. Note that a ratio greater than 6 samples per cycle is required to realize a range compression. This situation is often encountered in broad band channels. Principal seismic signal spectrum components have been observed at 1.2 Hz, and are conjectured to exist as high as 1.4 Hz. With the present 20 Hz data acquisition, 14.3 samples per cycle must be accommodated which permits the deletion of only one bit if no loss in performance is to be incurred. This 7 percent reduction is significant, and would presumably justify the additional instrumentation complexity if a 20 Hz sampling rate was essential to the subsequent process.

C.3 DATA SAMPLING

A direct method of data compression for transmission is the reduction of the sampling rate so as to approach the theoretical Nyquist rate requirement, followed by the use of reconstruction interpolation at the receiving end to reproduce the data continuum. This technique is well suited for data acquisition from LASA. It requires that only minimal changes be made in the existing system to reduce the sampling to a submultiple rate prior to transmission and allows selective reconstruction of the higher sample rate data within a general purpose computer when additional phase resolution is required.

If the sampling rate is chosen to be greater than twice the highest data frequency, sampling theory states that the original waveform can be completely reconstructed. Consider the signal f(t) with the Fourier transformation:

$$F(\omega) = \int_{-\infty}^{\infty} f(t)\, e^{-j\omega t} dt, \qquad \text{(C-1)}$$

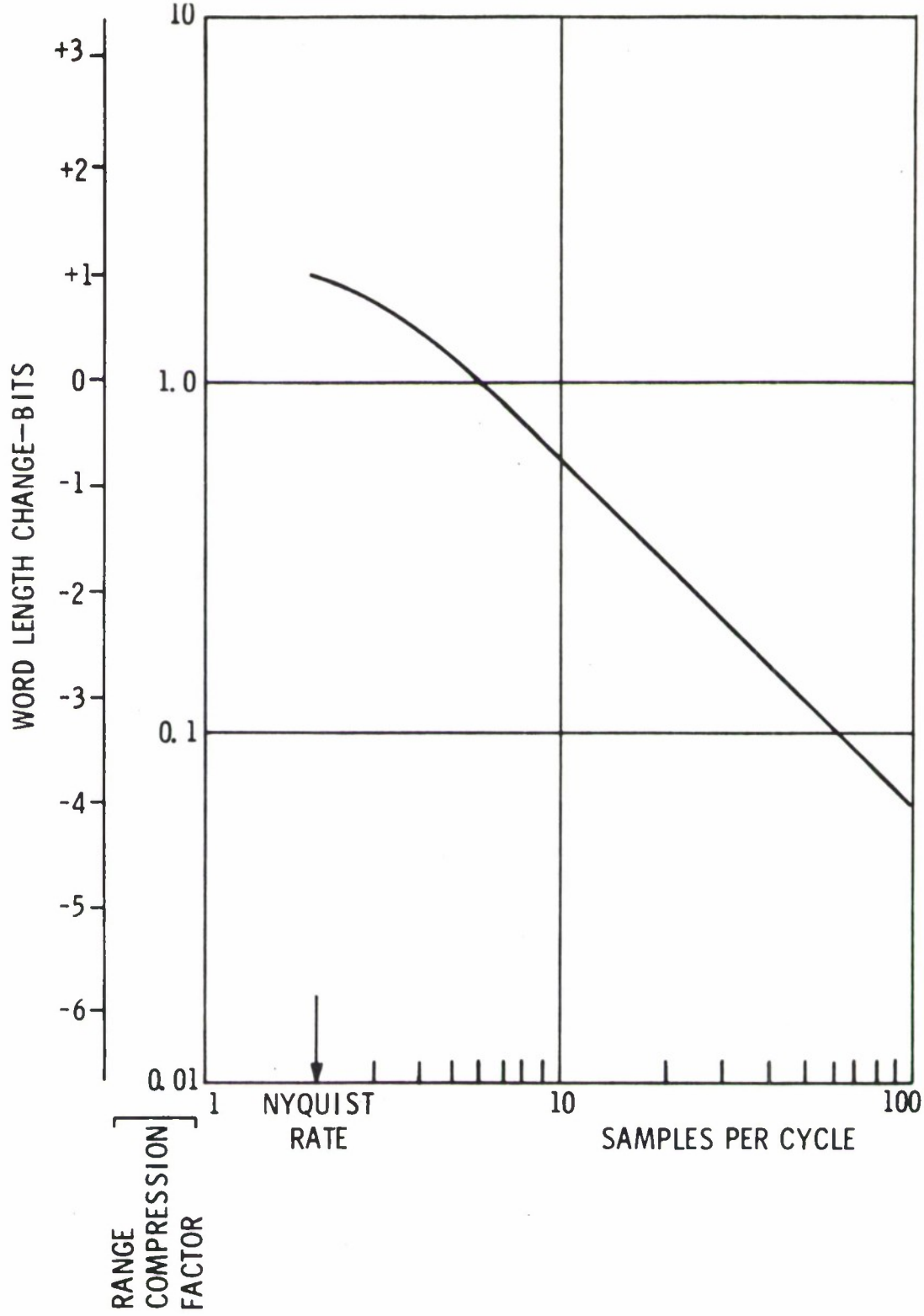

Figure C-1. Delta Modulation Characteristics

such that the signal is bandlimited ($|F(\omega)| = 0$ for $|\omega| \geq \omega_1$).

Defining the sampling frequency as $2\omega_2$ and the time interval between samples as T, the sampling frequency would then be chosen such that:

$$\omega_2 \equiv \frac{\pi}{T} \geq \omega_1. \tag{C-2}$$

Then f(t) can theoretically be recovered from its sampled values f(nT) by applying the expression:

$$f(t) = \sum_{n=-\infty}^{\infty} f(nT) \frac{\sin \omega_2 (t-nT)}{\omega_2 (t-nT)} \tag{C-3}$$

This transform corresponds to an ideal filter that passes without attenuation all frequencies below ω_2 and completely rejects frequency components introduced by the sampling process which exceeds ω_2.

A bandlimited signal cannot be realized, and some energy will always be encountered beyond the capacity of the sampled data channel ($|F(\omega)| \neq 0$ for $|\omega| \geq \omega_2$). Even if the sampling rate is chosen to be greater than twice the highest frequency of interest, the signal cannot be perfectly reconstructed, for new components corresponding to the data spectrum translated by the harmonic structure of the periodic sampling impulse train are present in the band of interest. This aliasing error constitutes the theoretical limit on data reconstruction fidelity. However, additional error is imposed by the practical limitation on the number of data points employed by the reconstruction algorithm, and this effect is examined in Appendix C.4.

In the present LASA system, a low-pass filter is included in each seismometer channel to severely attenuate data components exceeding 5 Hz. The amplitude response of the filter and the alias noise introduced into the data for 10 Hz and 20 Hz sampling rates are shown in Figure C-2 where the input has been modeled as wideband, uniform spectral density data. Lowering the cutoff frequency of the filter reduces the amount of noise aliased, or folded into the data spectrum. If the aliasing error at a reduced sampling rate is deemed unacceptable, alteration of the present filters should be considered.

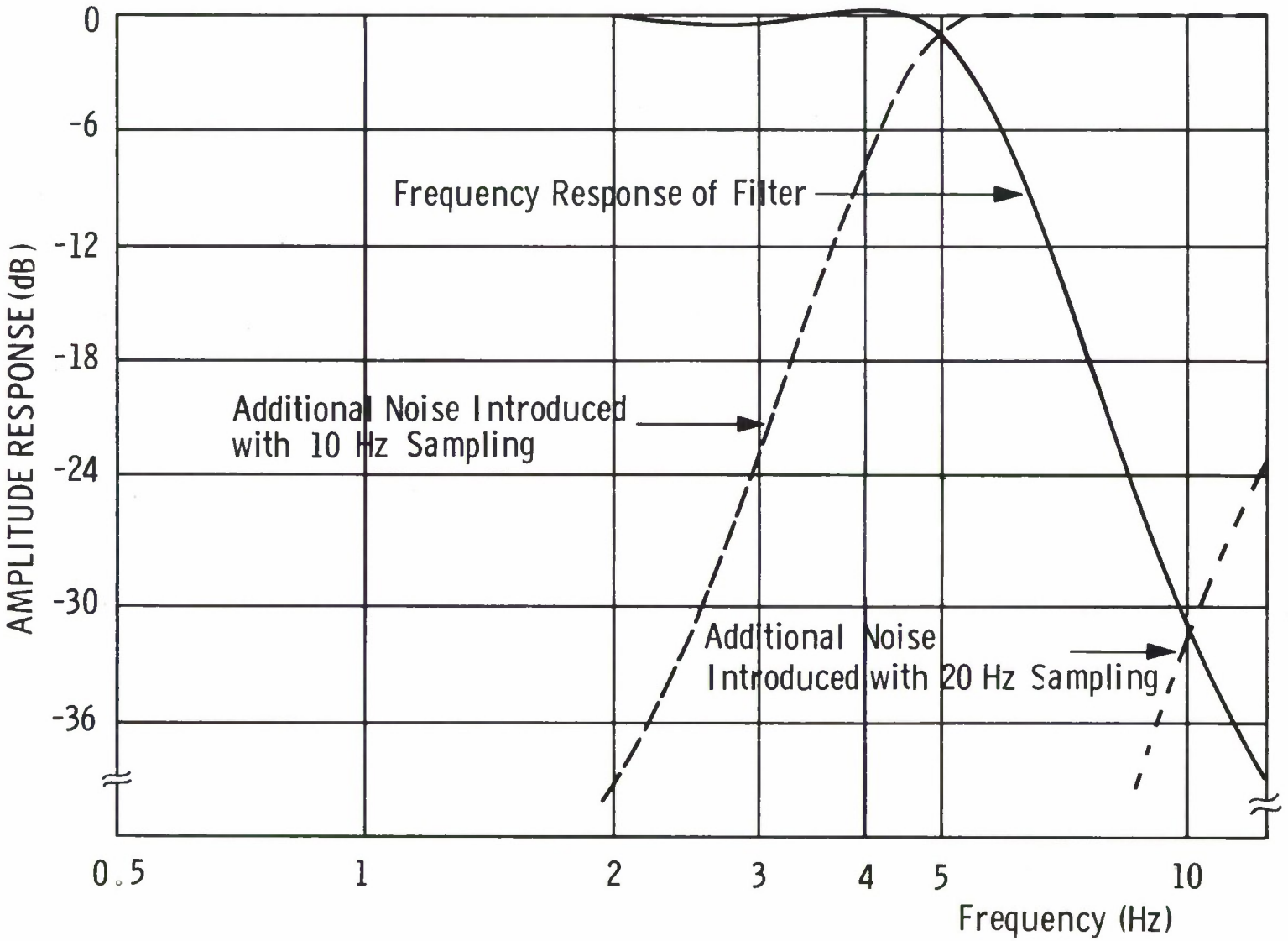

Figure C-2. Frequency Plane Aliasing

A useful technique for computing the upper bound on the aliasing error has been developed by Papoulis[8] and modified by Stickler[9]. The maximum error $|e(t)|$ in a reconstructed function f(t) is bounded by the inequality:

$$|e(t)| < \frac{2}{\pi} \int_{\omega_2}^{\infty} |F(\omega)| d\omega. \tag{C-4}$$

If $F(\omega)$ is bandlimited ($F(\omega) = 0$ for $|\omega| \geq \omega_0 > \omega_2$), the expression becomes:

$$|e(t)| < \frac{2}{\pi} \int_{\omega_2}^{\omega_0} |F(\omega)| d\omega. \tag{C-5}$$

This bound can be used as a guide for estimating the effect of sample rate reduction.

In the following analysis, data with a 20 Hz sample rate is generated from the 10 Hz data. The original 20 Hz data is utilized as a reference to evaluate the performance of several reconstruction algorithms. Thus, the input can be considered bandlimited at 10 Hz which corresponds to the capacity of the reference data. An upper bound on the aliasing error can be expressed as:

$$|e(t)| < \frac{2}{\pi} \int_{2\pi(5)}^{2\pi(10)} |F(\omega)| d\omega. \tag{C-6}$$

Observations from seismometer AO of subarray AO were employed for this analysis. The first record consisted of 51 seconds of seismic noise and the second was a 25 second period of data recorded for the Kamchatka Earthquake of April 8, 1966. The following upper bound of aliasing errors have been calculated from spectral density estimation data:

DATA	ESTIMATED ALIASING ERROR BOUND
Noise Record	-23.7 dB relative to the peak data magnitude
Kamchatka Earthquake	-31.9 dB relative to the peak data magnitude

C.4 DATA RECONSTRUCTION

Resolution requirements are often misconstrued as an essential sampling constraint, but actually they constitute a blend of sampling and reconstruction requirements. When communications represent a major system consideration, reconstruction techniques should be considered for acquiring the desired record resolution. The rudimentary theoretical assumptions are only approximated in practice and, since the most uncertain data points lie midway between the available datums, candidate interpolation algorithms for estimating these points have been experimentally evaluated.

Three methods of doubling data density by using linear symmetrical combinations of up to six consecutive points on each side of the estimated point were simulated. The base 10 Hz data was generated by selecting every other value of 20 Hz data, and hence the interpolated values can be compared to the originally observed values. The three methods are summarized as follows:

a. Lagrangian Polynomial Interpolation
Given a set of m+1 equidistant data values f(KT), K=j, . . . , j-m, there is only one polynomial $\phi(t)$ of degree m such that $\phi(KT) = f(KT)$ for $j-m \le K \le j$. $\phi(t)$ can be generated from the Lagrangian polynomials[10].

Polynomials of degree 1 and 3 were evaluated for reconstruction interpolation. The degree 1 or linear interpolation algorithm for the point equidistant between two samples is given by:

$$\hat{X}(nT) = \frac{X[(n+1)T] + X[(n-1)T]}{2} \qquad \text{(C-7)}$$

The degree 3 interpolation algorithm for the point in the center of the four samples is given by

$$\hat{X}(nT) = \frac{9\{X[(n-1)T] + X[(n+1)T]\} - \{X[(n-3)T] + X[(n+3)T]\}}{16}. \qquad \text{(C-8)}$$

b. Sinx/x Reconstruction Interpolation
The ideal sinx/x reconstruction is approximated by using N points on each side of a sample interval to reconstruct the midpoint. The algorithm for this case is given by:

$$\hat{X}(nT) = \sum_{k=1}^{N} \frac{2\{X[(n-2k+1)T] + X[(n+2k-1)T]\}\ (-1)^{k+1}}{(2k-1)\pi}, \qquad \text{(C-9)}$$

where N = 1, 2, 3, 4, 5, 6.

c. Optimum Discrete Filter Interpolation

The optimum or Wiener interpolation filter used here minimizes the interpolation error in the mean square sense under the constraint that the interpolated values are a linear combination of the sample values:

$$\hat{X}(t) = \sum_{k=-N}^{N-1} h_k X[(n+k)T] \text{ for the interval } (n-1)T < t < nT, \qquad (C-10)$$

where $\hat{X}(t)$ is the interpolated value of $X(t)$ at time t. The mean square error function is

$$MSE = E\left\{[\hat{X}(t)-X(t)]^2\right\}, \qquad (C-11)$$

where E denotes the expected value. Substituting for $\hat{X}(t)$ and minimizing the resulting expression with respect to the coefficients h_k yields, under the assumption that $X(t)$ is a wide sense stationary random process with autocorrelation $R_{xx}(\tau)$, the following set of equations which specify the proper coefficient values:

$$\sum_{k=-N}^{N-1} h_k R_{xx}[(\ell-k)T] = R_{xx}(\ell T-t) \qquad (C-12)$$

and $\ell = -N, -N+1, \ldots, N-2, N-1$.

These equations were evaluated for values of N from one through six using flat power spectrum data models from zero to 3 Hz and from 0.5 to 2.5 Hz.

This technique could be extended to yield the best interpolation estimate (in the mean square sense) of the signal for the case when signal and noise autocorrelation functions are individually described. Assuming that the signal and noise are uncorrelated, the coefficients h_k are specified by the following set of equations:

$$\sum h_k\left\{R_{ss}[(\ell-K)T] + R_{nn}[(\ell-K)T]\right\} = R_{ss}(\ell T-t) \qquad (C-13)$$

and $\ell = -N, -N+1, \ldots, N-2, N-1$ where $R_{ss}(\tau)$ and $R_{nn}(\tau)$ are the autocorrelation functions of the signal and of the noise respectively.

The optimum interpolation error for the 0.5-2.5 Hz spectrum case was within approximately 1 dB of the error for the 0-3 Hz spectrum case for the same algorithm data base. Only the latter is graphically represented. Figures C-3 and C-4 show the ratio of maximum error magnitude to maximum data magnitude when each of the algorithms is applied to the Kamchatka earthquake and seismic noise records. Figures C-5 and C-6 show the ratio of the power of the error to the total data power in dB for the two records. The power density for

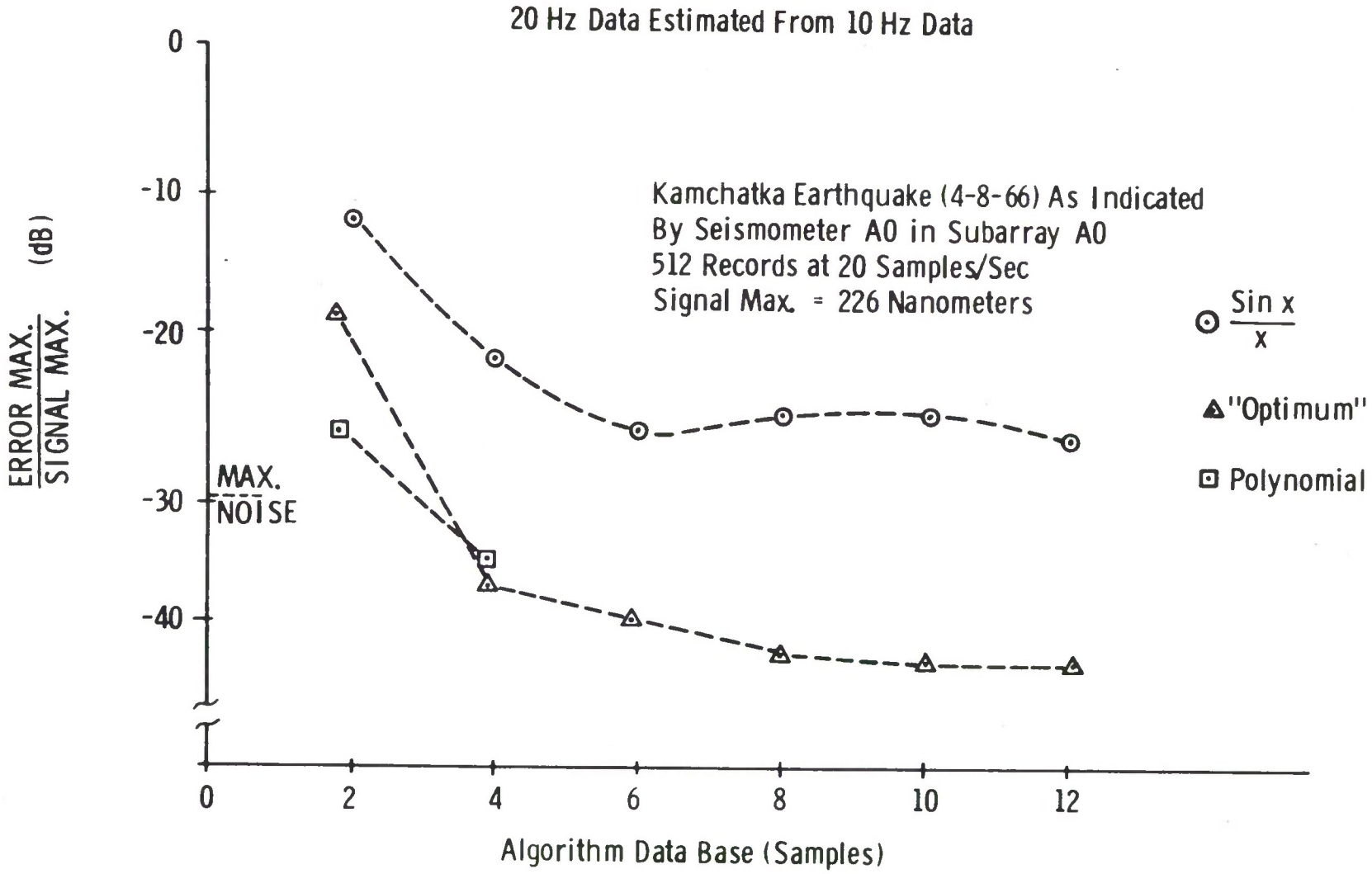

Figure C-3. Reconstructed Signal Error Bound

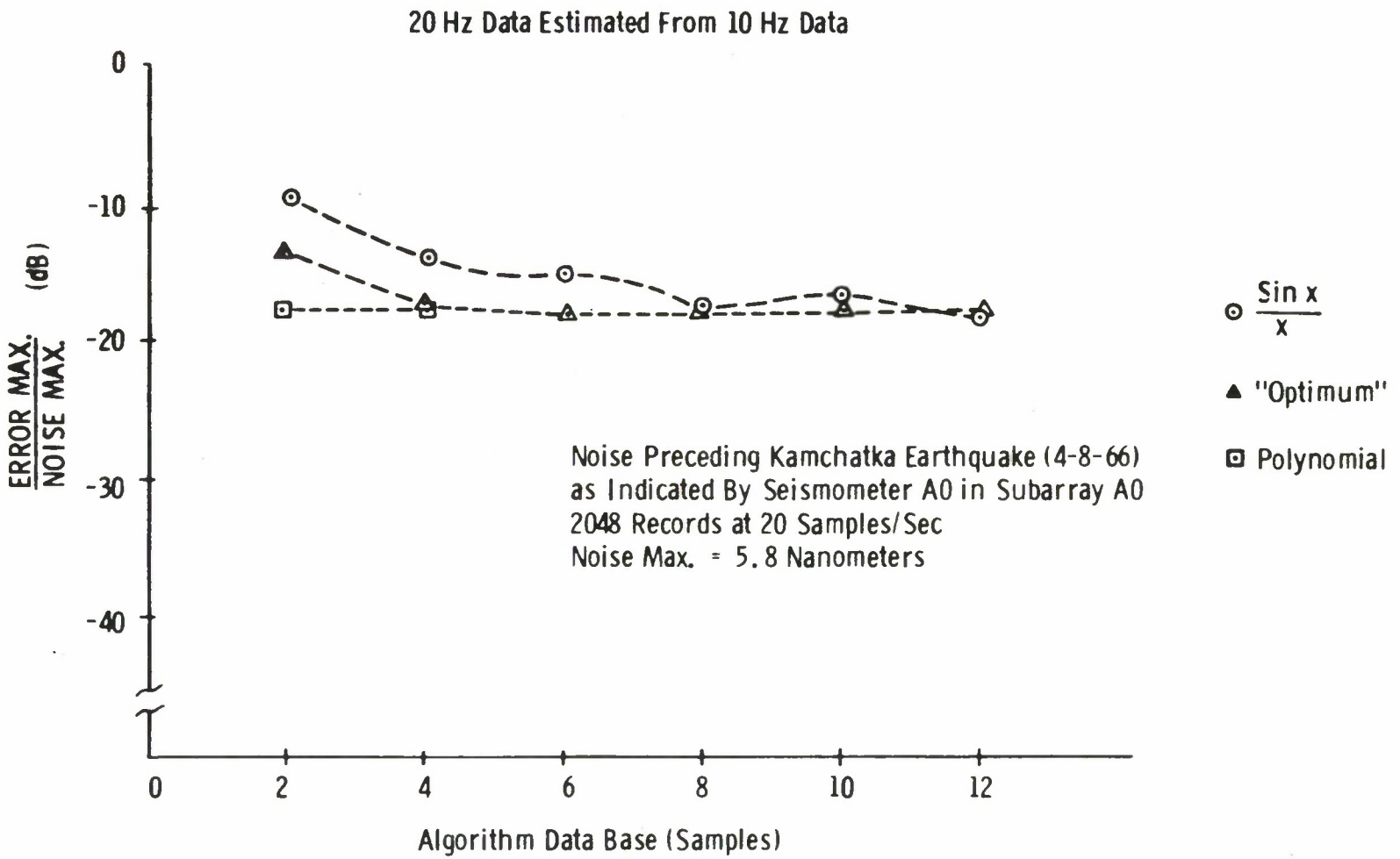

Figure C-4. Reconstructed Noise Error Bound

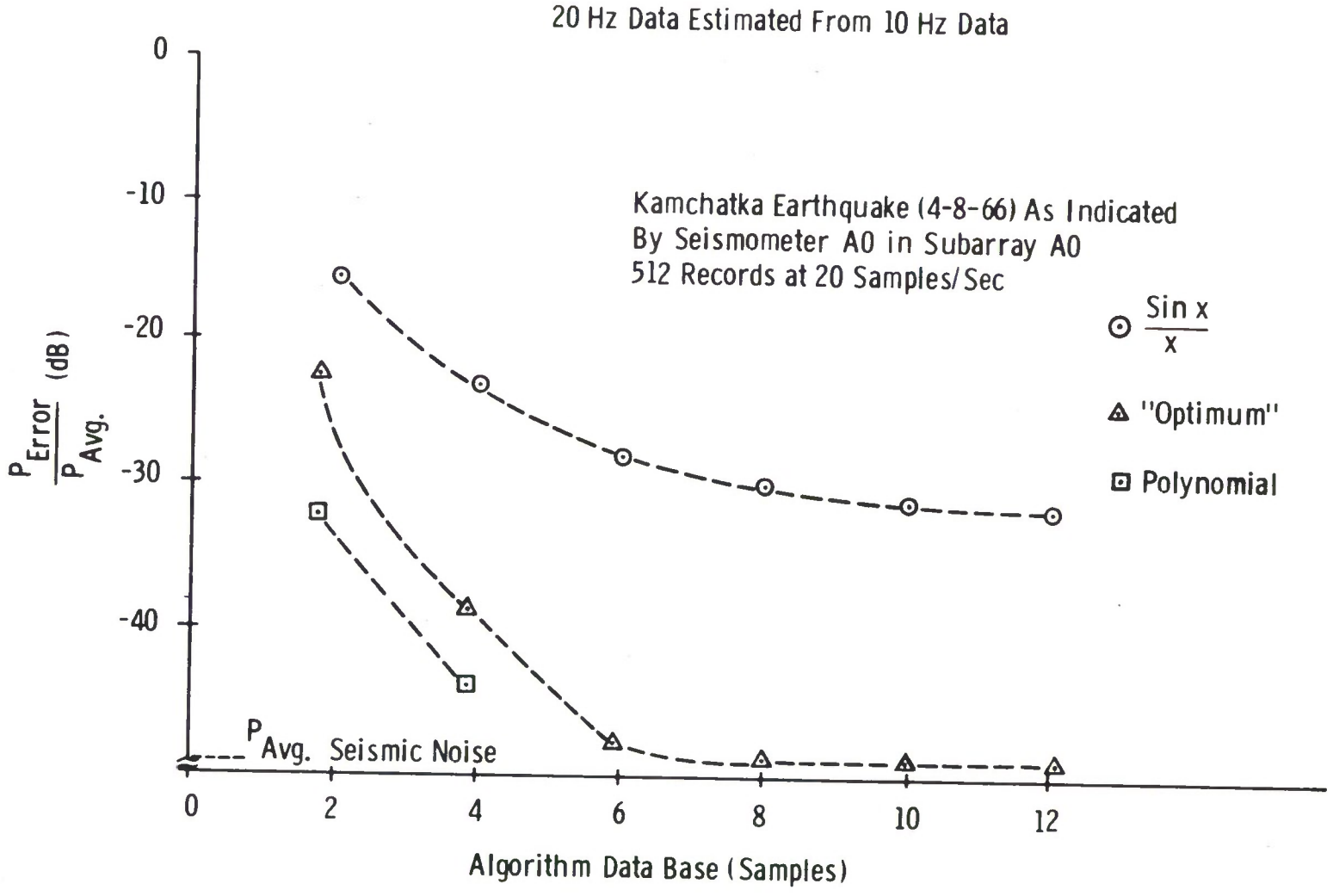

Figure C-5. Reconstructed Signal Error Power

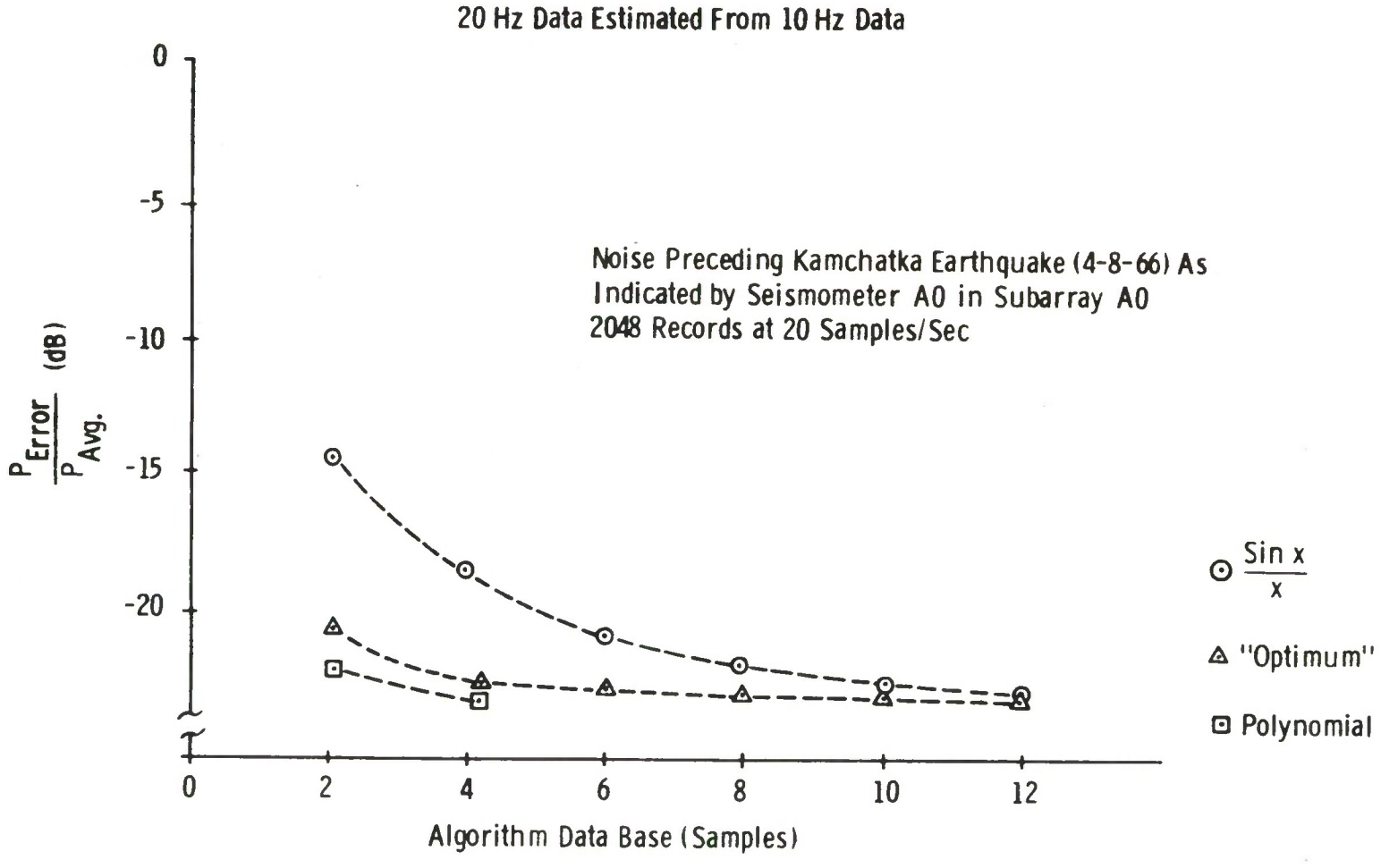

Figure C-6. Reconstructed Noise Error Power

the error between the actual values X(nT) and the estimated values $\hat{X}$(nT) generated by the 3rd order polynomial algorithm are illustrated by Figures C-7 and C-8.

Observation of these experimental results reveals a reconstruction performance which introduces an insignificant additional noise component consistent with the anticipated aliasing bound. Thus, an excessive sampling rate is presently implemented, and the compatible submultiple of 10 Hz appears sufficient to retain the message fidelity. This 50 percent communication requirement reduction precludes the desirability of delta modulation, for the principal component sampling ratio is no longer adequate to provide a significant range compression.

C.5 DATA ENCODING

Additional data compression can be achieved by examining the trade-offs between dynamic range and signal resolution for a floating point data word instead of the present fixed point format. In the fixed point format, the resolution of the signal is a function of its magnitude; large magnitude signals have excessive resolution to achieve a large dynamic range. By scaling the signal to operate near the maximum value acceptable, a minimum resolution over the entire dynamic range can be achieved with fewer data bits. Implementation complexity can be minimized by retaining the two's complement notation for negative numerical values and utilizing integer powers of two as the arithmetic base.

Figures C-9, C-10, and C-11 show the relationship between the resolution band and dynamic range as a function of word size for base 2, base 4, and base 8 floating points. The word size includes the sign and the exponent fields. Figure C-12 shows the relationship of the minimum resolution and dynamic range for the three formats. Base 2 and base 4 have the same minimum resolution for a given word length and dynamic range, but base 4 has a higher maximum resolution. In the dynamic ranges and word lengths of interest, base 2 and base 4 are both better than base 8.

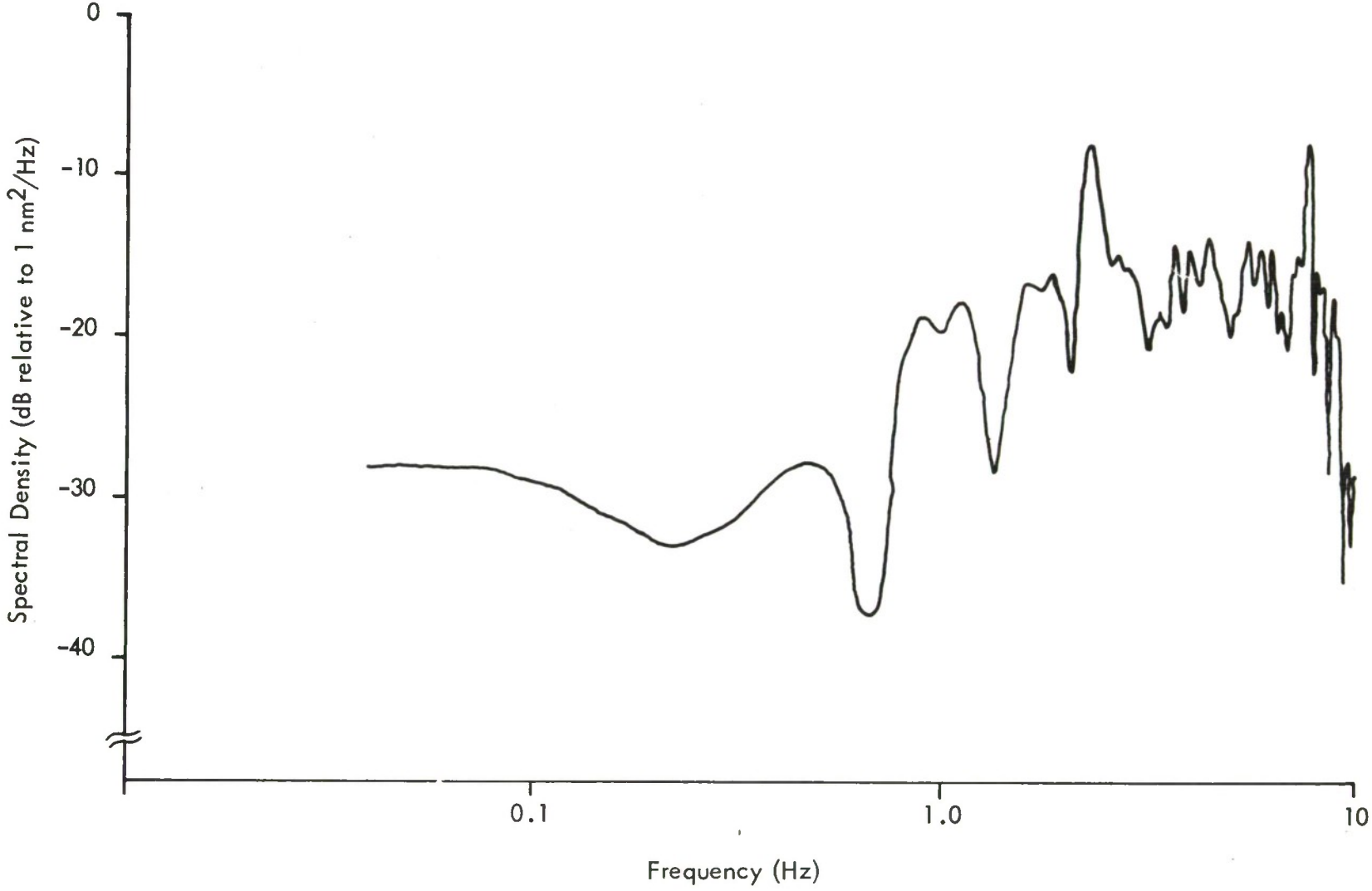

Figure C-7. Signal Error Spectrum–3rd Order Polynomial Reconstruction Algorithm

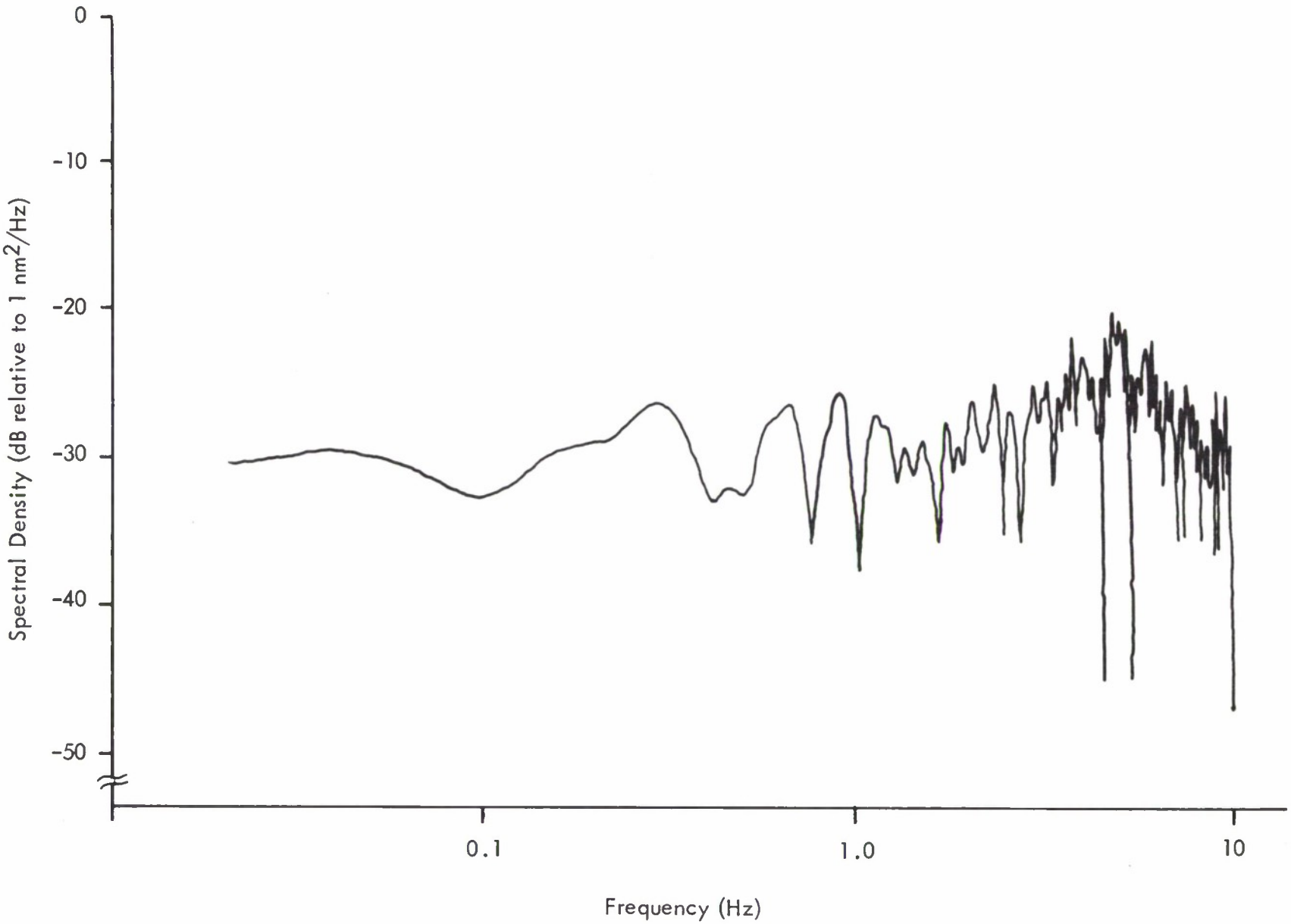

Figure C-8. Noise Error Spectrum—3rd Order Polynomial Reconstruction Algorithm

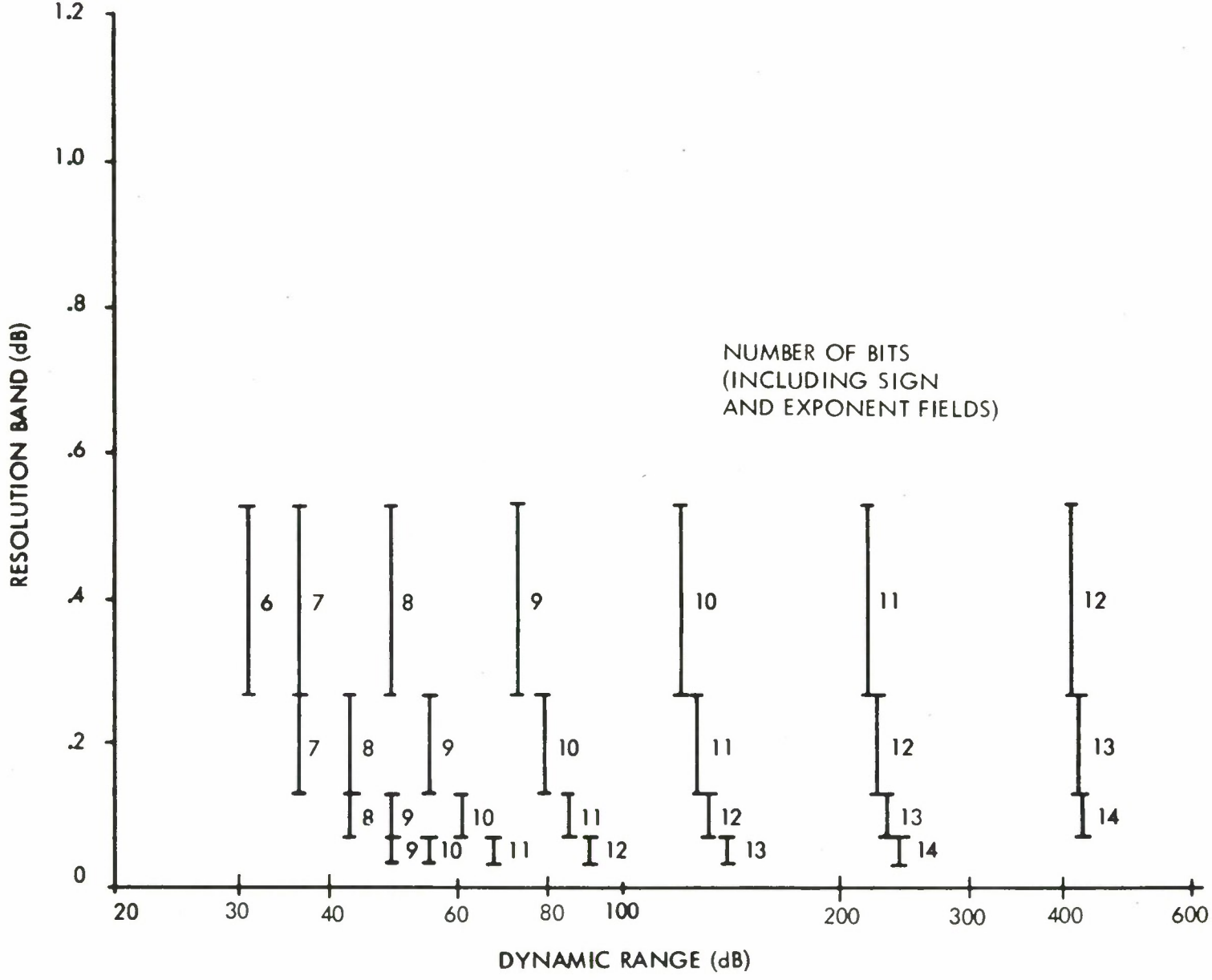

Figure C-9. Floating Point Base 2 - Encoding Characteristics

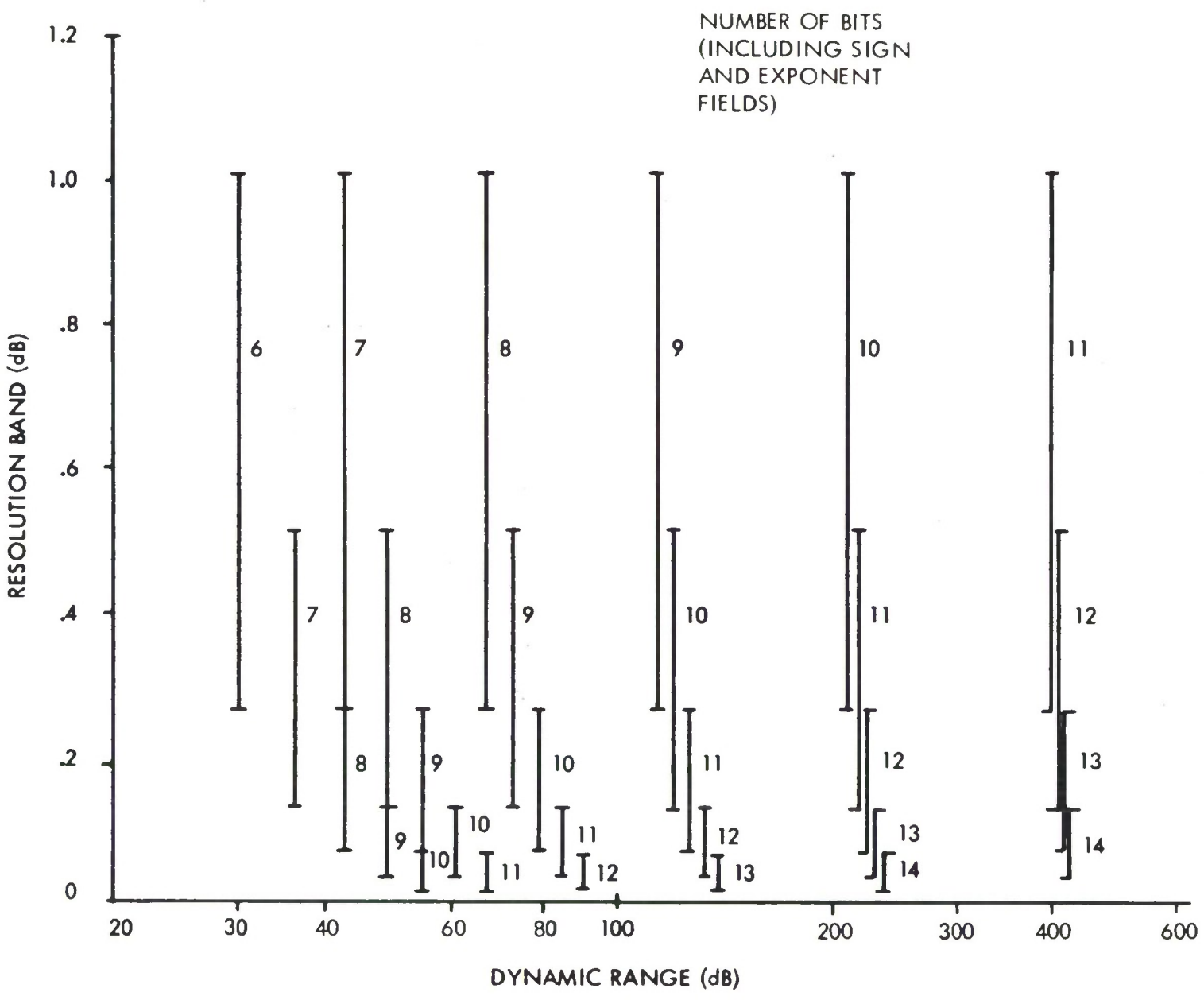

Figure C-10. Floating Point Base 4 - Encoding Characteristics

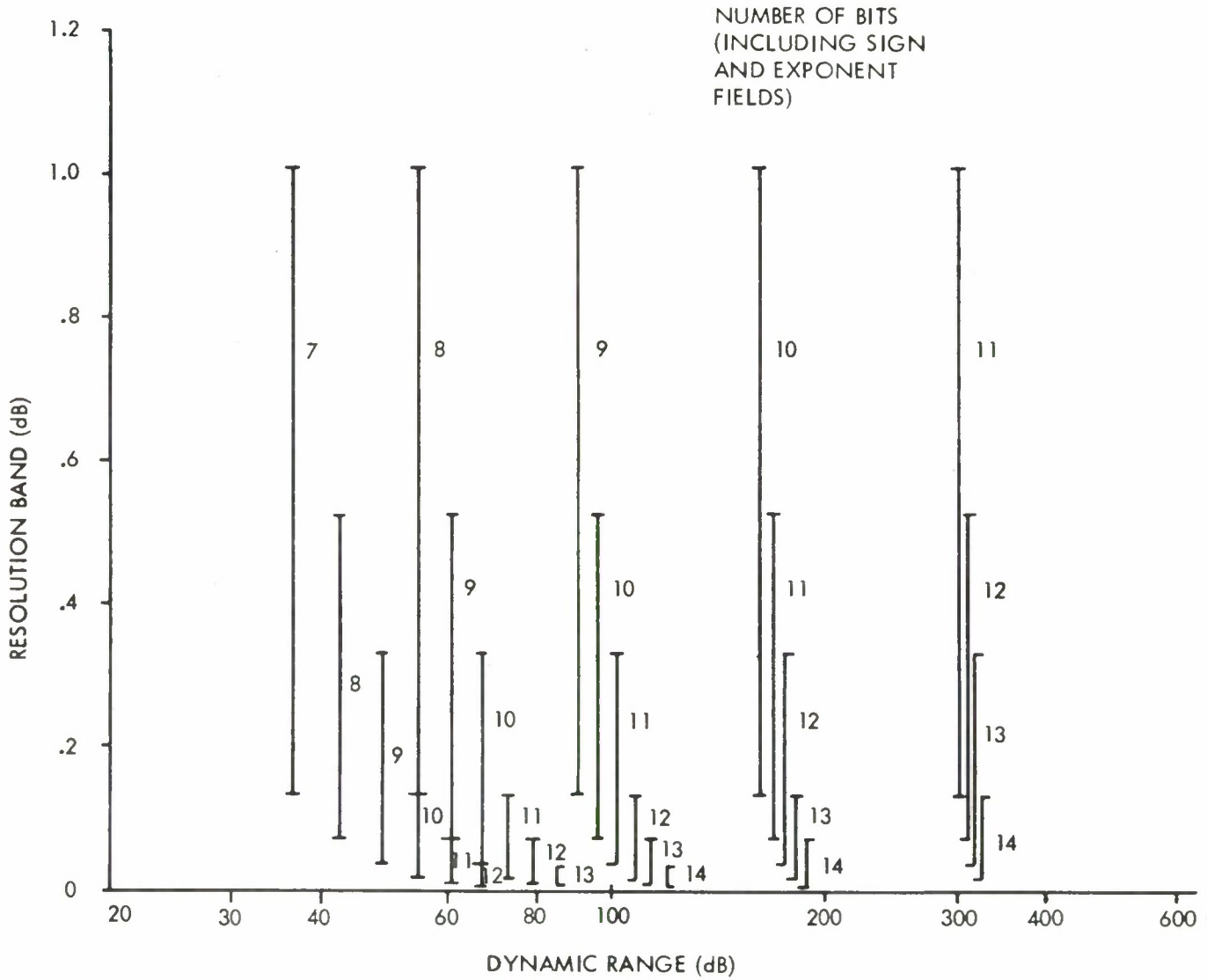

Figure C-11. Floating Point Base 8 - Encoding Characteristics

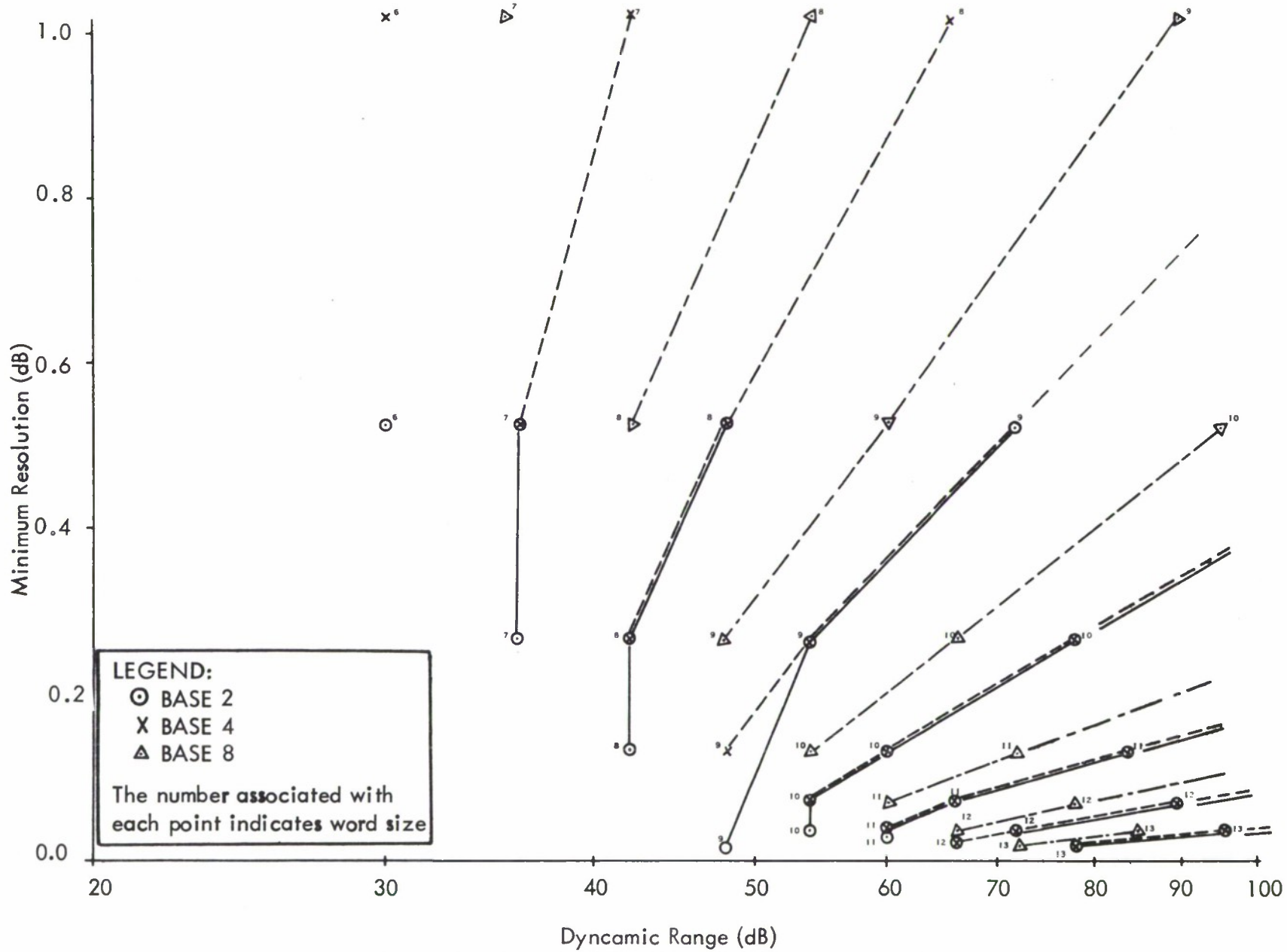

Figure C-12. Relative Encoding Characteristics

The most suitable selection for this specific application is base 4 modified floating point encoding. A 10-bit word is capable of representing a bi-polar value throughout a 78 dB dynamic range with a large signal resolution of 0.27 dB. The introduced quantization noise is at least 30 dB below the largest power of instantaneous signal or background noise, and 192 numerically illegal codes are available for fault signaling purposes. This technique is directly compatible with the present LASA instrumentation dynamic range, but no requirement for a quantum scaled 40 dB below the inherent noise is recognized. Since the processing techniques which attenuate the background noise are also effective on quantum noise, a rescaling by approximately 20 dB should be considered to extend the system's linear range to magnitude seven events. This recommendation is illustrated by Figure C-13, which also depicts the effective array resolution extension which prevails as a product of the beam forming process. Less than 0.01 dB of additional uncorrelated background noise is incurred at low levels, and even more extreme rescaling may be advisable when the subsequent processes are firmly established.

This communication concept extends the system performance while reducing the data rate to 100 baud per short period instrument. Signal analysis has demonstrated that the inner instrument ring of each LASA subarray can be deleted without adverse effects. Primary seismic data is then reduced to 39.9 Kb, and can be easily transmitted through the relatively economical Bell TELPIPE with an adequate 22 percent margin for secondary instrumentation and overhead. These techniques also illustrate the feasibility of employing voice grade lines for the data acquisition network coupling the subarrays.

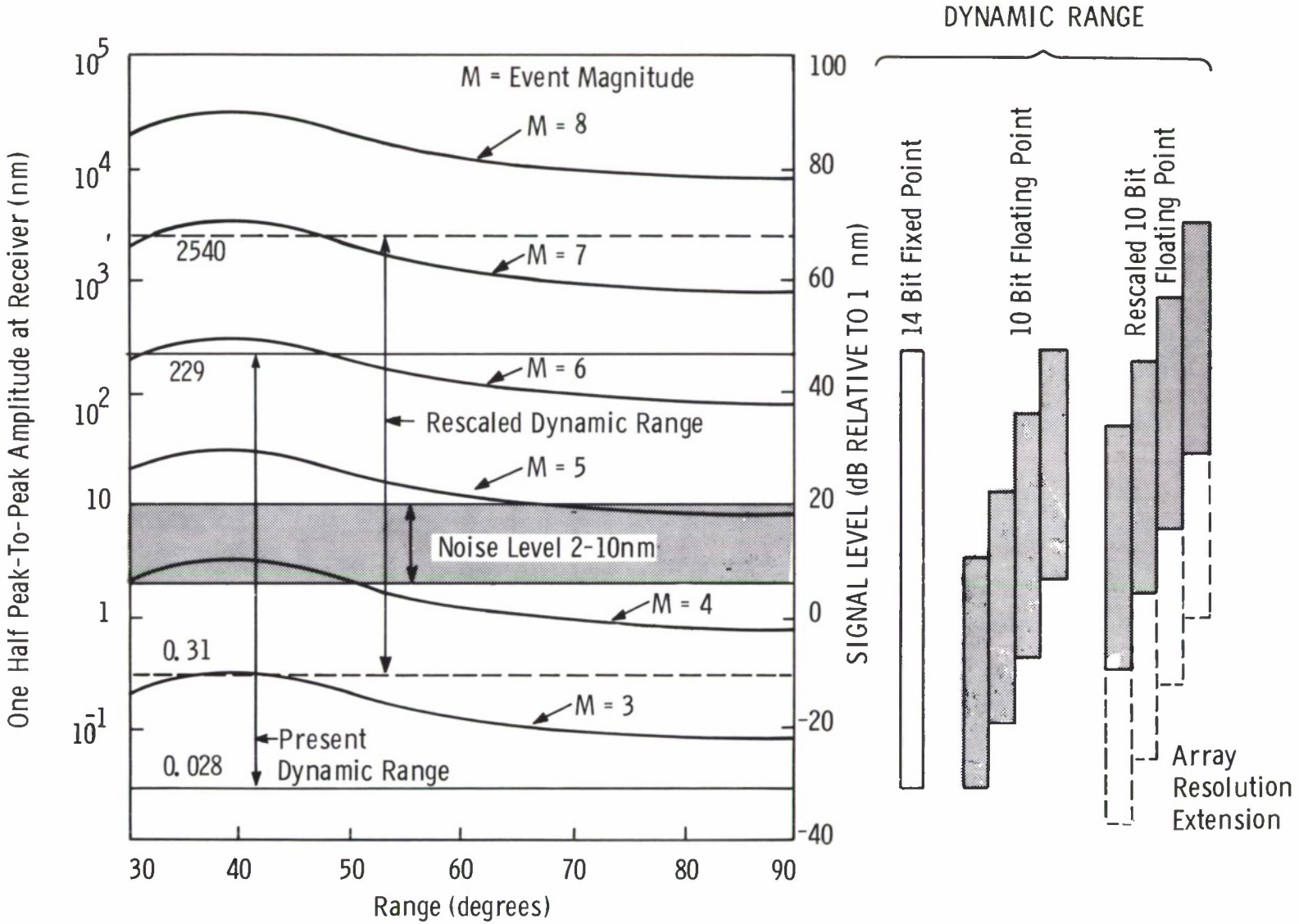

Figure C-13. Seismometer Digital Communications Scaling

Appendix D

DETECTION PROCESSOR SCALING

D.1 INTRODUCTION

Because of the finite word length limit in a digital computer, there are unavoidable errors due to quantization of the input, of the coefficients of the digital filters, and of the results of computation. A study of these quantization (or truncation) errors is important to ascertain the adequacy of implementation, to permit a prudent assignment of variable scaling, and to evaluate the numerical error present at each process node.

D.2 SCALING

The effects of quantization are modeled as additive random noise. These contributions are combined with the estimated data noise encountered at each stage of the Detection Processor, and the composite noise propagation is traced through the system. The results are in reasonable agreement with preliminary experimental observations.

D.2.1 Seismometer Data

The output of a single seismometer is digitized as a 13-bit word plus sign at a quantum level (Q) of 0.028 nm. The quantization error is assumed to be a random variable which is uniformly distributed and uncorrelated from sample to sample. Since two's complement representation is used within the computer, the quantization error bias (B) is $\frac{-Q}{2}$ and the variance is $Q^2/12$.

The natural background noise is observed to be a variable with zero mean and a standard deviation σ of approximately 3 nm, or roughly 100 times the

quantization level. The noise power due to quantization is therefore five orders of magnitude lower than the power due to the background noise, and the former may be neglected for further practical consideration.

Summarizing, at the seismometer level,

$$\begin{aligned} Q &= 2.8 \times 10^{-2} \text{ nm} \\ B &= -Q/2 = -1.4 \times 10^{-2} \text{ nm} \\ \sigma &= 3 \text{ nm} = 1.07 \times 10^{2}\, Q. \end{aligned} \tag{D-1}$$

D.2.2 Subarray Beamforming

Although the microcode for this process has the capability to scale down large magnitude inputs, it is not considered in this model. A prescaling right shift of five or fewer binary digits will not effect the process parameter selection. The subarray beamforming is carried out by properly delaying and summing the outputs of the 25 seismometers in the subarray. Since addition only is involved in this implementation, no other computational error is introduced.

At the subarray beam level, there is a gain in signal-to-noise ratio. For Longshot, the observed unfiltered subarray gain was 4.5 dB, or a factor of 1.68. This broad band apparent gain is utilized to estimate the residual noise at the conclusion of the process. Thus, at the subarray beam level,

$$\begin{aligned} Q &= \frac{2.8 \times 10^{-2}}{25} = 1.12 \times 10^{-3} \text{ nm} \\ B &= -1.4 \times 10^{-2} \text{ nm} = -1.25 \times 10\, Q \\ \sigma &= \frac{1.07 \times 10^{2} Q}{1.68} \times 25 = 1.59 \times 10^{3}\, Q \end{aligned} \tag{D-2}$$

D.2.3 Recursive Filtering

The filter selected for initial detection processor evaluation is a third order bandpass Butterworth formulation characterized by the parameters appearing in Table D-1.

TABLE D-1

FILTER CHARACTERISTICS

Parameter		Value
Sample Period	T	0.1 Seconds
Lower Corner Frequency	f_1	0.9 Hz
Upper Corner Frequency	f_2	1.4 Hz
Output/Input Bound Ratio	$\sum_{n=0}^{\infty} \lvert c_n \rvert$	1.59
Implementation Bias Magnification	$\sum_{n=0}^{\infty} d_n$	12.38
Implementation Noise Magnification	$\sum_{n=0}^{\infty} d_n^2$	3264.47

The filter function,

$$H(Z) = \frac{K\,(1 - Z^{-2})^3}{1 + b_1 Z^{-1} + b_2 Z^{-2} + \ldots + b_6 Z^{-6}} \quad , \qquad \text{(D-3)}$$

is obtained by implementing the difference equation in accordance to Figure D-1. Theoretical values of the coefficients are listed in the first column of Table D-2.

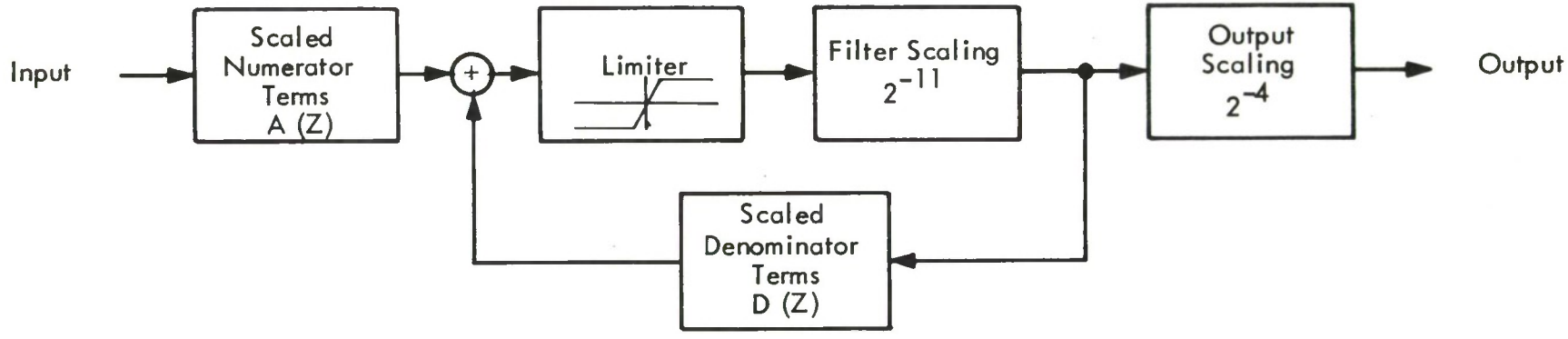

Figure D-1. Recursive Filter

TABLE D-2

FILTER COEFFICIENTS

Parameter	Value		
	Theoretical	Machine Scaled	Implemented
K	0.002898		3
b_1	-4.081417	-8358.74	-8359
b_2	7.955923	16293.73	16294
b_3	-9.092820	-18622.09	-18622
b_4	6.444996	13199.35	13199
b_5	-2.677543	-5483.61	-5484
b_6	0.532075	1089.69	1090

The scaling factor of 2^{-11} relating the theoretical and machine scaled values is implied by the objective to minimize the encountered quantization while accommodating the largest denominator coefficient (b_3) within the 15 bit fixed point computation word. Integer numbers must be employed to approximate the machine scaled values.

The effects of fixed point word saturation and the resulting phenomenon of limit cycles have been experienced during processor development. This may be prevented by sufficiently restricting the input so as to preclude an excessive output value. The output to input bound ratio corresponds to the sum of the magnitudes of the impulse response of the filter. In this instance,

$\sum_{n=0}^{\infty} |c_n|$ is 1.59, thereby establishing an input magnitude bound of

1.25×2^{14} quantum units if linear operation is to be assured. The filter

scaling coefficient (K) restriction is

$$K \leq \frac{0.002898 \times 2^{11}}{1.59} = 3.73$$

which utilizes input saturation to preclude saturation of the filter process. The largest permissable integer is 3, and thus the transfer function numerator is implemented as:

$$A(z) = 3 \times 2^{-11} (1 - Z^{-2})^3 .$$

This establishes a new quantization level (within the filter pass band):

$$Q = \frac{0.00112 \times 0.002898}{3 \times 2^{-11}} = 2.22 \times 10^{-3} \text{ nm.} \qquad \text{(D-4a)}$$

Figure D-2 is a plot of the filter response calculated with the theoretical coefficients. The response calculated with the implemented coefficients (Figure D-3) gives an almost identical curve that has been shifted downward as a result of scaling the numerator to prevent filter saturation. The normalized difference between the response curves is illustrated in Figure D-4.

Truncation errors encountered in the filter process contribute to the output noise level. Consider shifting a word of m digits right r places and then truncating to create an effective word length of m-r digits. The truncation error due to the right shift is equivalent to the difference between the prevalent quantization errors associated with the m bit and m-r bit word lengths. The bias and variance of the error component are related to the quantum level:

$$B_r = -(1-2^{-r}) Q/2$$

$$\sigma_r^2 = (1-2^{-2r}) Q^2/12,$$

where Q represents the quantization level after the right shift. The second term in each of the above expressions is negligible when evaluating the effects of the filter scaling shift (r=11).

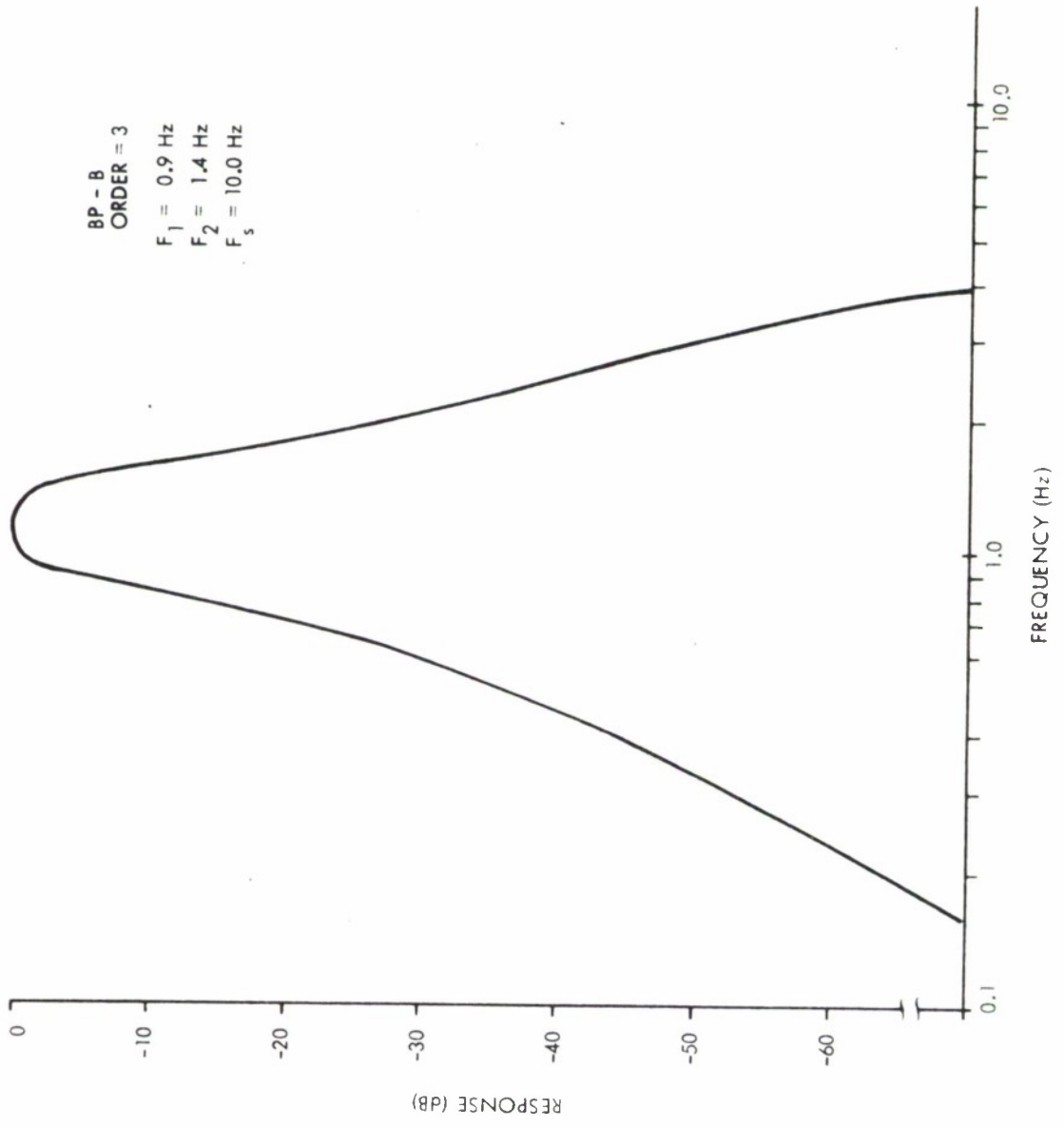

Figure D-2. Frequency Response for Theoretical Filter

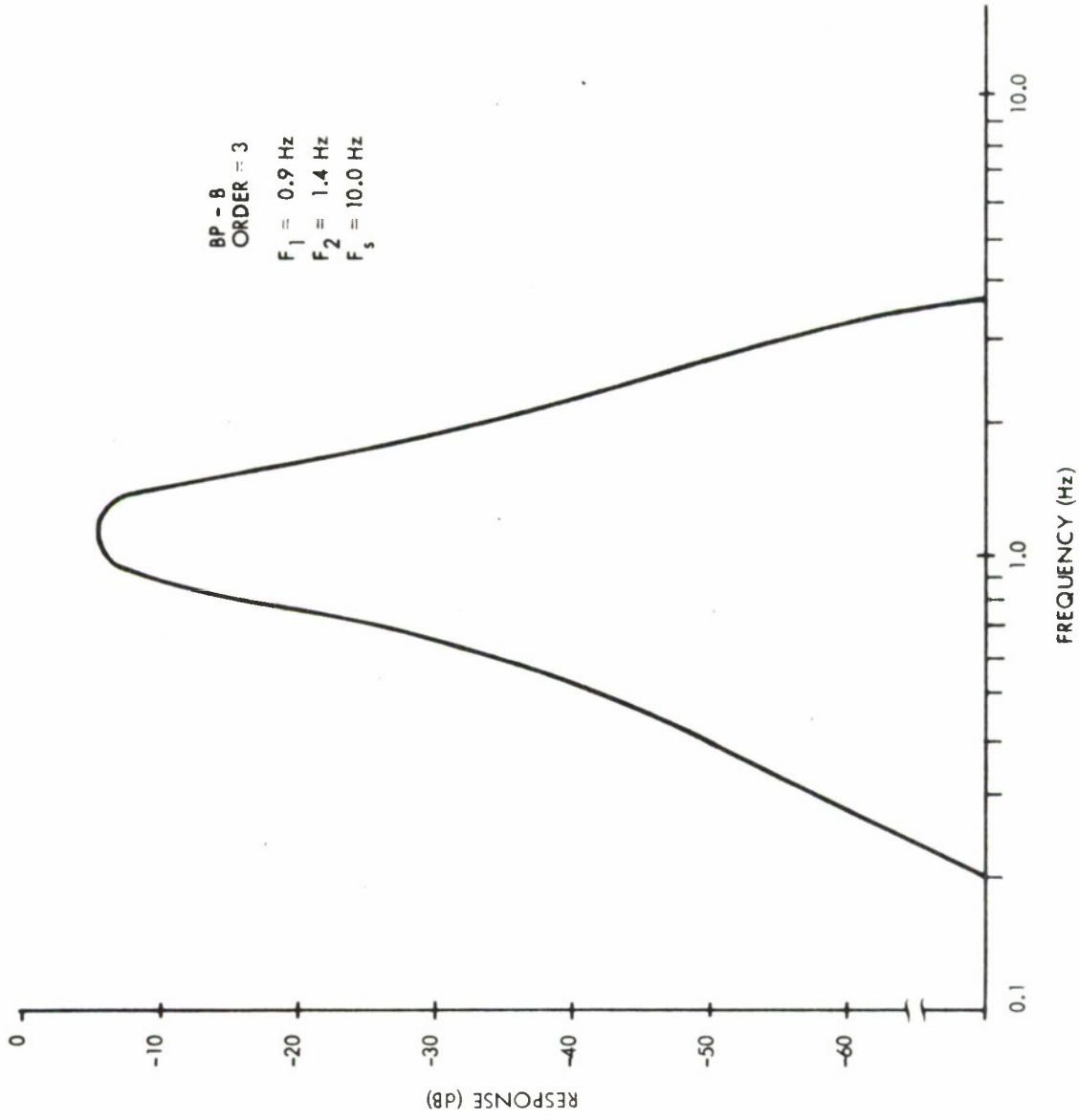

Figure D-3. Frequency Response for Actual Filter

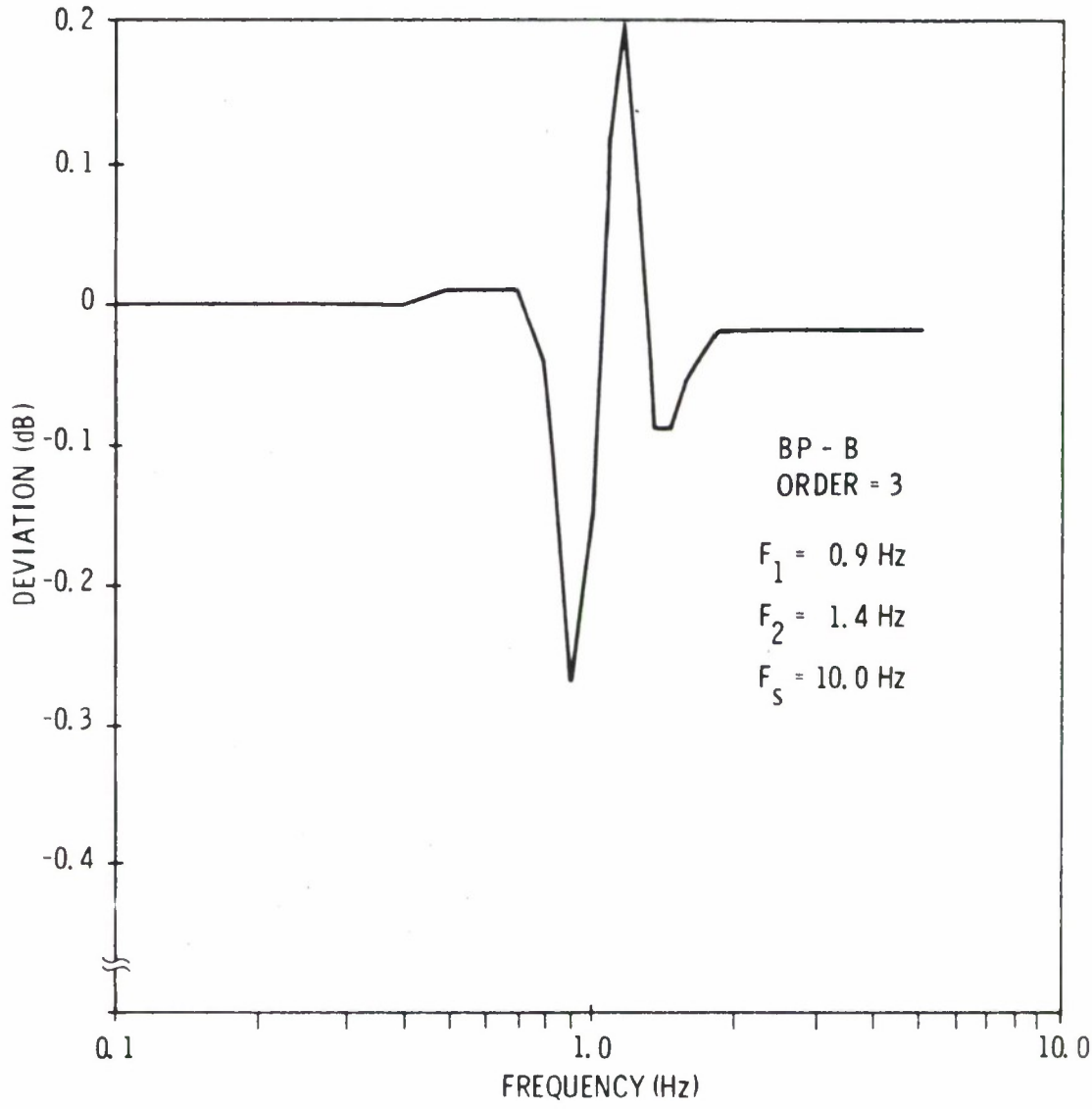

Figure D-4. Deviation of Frequency Response for Actual Filter from Theoretical Filter

Statistical characteristics of the truncation error generated in the filter recursive loop are:

$$B_F = (-Q/2) \sum_{n=0}^{\infty} d_n = -6.19\,Q$$

$$\sigma_F = \sqrt{(Q^2/12) \sum_{n=0}^{\infty} d_n^2} = 1.65 \times 10\,Q$$

where d_n is the unit impulse response of the filter denominator implementation. The errors are assumed to be uniformly distributed and uncorrelated from sample to sample.

No bias component is propagated through the filter since a null transfer relation exists at zero frequency, as is verified by the final value theorem:

$$\sum_{n=0}^{\infty} c_n = \lim_{Z \to 1} H(Z) = 0.$$

For Longshot, the observed gain in the signal-to-noise ratio in the recursive filter is approximately 18.5 dB, or an amplitude ratio of 8.35. To establish an output noise estimate, the signal is assumed to be coherent and the gain due entirely to noise reduction. The standard deviation of this propagated output noise component is:

$$\sigma_n = \frac{(1.59 \times 10^3\,Q)\,(1.12 \times 10^{-3})}{8.35\,(2.22 \times 10^{-3})} = 9.62 \times 10\,Q.$$

The composite noise output estimate can thus be expressed as:

$$B = -6.19\,Q$$

$$\sigma = \{(1.65 \times 10)^2 + (9.62 \times 10)^2\}^{1/2}\,Q = 9.8 \times 10\,Q \qquad \text{(D-4b)}$$

D.2.4 Filter Output Scaling

The output of the recursive filter is right shifted four bit positions so as to best match the dynamic range of the LASA beamformer and the preceding process. This alters the quantum level:

$$Q = (2.22 \times 10^{-3}) \times 2^4 = 3.55 \times 10^{-2} \text{ nm.} \qquad \text{(D-5a)}$$

Additional error is introduced by the shift, and the bias and standard deviation are now:

$$B = -\frac{6.19\,Q}{16} - \frac{Q}{2}(1-2^{-4}) = -8.56 \times 10^{-1}\,Q$$

$$\sigma = \sqrt{\left[\frac{(9.8 \times 10)Q}{16}\right]^2 + \frac{Q^2}{12}(1-2^{-8})} = 6.11\,Q. \qquad \text{(D-5b)}$$

D.2.5 LASA Beamforming

The LASA beams are formed from the delayed sum of 21 subarray beams. Again, there are only additions involved. The gain in LASA beamforming is approximately 11 dB, or an amplitude factor of 3.55.

$$Q = 3.55 \times 10^{-2}/21 = 1.69 \times 10^{-3} \text{ nm}$$

$$B = -(8.56 \times 10^{-1}) \times 21\,Q = -1.798 \times 10\,Q \qquad \text{(D-6)}$$

$$\sigma = \frac{6.11 \times 21\,Q}{3.55} = 3.61 \times 10\,Q$$

The predictable bias should be removed prior to rectification so as to minimize the post detection noise. This can be accomplished by implementing a 22nd input channel which inserts a compensating positive signal of 18 quantum units. The estimated residue is only 2×10^{-2} Q, or about 3×10^{-5} nm.

D.2.6 Rectification

A sum of absolute magnitudes is obtained for every mutually exclusive group of three successive samples, and this value is right shifted two bit positions. The subsequent quantum value is:

$$Q = \frac{4}{3} \quad (1.69 \times 10^{-3}) = 2.25 \times 10^{-3} \text{ nm.} \tag{D-7a}$$

Assuming a Gaussian distribution, the bias of the output of a full-wave linear rectifier with unity gain is evaluated as $\sqrt{\frac{2}{\pi}}$ times the standard deviation of the input when the mean is zero[11].

$$B = \frac{3}{4}\left(\sqrt{\frac{2}{\pi}}\right)\left(3.62 \times 10\, Q\right) = 2.17 \times 10\, Q. \tag{D-7b}$$

The standard deviation relationship is also evaluated as:

$$\sigma = \frac{3}{4} \quad (0.603) \quad (3.62 \times 10)Q = 1.64 \times 10\, Q. \tag{D-7c}$$

D.2.7 Short Term Average

An accumulation of three of the above groups corresponds to a 1.8 second short term window, which is consistent with the recommendations of the post-detection integration analysis[1]. This establishes the final output characteristics as:

$$Q = \frac{1}{3} \quad (2.25 \times 10^{-3}) = 7.5 \times 10^{-4} \text{ nm}$$

$$B = 3 \quad (2.17 \times 10)Q = 6.51 \times 10\, Q \tag{D-8}$$

$$\sigma = 3 \quad (1.64 \times 10)Q = 4.92 \times 10\, Q.$$

D.2.8 Long Term Average

The background noise level is estimated so as to permit the application of a floating threshold criterion. An 80-second history has been found necessary

to obtain consistent long term averages. An exponential filter of the form

$$H(Z) = \frac{2^{-\alpha}}{1-(1-2^{-\beta})\,Z^{-1}} \qquad \text{(D-9)}$$

has been implemented to preclude the requirement for maintaining such an extensive history within the processor. This is accomplished with the configuration shown in Figure D-5.

The factor $(1-2^{-\beta})$ represents the time constant of the exponential filter. Figure D-6 depicts the values of β versus time constant normalized to the sample period. β was chosen to be 6, which corresponds to a time constant of 113 seconds. The value of 1 was selected for α so that the bias error generated in the filter would alter the noise estimate by only 0.1 dB.

With this parameter set, the dc gain of the filter can be shown to be 32; and the quantization is:

$$Q = \frac{7.5 \times 10^{-4}}{32} = 2.34 \times 10^{-5} \text{ nm.} \qquad \text{(D-10a)}$$

Both internally generated noise and propagated noise are evident at the output. Their contributions are evaluated as:

$$B = 32\,(6.51 \times 10)\,Q - \frac{Q}{2}\sum_{n=0}^{\infty} d_n$$

and (D-10b)

$$\sigma = \sqrt{(4.92 \times 10Q)^2 \sum_{n=0}^{\infty} c_n^2 + \frac{Q^2}{12}\sum_{n=0}^{\infty} d_n^2}$$

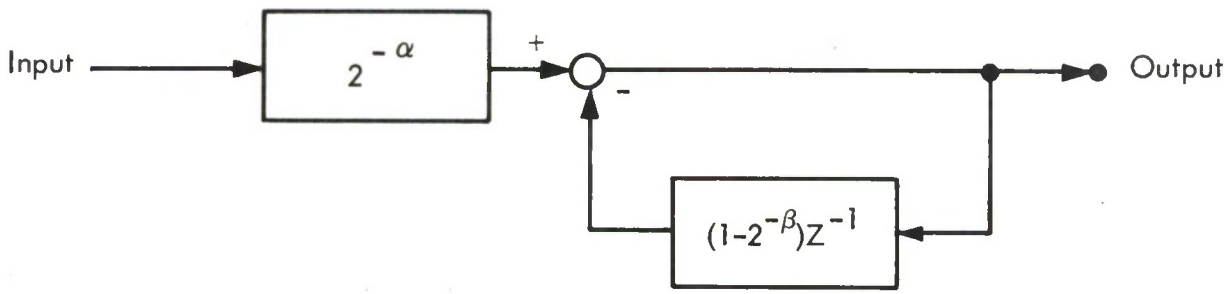

Figure D-5. Exponential Filter

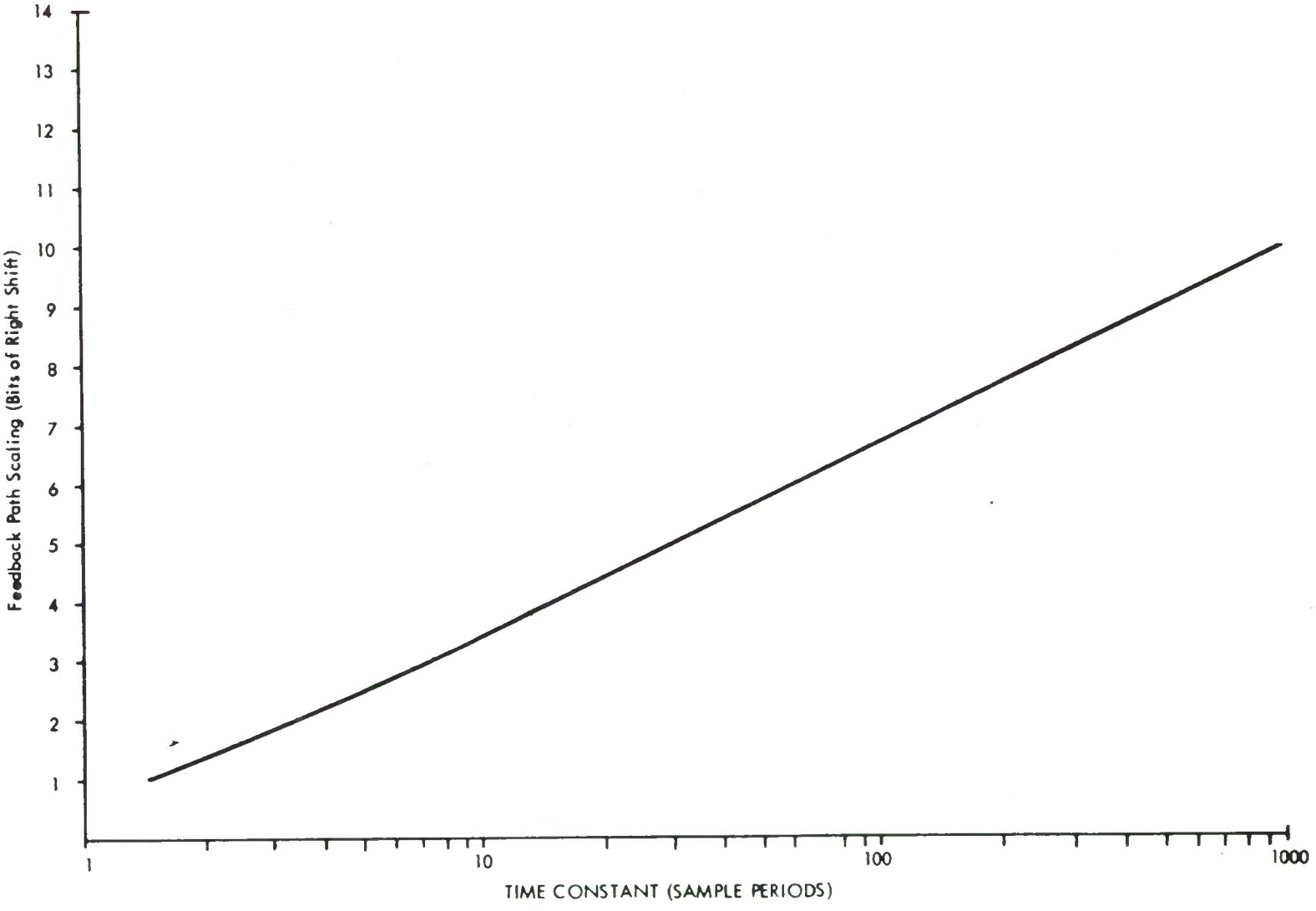

Figure D-6. Time Constant of Exponential Filter

where:

$$\sum_{n=0}^{\infty} d_n = 64$$

$$\sum_{n=0}^{\infty} c_n^2 = 8 \qquad \text{(D-11)}$$

$$\sum_{n=0}^{\infty} d_n^2 = 32$$

Thus, $B = 2.05 \times 10^3 Q$

(D-12)

and $\sigma = 1.39 \times 10^2 Q$

D.3 SUMMARY

These quantizations and errors for the Detection Processor implementation are summarized in Figure D-7. The standard deviations tabulated are based upon the noise measurements and gain performance measured for Longshot.

Detection Processor Scaling

LEGEND	PROCESS PARAMETERS			COMPOSITE NOISE	
	SAMPLING RATE	QUANTUM	SATURATION	BIAS	STANDARD DEVIATION
	SAMPLES PER SECOND	NANOMETERS	NANOMETERS	NANOMETERS	NANOMETERS
A	10	0.028	229	-0.014	3
B	10	0.00112	36.7	-0.014	1.79
C	10	0.00222	72.6	-0.014	0.22
D	5	0.00169	55.4	0	0.06
E	1.67	0.00075	24.6	0.048	0.037
F	0.55	2.34×10^{-5}	0.767	0.048	0.0033

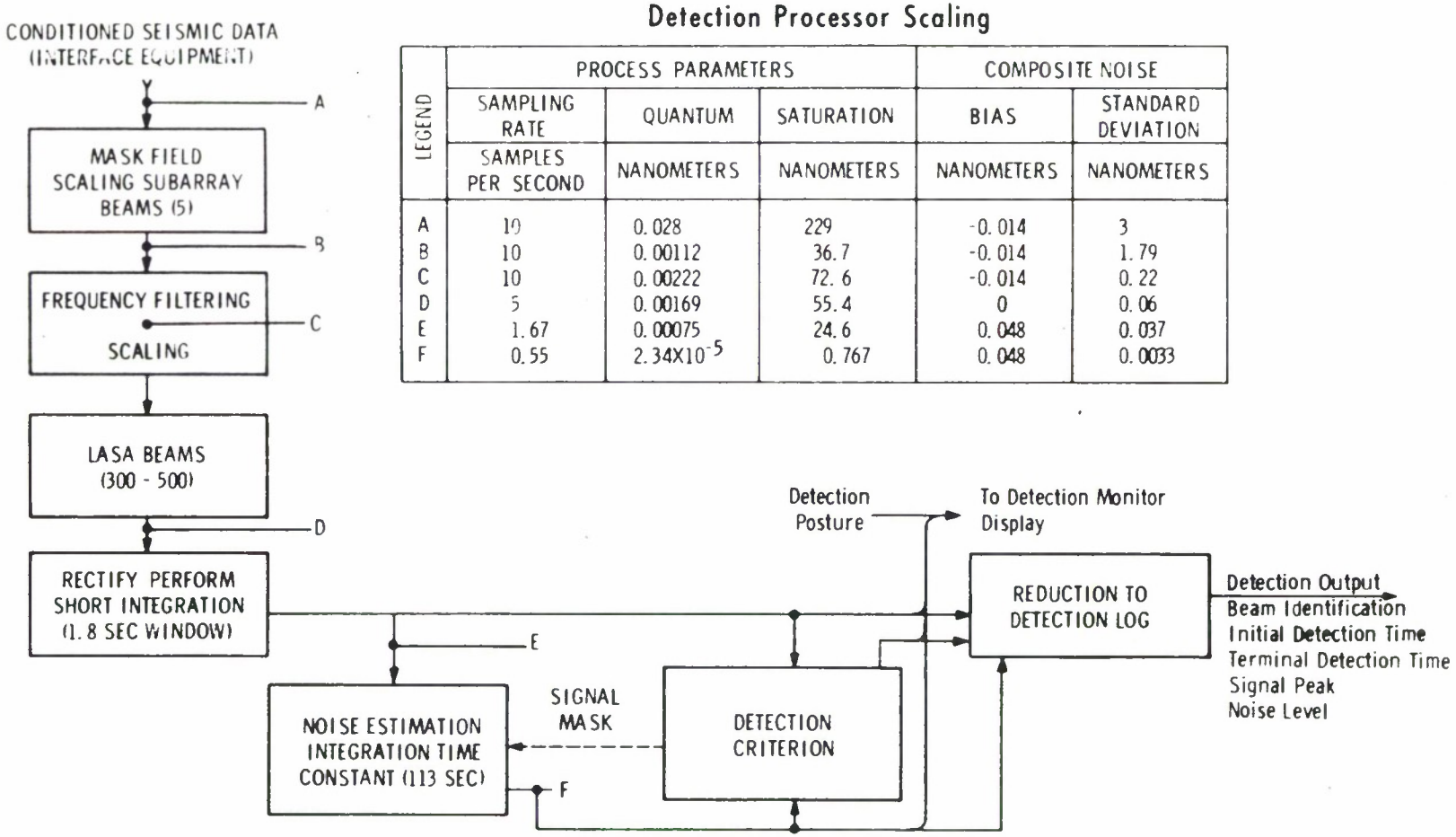

Figure D-7. Detection Processor Scaling

Appendix E

EXPERIMENTAL DISPLAY

To provide rapid recording of waveforms for support of studies during the experimental phases of the LASA Signal Processing system, a strip chart recorder interface is being added to the experimental display control unit. Simultaneous recording of multiple time-varying states for both detection and event processing during on-line operation will be possible.

The strip chart recorder will utilize the experimental display interface with the System/360 through the 2701 parallel data adapter. (See Figure E-1.) A maximum of eight output channels will be available, and data recording will be performed at a faster than real-time rate. In addition, start and stop of the paper transport will be under control of the CPU. Waveform identification, starting time, scaling, and time interval can be provided prior to each record with a binary coding. The width of the time interval pulse represents a known time record while the amplitude represents a known input magnitude. By shifting the magnitude of the time interval pulse the same as data, a known amplitude reference is provided. An example of a typical recording is shown in Figure E-2.

A data buffer consisting of the following information has been defined: display indicator half-word, channel identification sequence, starting time sequence, time interval pulse, followed by waveform intensities arranged sequentially for each time sample. This buffer sequence is shown in Figure E-3. The high order byte of the indicator half-word (bits 0 thru 7) is used to start the strip chart recorder paper transport and indicate the number of channels being recorded. This information is used to control the data timing. Once the

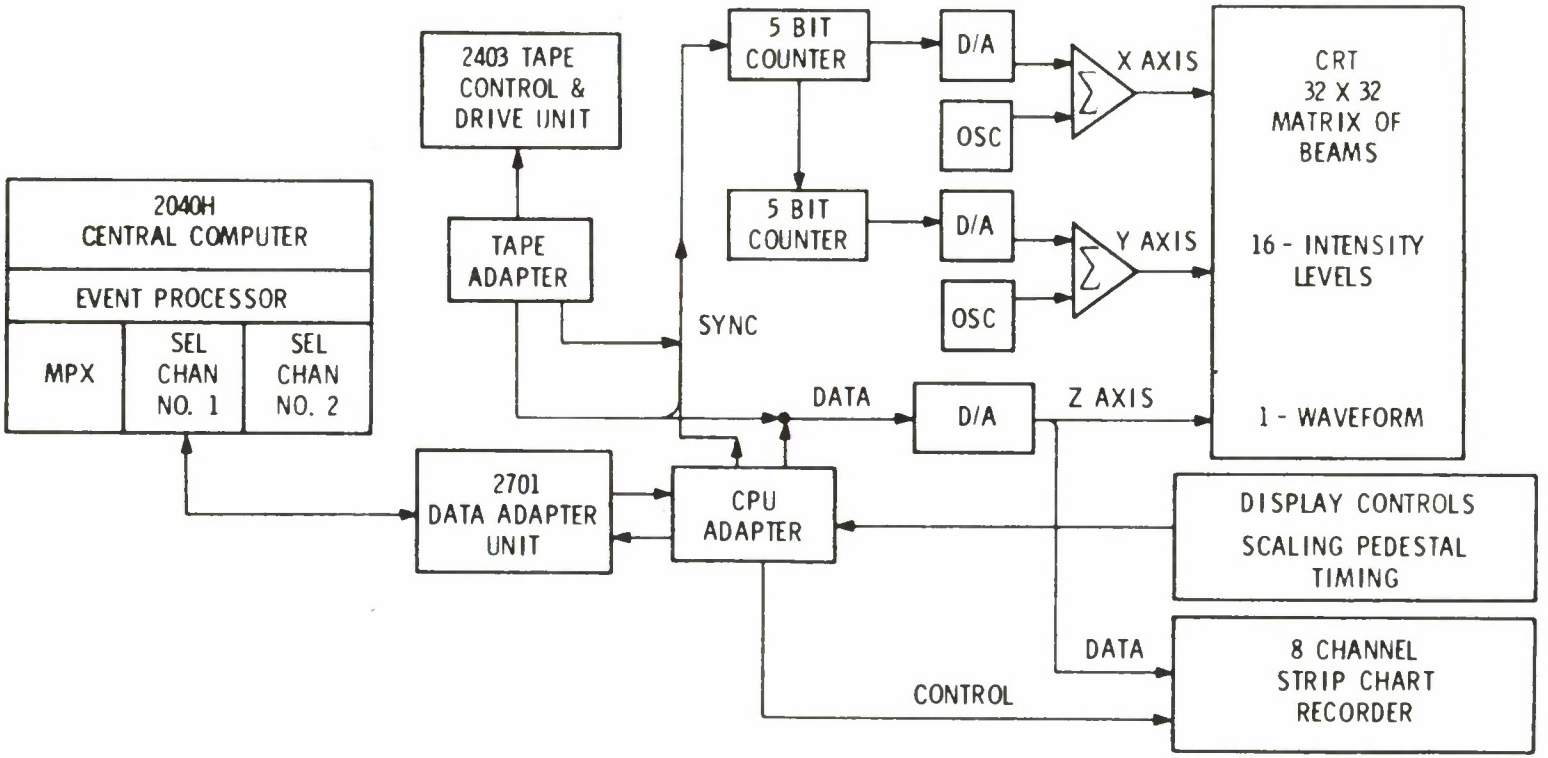

Figure E-1. Experimental Display

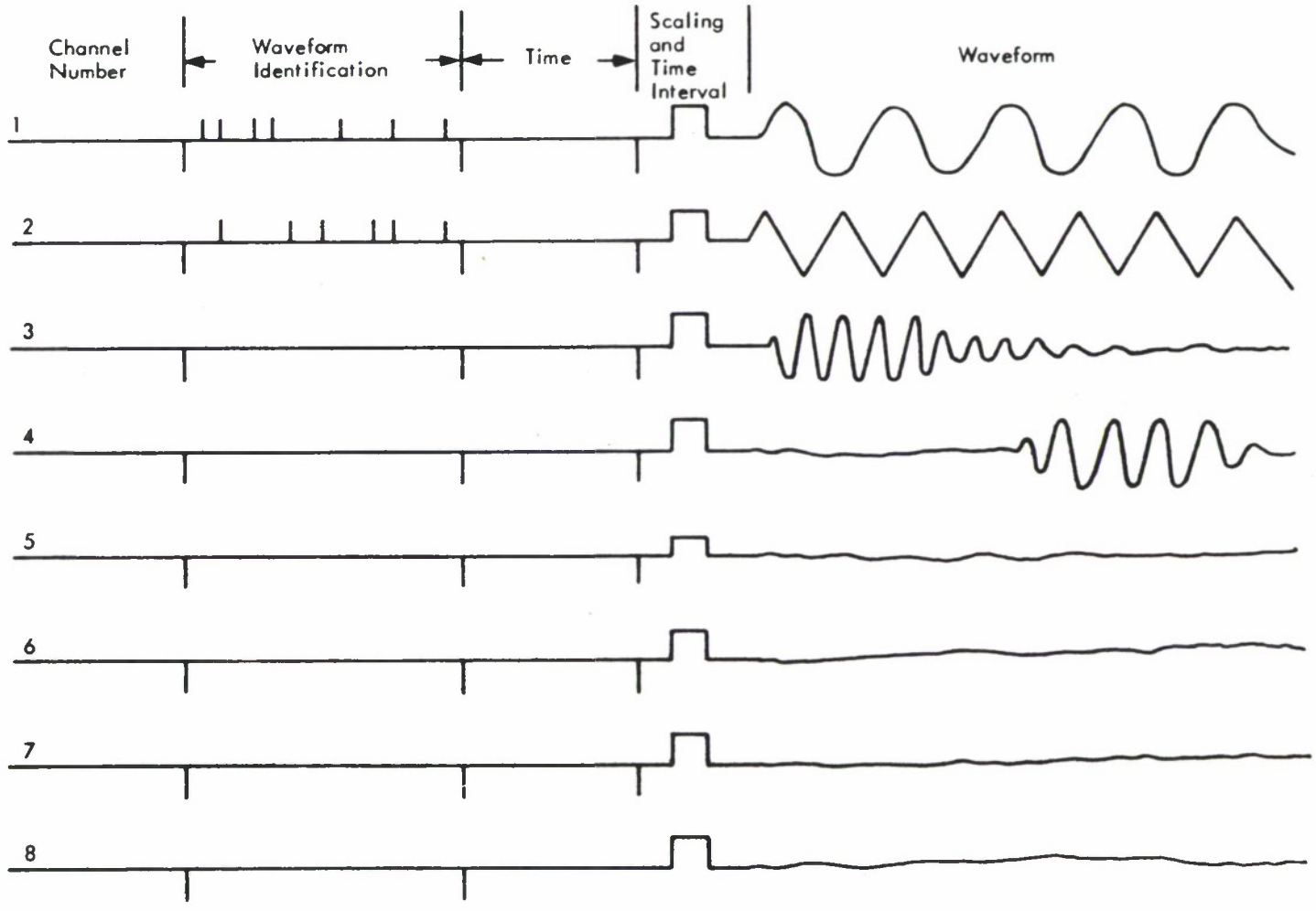

Figure E-2. Illustrative Strip Chart Record

Indicator Halfword

Start Mark Channel #1
"
"
Start Mark Channel # (8 max)

Start Mark Sequence

Zero Value #1
"
"
Zero Value # (8 max)
Bit 0 Channel #1
Bit 0 Channel #2
"
"
Bit 0 Channel # (8 max)
"
"
"
Bit 15 Channel #1
"
Bit 15 Channel # (8 max)

Channel Identification Sequence

Start Mark Sequence
Time Sequence
Time Interval Pulse Sequence
10 Zero Value Sequences
Data Sample T1 Channel #1
Data Sample T1 Channel #2
"
"
Data Sample T1 Channel # (8 max)
Data Sample T2 Channel #1
"
"
"
Data Sample T_n Channel # (8 max)

DATA FORMAT

0	1 2 3 4 5 6 7 8 9	10-15
SIGN	Amplitude Data Two's Complement Format	Not Used

INDICATOR HALFWORD FORMAT

0	1 2 3	4 5 6 7	8-15
START CHART	No. of Chan-nels	Not Used For Control Indicator Only	Not Used

Figure E-3. Data Buffer Sequence

data transfer has been started, the operation continues as a background program with data transfer under control of the interface timing. The number of half-words indicated in the indicator byte is transferred in a burst at a rate of approximately 200K bytes per second. After transmission of the last half-word in the burst, the 2701 control unit will not respond that it has received the data until it is time to transmit a new burst of half-words. The time between transmitting bursts must be sufficient to permit the strip chart recorder writing pen to respond to the change. The operator will be able to control the time between the start of the bursts in discrete steps from 8.33 milliseconds to 0.2 seconds. For records with low sample rates, recording time will be much faster than real data time. As an example, a two minute record with a sample rate of five samples per second and a recorder setting for an interval between the start of data bursts of 25 milliseconds would require 15 seconds to record. The record time is independent of the number of waveforms recorded (1 through 8).

Initiation of a strip chart recording operation requires the presence of a data buffer, selection of the strip chart recorder mode, setting the scaling control and activating the interrupt pushbutton on the display control panel. An ATTENTION is presented to the CPU, which shall respond by scanning the display control settings. When scaling is required, the data in the data table (all except the indicator half-word) is shifted left the required number of bit positions while retaining the proper sign for the data. If the scaling results in overflow of data bits, the magnitude is set to its maximum value while retaining its original sign. This shifted data is used to assemble a new data table for recording. The original data table is retained in case the operator requires a different scaling setting for data that has overflowed in the scaling operation. After completion of the scaling operation, the CPU initiates a WRITE operation. If the operator changes a control setting during the write operation, the CPU will receive a DEVICE END and ATTENTION status from the 2701 control unit. The CPU initiates a READ operation for scanning the control settings, performs the necessary scaling, and restarts the data transfer

from the beginning of the new data buffer. The display control operation has been previously described in conjunction with the beam display operation[5].

The selection of the waveforms being displayed, starting time for the data buffer, and generation of the original data buffer are under control of another I/O device. All seismometers, subarray beams, LASA beams, and other desired waveforms will be assigned an identification number to be used for selection and record identification. If data being presented has been recorded at different sample rates on the data tape, the data buffer is generated to correspond to the highest sample rate with either the value at the last sample time or an interpolated value inserted for time periods where data does not exist.

Appendix F

ARRAY-PROCESSING DESIGN SYNTHESIS

F.1 INTRODUCTION

The purpose of this appendix is to identify an array-processing design synthesis procedure upon which an experimental data measurement plan can be based. Using the limited data base processed at this time, certain key system design parameters can be measured and used to determine expected system performance.[1,2,3,4]

It is intended to extend the synthesis procedure presented here, unify the approach, and provide substantially more experimental verification. In addition, a cost analysis along the lines suggested herein is under study and may be integrated to relate cost trade-offs to system performance. In this manner, an array-processing synthesis technique can be developed pertinent to overall system objectives, optimally configured to take advantage of cost trade-off's, and expressed in terms of measurable variables to enable experimental verification.

F.2 THEORETICAL CONSIDERATIONS

The communications requirements, system gain, and location accuracy are of interest to large seismic array-processing design synthesis.

F.2.1 Data Transmission

The dynamic range of field instruments seldom exceeds 50 dB, and the ratio of resolution to dynamic range is usually about 1 percent. In the case at hand, we are interested in a dynamic range of well over 70 dB and a resolution

of the order of 1/4 dB. Since the instruments will, in all probability, be remotely located, a data transmission system will be required. Generally speaking, it is desirable to reduce the data rate (bits per second) to a minimum value while maximizing channel loading within available capacity.

The dynamic range of a floating point modulo 4 communication channel and the word length requirement for several values of resolution are discussed in Appendix C. This data formatting technique is easily coded and decoded and can be supported over standard voice grade telephone lines. It is noted from Figure F-1 that a 10 bit data word length will yield a dynamic range of about 78 dB with a resolution of approximately 1/4 dB. From the spectral density data shown in Section F.3.3, it is reasonable to suggest a sampling rate of 10 Hz, which is over three times the frequency where the signal is 30 dB down from its maximum value.

If one allows 20 percent of the channel capacity for low frequency sensors (e.g., long-period instruments, etc.), synchronization and framing, error coding, and parity, the data rate is:

$$R = 120N \text{ bits/second,} \qquad \text{(F-1)}$$

where N is the number of short-period sensors. Selecting the 2400 baud line as a typical voice grade line, one might consider the smallest instrument-converter-communications component group as 20 short-period instruments sampled at 10 Hz and several low frequency sensors whose aggregate data rate is less than 200 bits/second. By employing many identical groups, design costs are minimized and a direct measure of sub-system costs becomes available in terms of a system performance parameter.

F.2.2 Gain

Consider an array of sensors in which it is desired to steer many conventionally [1,2] formed beams. Let $x_n(t)$ be the output of the n^{th} sensor, then the m^{th} beam output is:

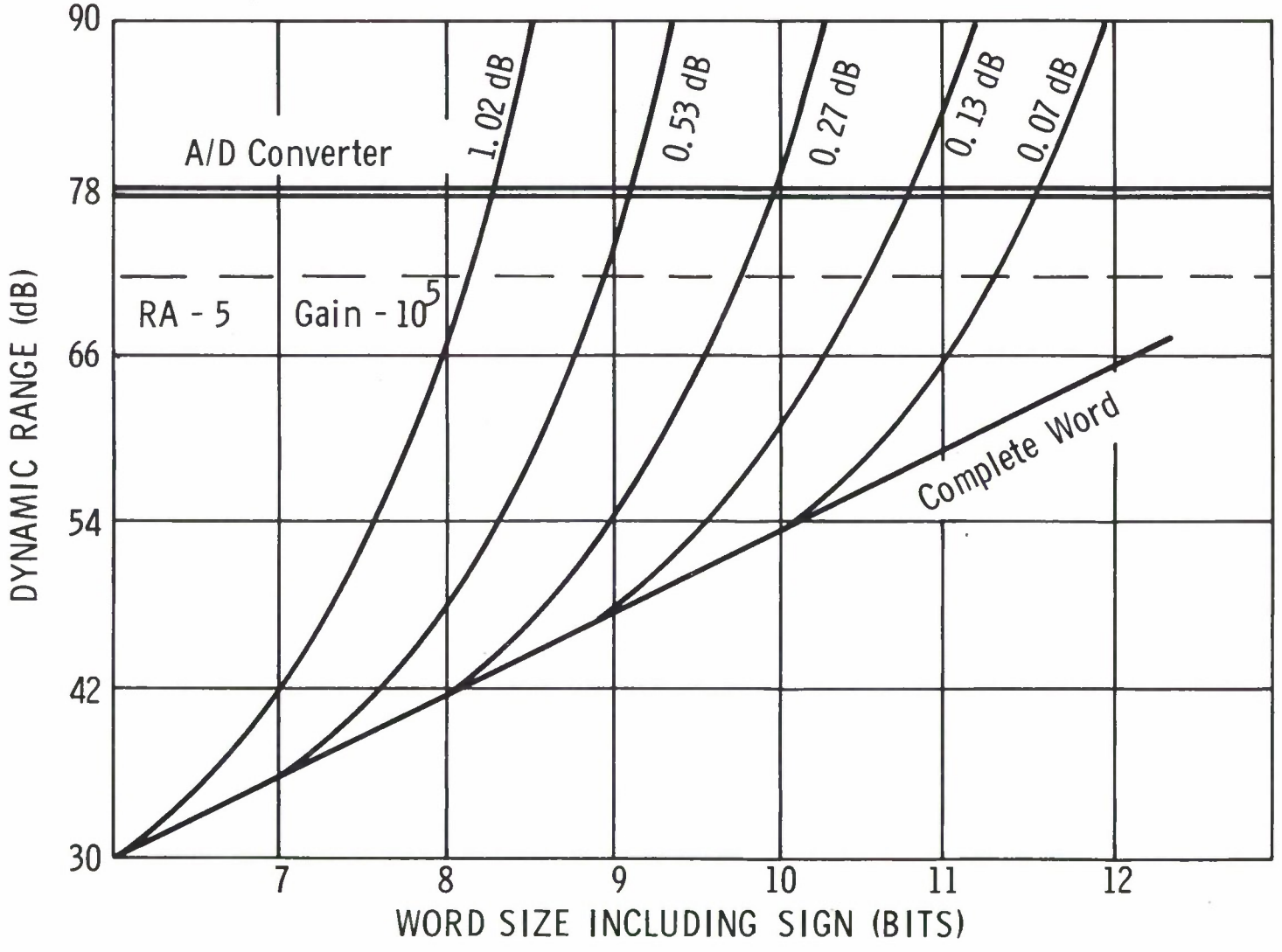

Figure F-1. Modified Floating Point—Data Encoding Modulo 4

$$B_m(t) = \frac{1}{N}\sum_{n=1}^{N} x_n(t + \tau_{mn}), \qquad \text{(F-2)}$$

where N is the number of sensors in the array and τ_{mn} is the time delay. Defining gain as the ratio of the average signal power to the average noise power of the beam output divided by the ratio of the average signal power to the average noise power at a sensor, it can be shown that:

$$G = 10 \log_{10} \frac{1+ (N-1)\ \rho_s}{1+ (N-1)\ \rho_n} \text{ dB}, \qquad \text{(F-3)}$$

where ρ_s and ρ_n are the average signal and noise correlation coefficients, respectively.

Equation F-3 is depicted in Figure F-2 for several values of ρ_n as a parameter. First note that only when ρ_n is very small does the denominator of Equation F-3 approach unity (e.g., neglect trivial case). On the other hand, when $\rho_s = 1/2$, a loss of an additional 3dB is incurred.

Using the classical assumption, that is, the signal is correlated ($\rho_s = 1$) and the noise is uncorrelated ($\rho_n = 0$), Equation F-3 reduces to:

$$G = 10 \log_{10} N \text{ dB}. \qquad \text{(F-4)}$$

Unless the noise correlation is small, indiscriminant addition of instruments will not always yield more gain. A more general relationship and perhaps one that would be more directly applicable to array synthesis is the dependence of the correlation coefficient on element spacing.

Let us further assume that we desire to place a large number of elements in a given space such that we are interested in noise correlation coefficients of the order of 10^{-2}. Using the standard deviation as an indication of the quality of the measurement, it can be shown that:

$$\sigma_n = \sqrt{\frac{1}{2WT}}, \qquad \text{(F-5)}$$

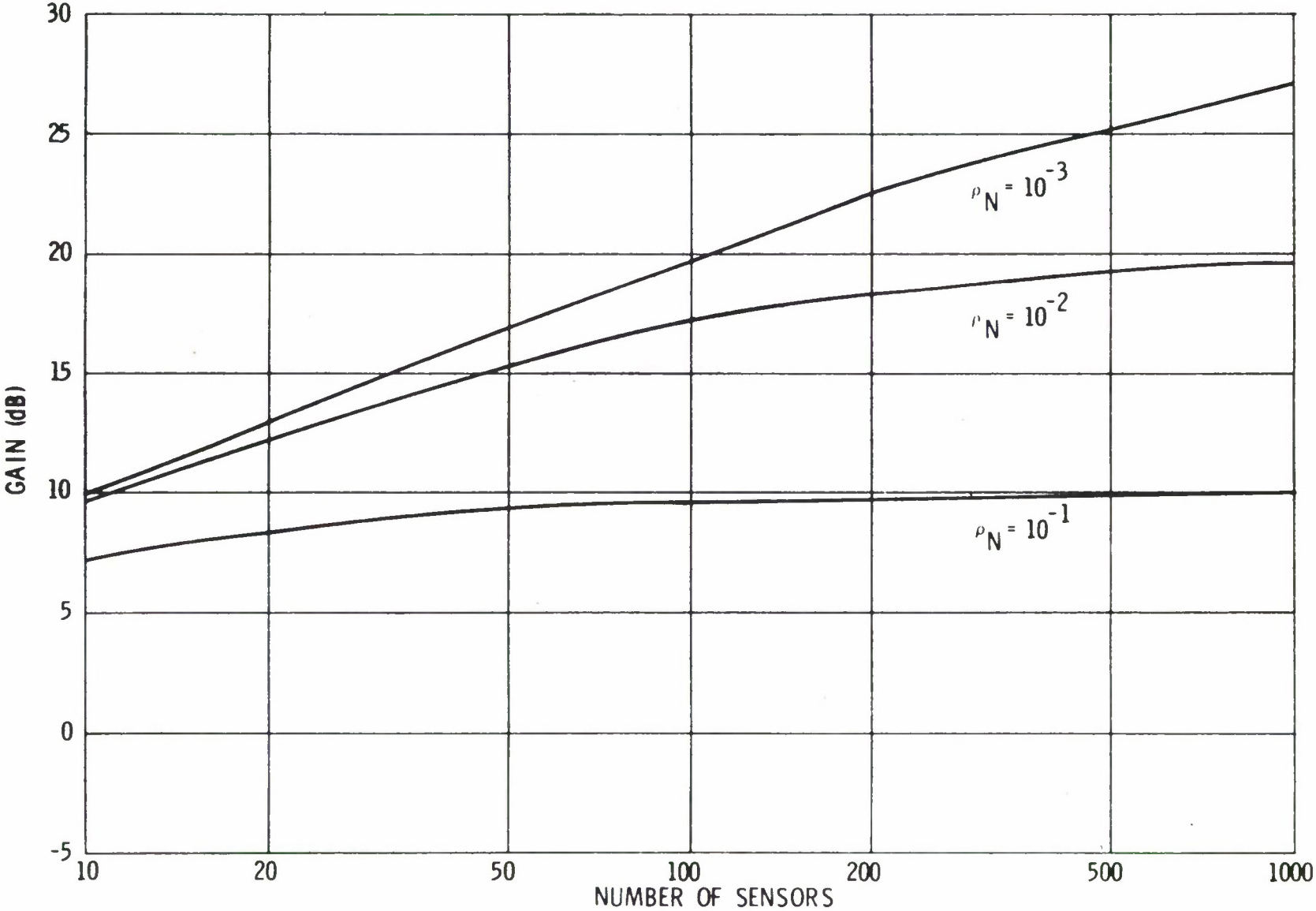

Figure F-2. Array Gain

where W is the noise bandwidth in Hz and T is the record length in seconds. From the spectral estimates presented in Section F.3.3, we select W = 1/2 Hz. If σ_n is to be less than the value of ρ_n, we require a minimum record length of almost three hours.

In order to use pair-by-pair correlation to obtain the average correlation coefficient, the effects of directional noise must be considered. In view of this and the aforementioned restrictions, it seems reasonable to suggest that correlation measurements be compared to gain measured directly by conventional beamforming and average power techniques.

F.2.3 Sampling

In Section F.2.1, it is suggested that a sampling rate of 10 Hz would be adequate. Since data reconstruction techniques permit extension of the effective sampling rate, high frequency data can be retrieved with little error. (See Appendix C.) Since this procedure would not be applied on a routine basis in an operational sense, it would be reasonable to sample at a rate commensurate with the real-time requirement. The loss in conventional processing gain as a result of sampling[1] is:

$$\bar{G}_1 = \frac{5 \log_{10} e}{6} (2\pi f \Delta T)^2 \text{ dB}, \qquad \text{(F-6)}$$

where f is the signal frequency in Hz and ΔT is the sample period in seconds. Equation F-6 is depicted in Figure F-3. When the signal frequency is less than 1.5 Hz, a loss of less than 0.5 dB is incurred when the sensors are sampled at 10 Hz.

F.2.4 Time Delays

Conventional beamformed array processing requires that the time delays τ_{mn} employed in Equation F-2 be determined for the teleseismic surveillance region between 0.04 sec/km and 0.08 sec/km.

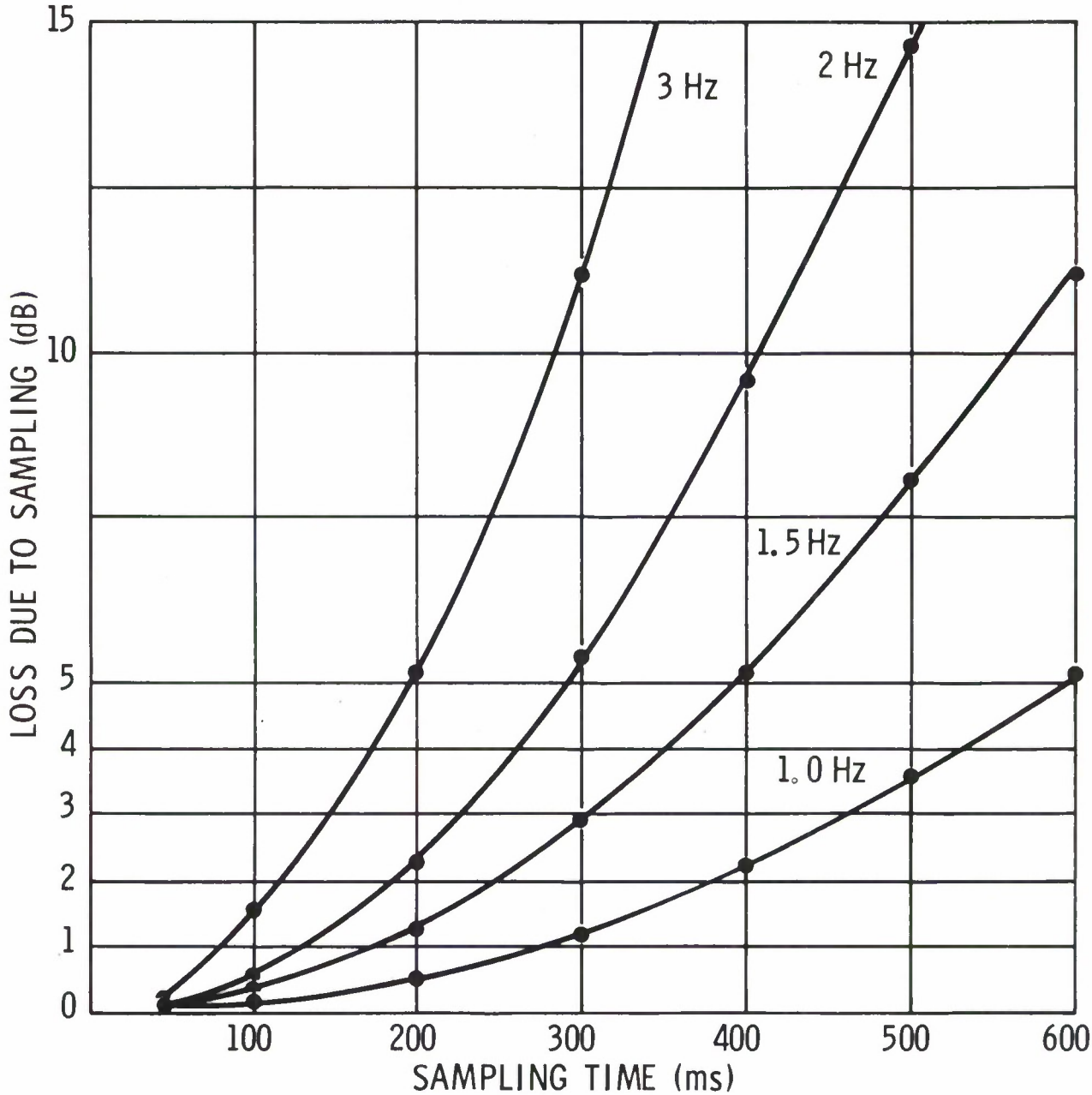

Figure F-3. Sampling Loss

These delays will be, in general, non-planar functions of both range and azimuth, and it is planned to employ existing data to establish the initial time delay library. Through system usage, the library will be updated and improved. Interpolation between regions for which data exists or admittance of events whose origin is not in the teleseismic region may reduce the number of calibration events required. Through a knowledge of event hypocenter, the data base for the inverse velocity space to geographic coordinate conversion can be developed.

This procedure separates array phasing and event location into two tasks. Measurement of phase speed in inverse velocity space yields the appropriate time delays through the wave front approximations. The geographic event location is then obtained by conversion from inverse velocity space by appropriate tables. The absolute location accuracy is dependent upon the assumed model, which can only be improved through calibration.

An error in the time delay, therefore, has two distinct effects. First, the beam is defocused and a loss[3] is incurred:

$$\bar{G}_2 = (10 \log_{10} e)\ (2\pi f \sigma_T)^2 \text{dB}, \qquad \text{(F-7)}$$

where f is the signal frequency in Hz and σ_T is the standard deviation of the steering error in seconds. Equation F-7 is depicted in Figure F-4.

Referring again to the spectral density estimates in Section F.3, we note that little signal energy is received above 1 Hz. Using the 1 Hz curve and limiting the loss to 1 dB, the total steering (including wave front approximations) standard deviation error must be less than 75 ms. For regions where this is not possible, the loss manifests itself as beam defocusing and array performance is degraded. It is also pointed out that the steering delays error may be dependent upon array aperture and no attempt has been made here to take this additional loss into account.

The second effect is the uncertainty in event location. The relative accuracy of the event location process can be described in terms of the system's

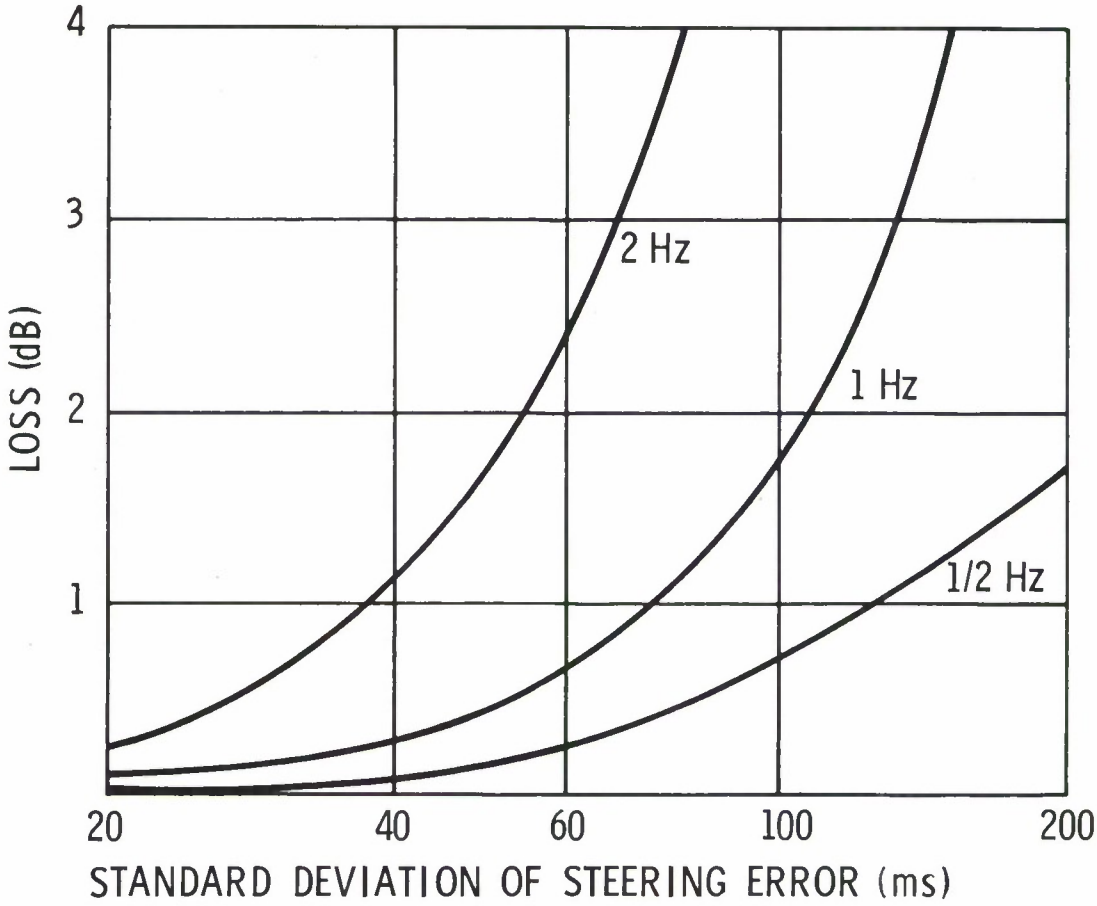

Figure F-4. Phasing Loss

ability to measure time in a noise background and the array aperture. Under Gaussian assumptions for the noise background and statistical independence of noise at the elements, it can be shown that the root mean square of the relative location error for a typical range angle of 58^{o} (6400 Km) is:

$$L \cong \frac{10^5}{\pi f R_E} \sqrt{\frac{1}{2WT} \cdot \frac{1}{S/N}} \text{ Km}, \qquad \text{(F-8)}$$

where f is the signal frequency, R_E is the radius of the circular array and WT is the gain-bandwidth product.

In order to assess the absolute location accuracy in a form suitable for experimental evaluation, Equation F-8 should be extended to take into account signal decorrelation and k-space to geographic conversion bias effects. It is pointed out that these bias errors appear experimentally inseparable and are only minimized through calibration. Their contribution to the location error has not been taken into account herein.

F.3 EXPERIMENTAL RESULTS

The experimental data used in this section was taken from LASA. It is presented to demonstrate the utilization of the theory, to indicate the feasibility of the processing concepts hypothesized in Section F.4, and to depict how the results of field tests may be used to predict expected array-processing system performance. Although the data sample is extremely small, it is believed to be typical and representative of prevailing conditions at LASA.

F.3.1 Gain

For the particular array geometry of LASA, several of the subarrays may be combined to yield many different array configurations. Using selected instruments, the validity of the classical conventional processing gain formula ($10 \log_{10} N$) can be experimentally verified for varying conditions. Depicted in Figures F-5 and F-6 (solid lines) is the conventional processing loss as a function of the number of LASA sensors utilized for three array apertures (20,

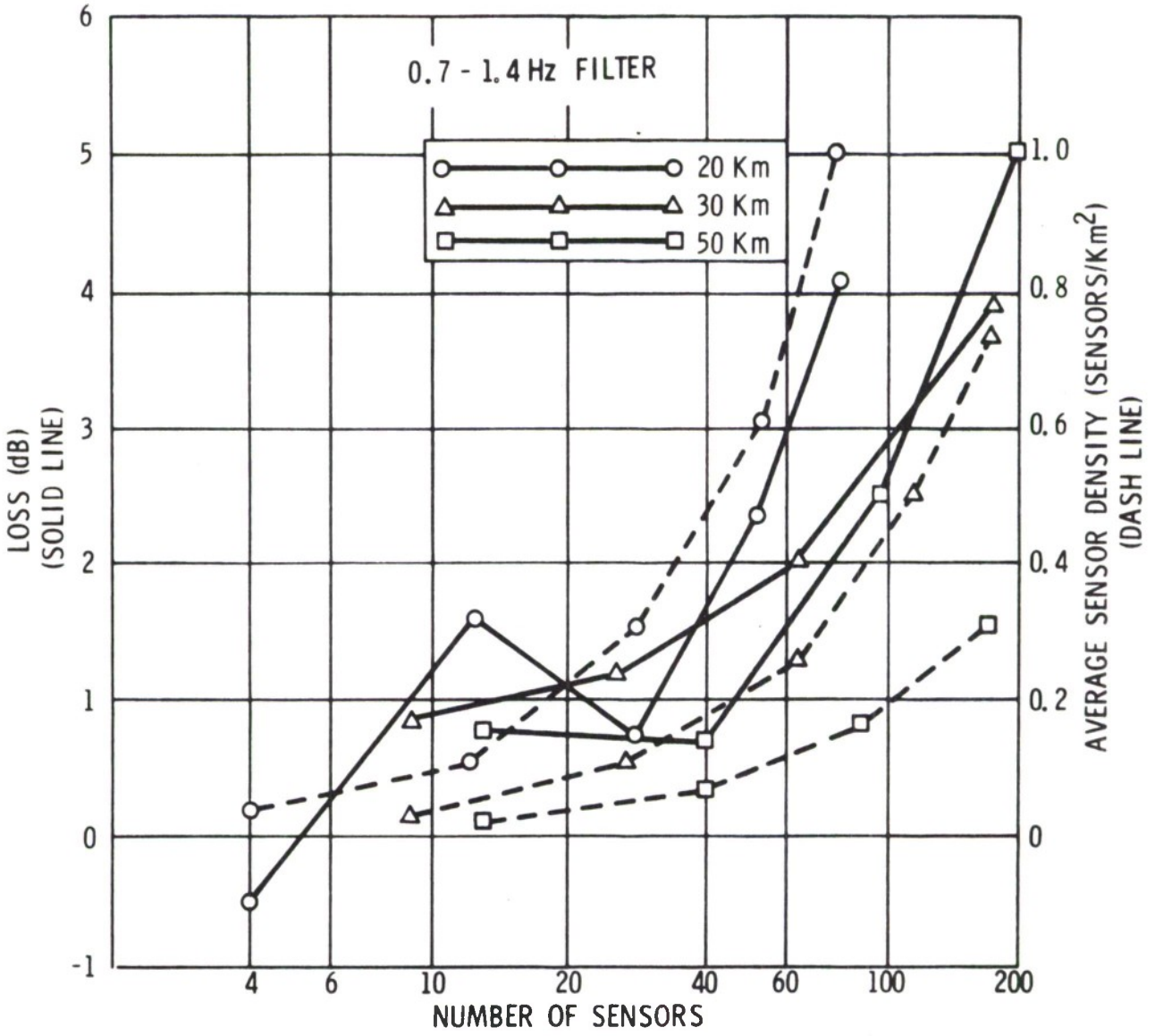

Figure F-5. Conventional Processing Loss (0.7 - 1.4 Hz)

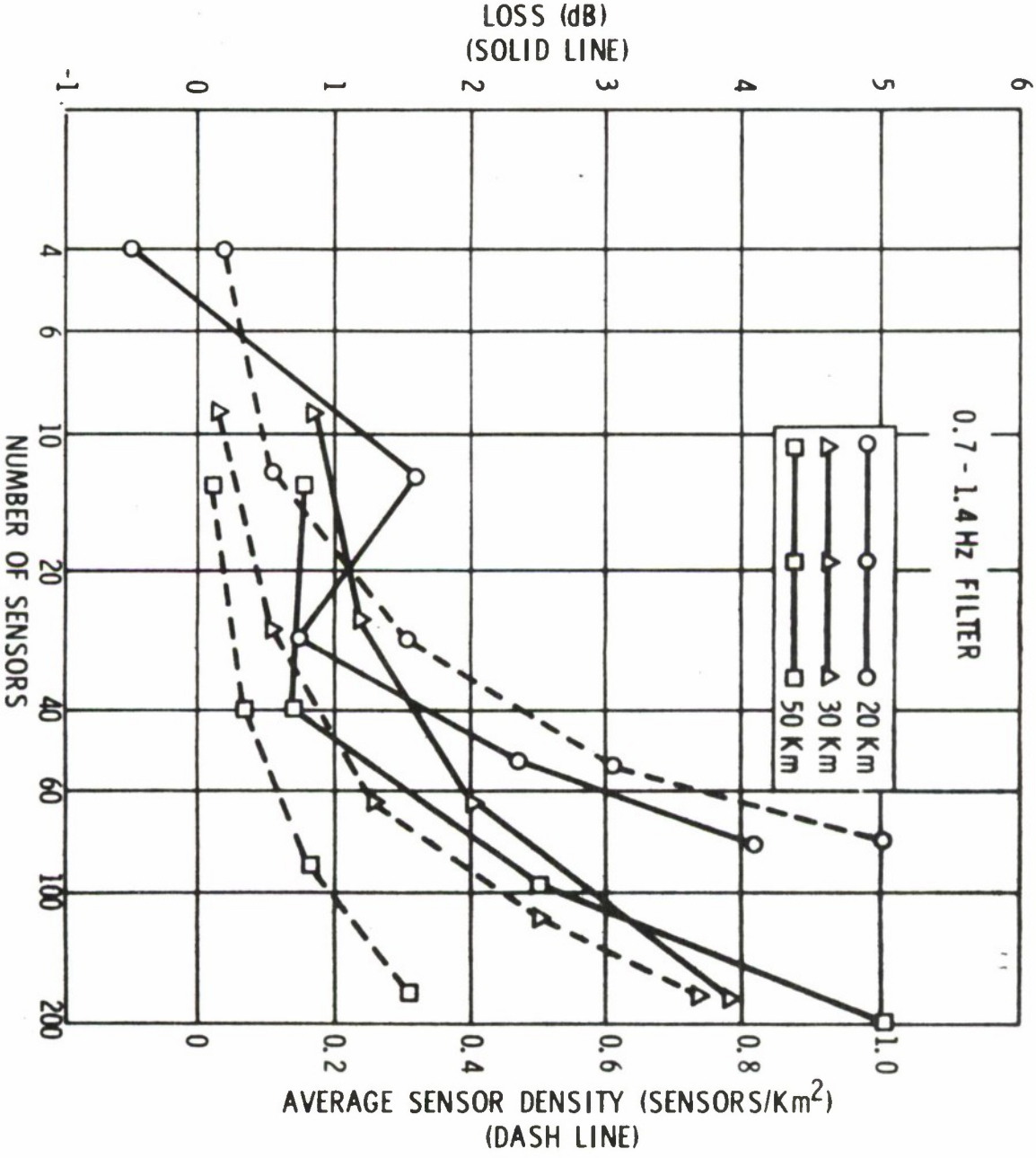

Figure F-6. Conventional Processing Loss (0.9 - 1.4 Hz)

30, and 50 kilometers). In Figure F-5, a 0.7-1.4 Hz third order Butterworth bandpass filter was employed and in Figure F-6, the filter 3 dB points were 0.9-1.4 Hz. The dashed lines in figures F-5 and F-6 (right ordinate) indicate the number of sensors divided by the square of the average distance between sensors used in the corresponding gain measurement. The scale should be modified by the factor $1/\pi$ when comparing the quasi density expressed here to circular area densities.

The principal conclusion drawn from this and other data is that through proper element spacing, conventional processing [1,2] and appropriate frequency filtering [4], it is possible to obtain gains which are within about 1 or 2 dB of theoretical values when fifty elements are densely packed. It is inferred that through proper spacing, considerably more elements can be employed with equivalent results.

F.3.2 Noise Correlation

The average element spacing available from LASA required to support conventional processing is perhaps not a useful design parameter. A more conservative criterion, minimum element spacing, will also be considered.

Exhibited in Figure F-7 are many values of the noise correlation coefficient as a function of the spacing between instruments for one sample of noise. Combinations of the sensors in selected LASA subarrays were used; and the previously specified 0.9-1.4 Hz filter was employed. Note that the average correlation coefficient passes through zero at approximately five kilometers. Because of the anticipated variations in the zero crossover point, we will employ a modest margin and use 6 kilometers. Without regard to beam pattern, a uniformly distributed array, such as one developed by contiguous equilateral triangles or squares, will require near minimum area and provide near maximum gain for a small number of sensors.

In order to employ correlation techniques, the noise directionality must be taken into account. To support the inherent isotropic conjecture, 313 beams,

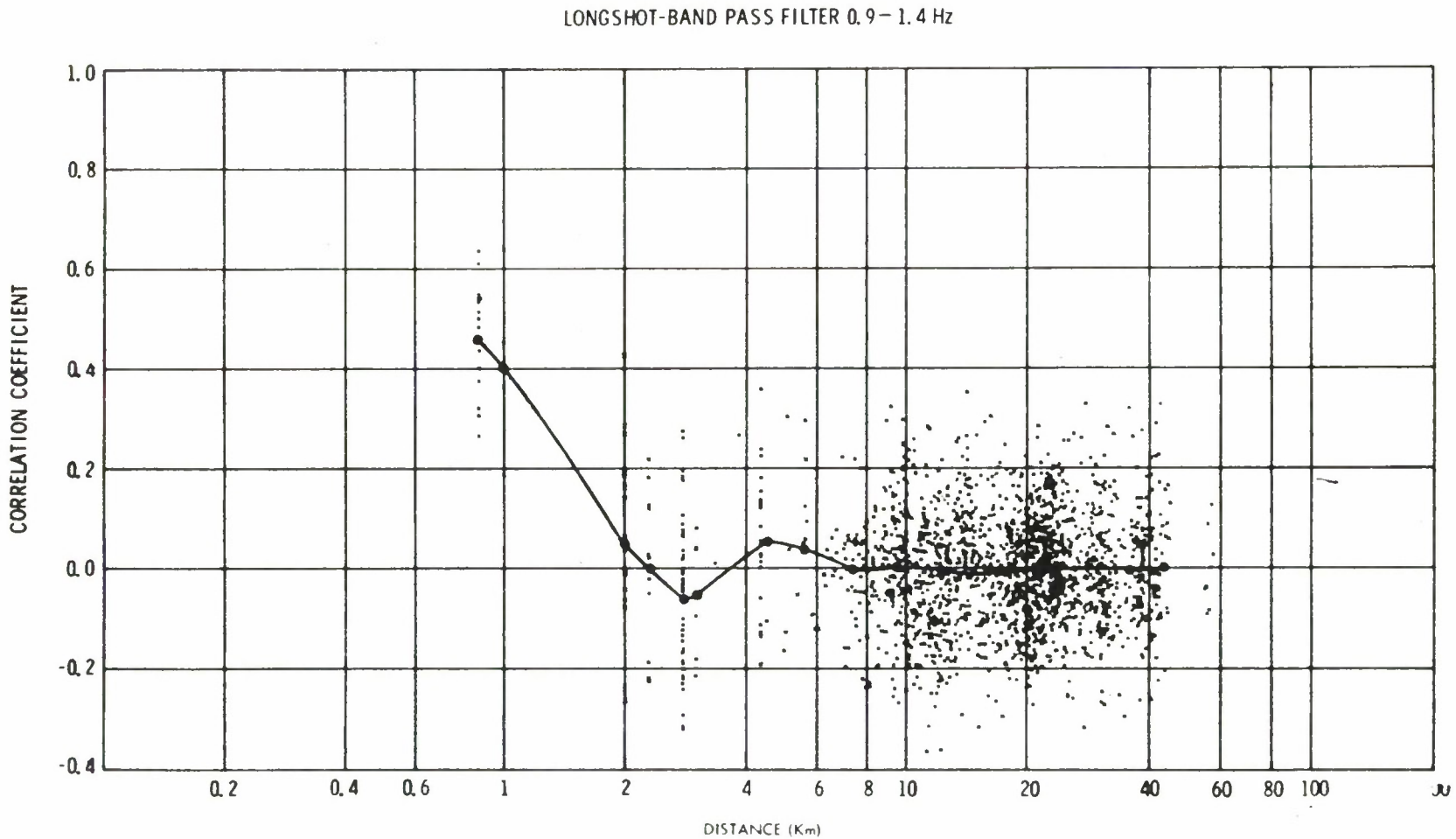

Figure F-7. Correlation Coefficient vs. Distance Between Instruments

whose centers formed the vertices of equilateral triangles of leg length 5×10^{-3} sec/Km were formed in the circle of radius 8×10^{-2} sec/Km. For this sample, the maximum deviation of each beam output was found to be less than 3 dB.

The temporal stability of this apparent isotropic condition has not been investigated, nor has a statistically significant data base been established to indicate that these results are typical.

F.3.3 Spectral Density

The pertinent bulletin characteristics of the events[4] presented in this section are tabulated in Table F-1. Their spectral density functions in decibels referenced to one nanometer, are exhibited in figures F-8 and F-9. Typically, this data is a composite of 13 seconds of event data and 50 seconds of record preceeding the event.

For Longshot the traces peak at about 1.0 Hz. Note that good subarray and array gain is experienced below 1.0 Hz. However, above 1.0 Hz, the subarray performs almost as well as the array. Note also the improvement in subarray gain at frequencies above 1.0 Hz.

TABLE F-1
BULLETIN DATA

Longshot	Event	Earthquake
10/29/65	Date	4/8/66
21:08:35.5	LAO Arrival	01:56:40.2
Rat Island	Location	East Coast of Kamchatka
51.44°N 179.18°E	Latitude/Longitude	51.2°N 157.7°E
47.15°	Range	58.81°
304.55°	Azimuth	313.0°
6.1	Magnitude	5.9

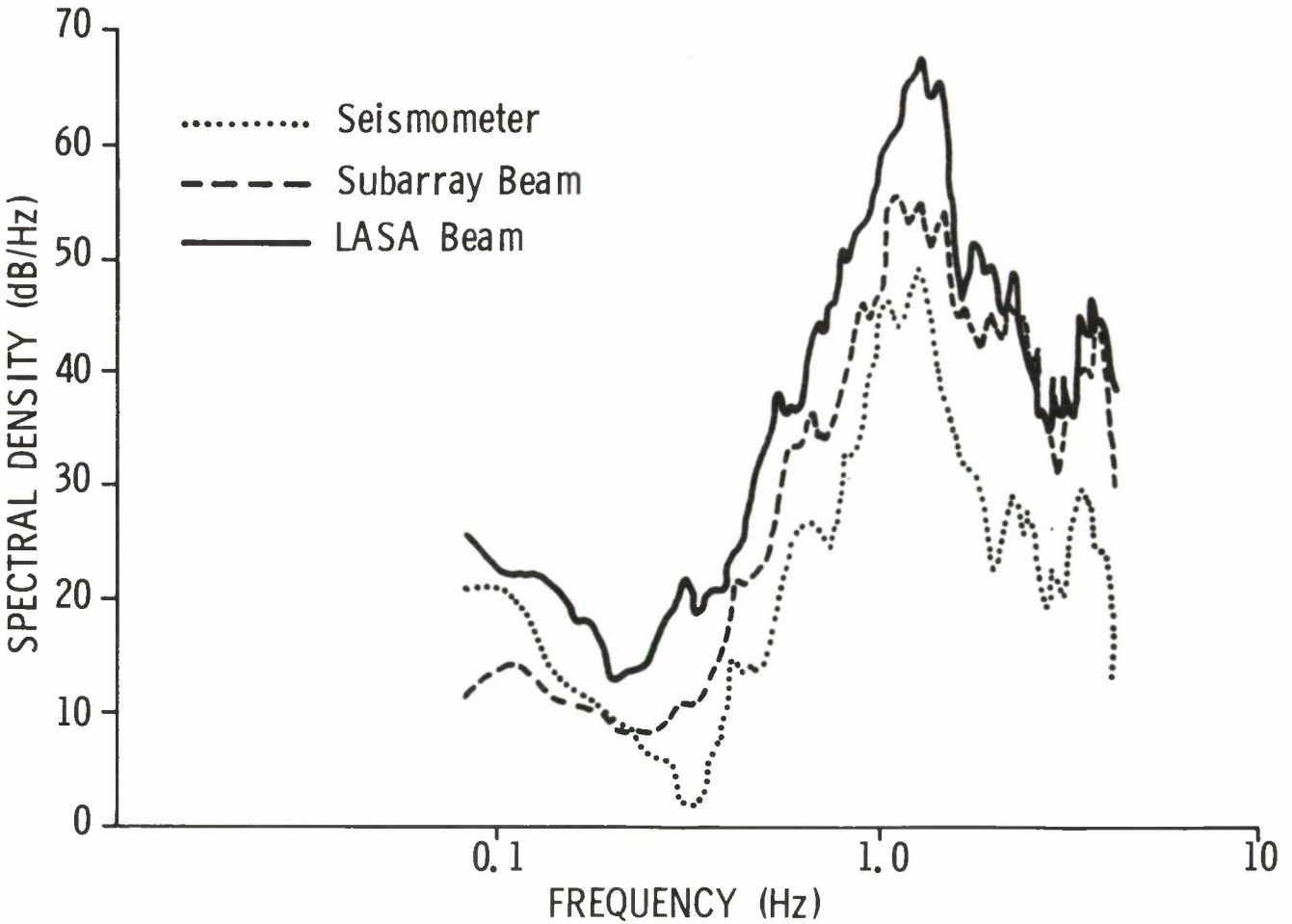

Figure F-8. Longshot S/N Spectrum

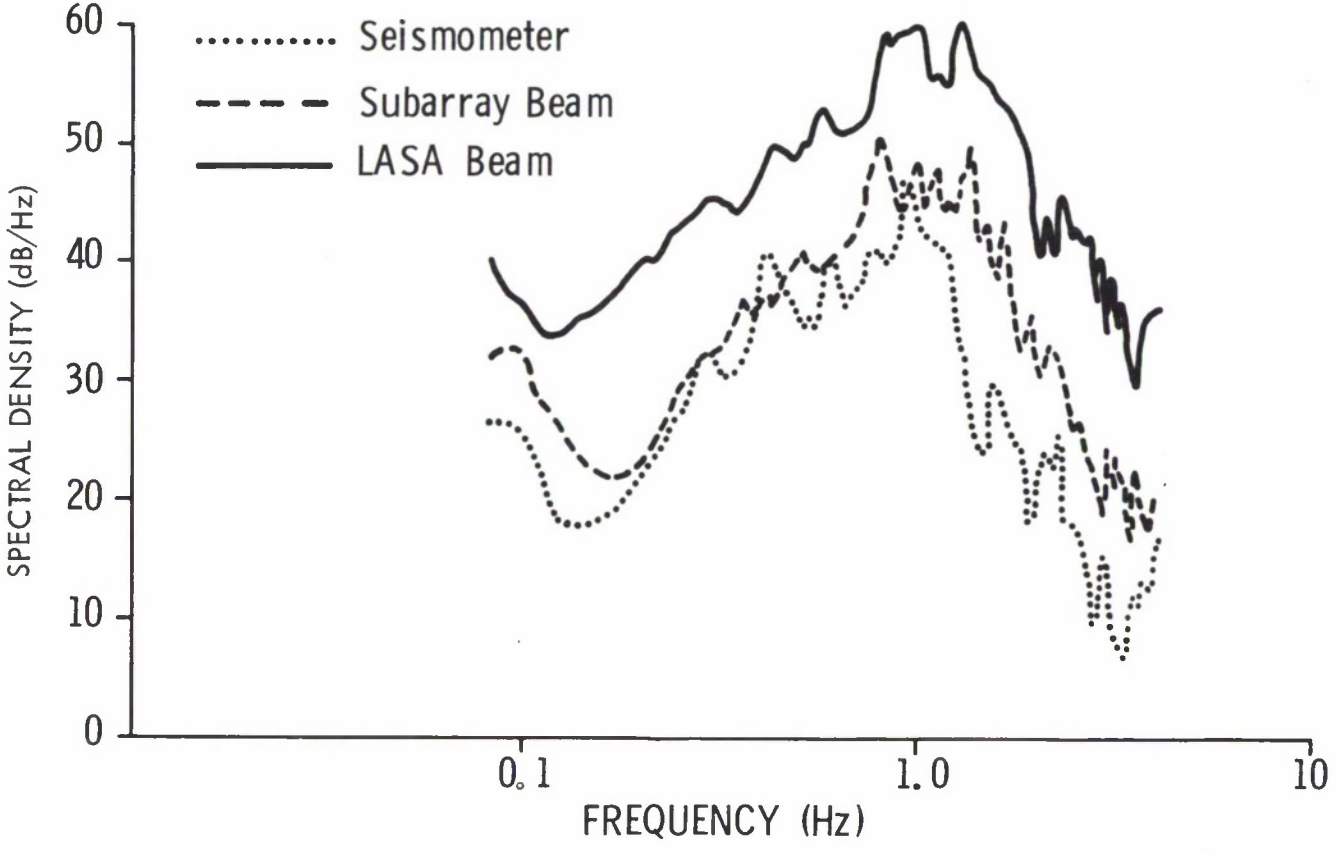

Figure F-9. Kamchatka S/N Spectrum

For the Kamchatka event, a wider signal spectrum is observed; however, the principle signal spectrum is less than 1.2 Hz. Good composite subarray gain is achieved throughout the spectrum, while good subarray gain is only achieved above 1.0 Hz.

Both spectral estimates support the conjecture that noise coherence at low frequencies exists and from Section F.3.2 it can be inferred that the poor subarray gain is due to the element spacing within the subarrays.

Since the signal duration of Longshot is small compared to the record length used, it is suggested that the poor composite subarray performance above 1 Hz may be due to signal reverberation. This has not been experimentally tested, nor has there been sufficient data analyzed to warrant this implication.

F.4 SYSTEM HYPOTHESIS

The array-processing requirements naturally divide into detection and event functions.[1,2] The detection function[3] primarily determines the existence of an arrival and its approximate location. The association of several arrivals into an event and the estimation of event magnitude, location and depth is the event function.[4] Classification is considered a post-event processing function and beyond the scope of this document.

The detection function is primarily a real-time function (i.e., it must be accomplished in a manner so as to not fall behind), while the event function primarily requires a processing capability based on the event occurrence rate. The detection function operates on a power threshold ratio and decision logic criterion over a frequency band where the signal to noise ratio peaks. The event function, on the other hand, requires maximal gain and fidelity (or at least more than the detection function) to insure waveform preservation, arrival identification, location accuracy and an appropriate evasion capability level. The detection function implies area surveillance. To insure arrival

inclusion in event processing, the event function requires only a beam coverage density over the area of the detection location uncertainty.

In addition, the detection function is normally specified by a detection capability and a false alarm probability, while the event function is specified by geophysical parametric estimates of arrival magnitude, hypocenter, and time of origin. Typically, more information is required in event processing than for detection processing.

The above noted dichotomies strongly suggest a multi-level array configuration. Depicted in Figure F-10 is a hypothetical array-processing system from which some quantitative performance trade-offs can be estimated.

To provide a basis for design synthesis, the system objectives require specification. For detection, we will arbitrarily require a conventionally beamformed array gain of 20 dB. The detection capability can be expressed as:

$$D_c = G_p - T_c, \text{ dB}, \tag{F-9}$$

where G_p is the total processing gain, including both filter and array gain and T is the detector threshold margin. For reasonable false alarm rates anticipated from the threshold decision logic[4], we conservatively assume that the filter gain and the threshold margin, are approximately equal. Then, D_c is essentially the gain with respect to a filtered trace; and, therefore, N=100.

For the event function objectives considered here, the location requirement is probably the most demanding. The event array capability can be expressed in terms of the event array gain and its filter gain, namely:

$$E_C = G_E + G_F, \text{ dB}. \tag{F-10}$$

However, the event location is a function of both event array gain (neglecting filter gain), and the array aperture expressed as the event array radius (R_E). Here, we will arbitrarily require a location accuracy of 50 kilometers when the signal to noise ratio (S/N) on the processed output is about 12 dB.

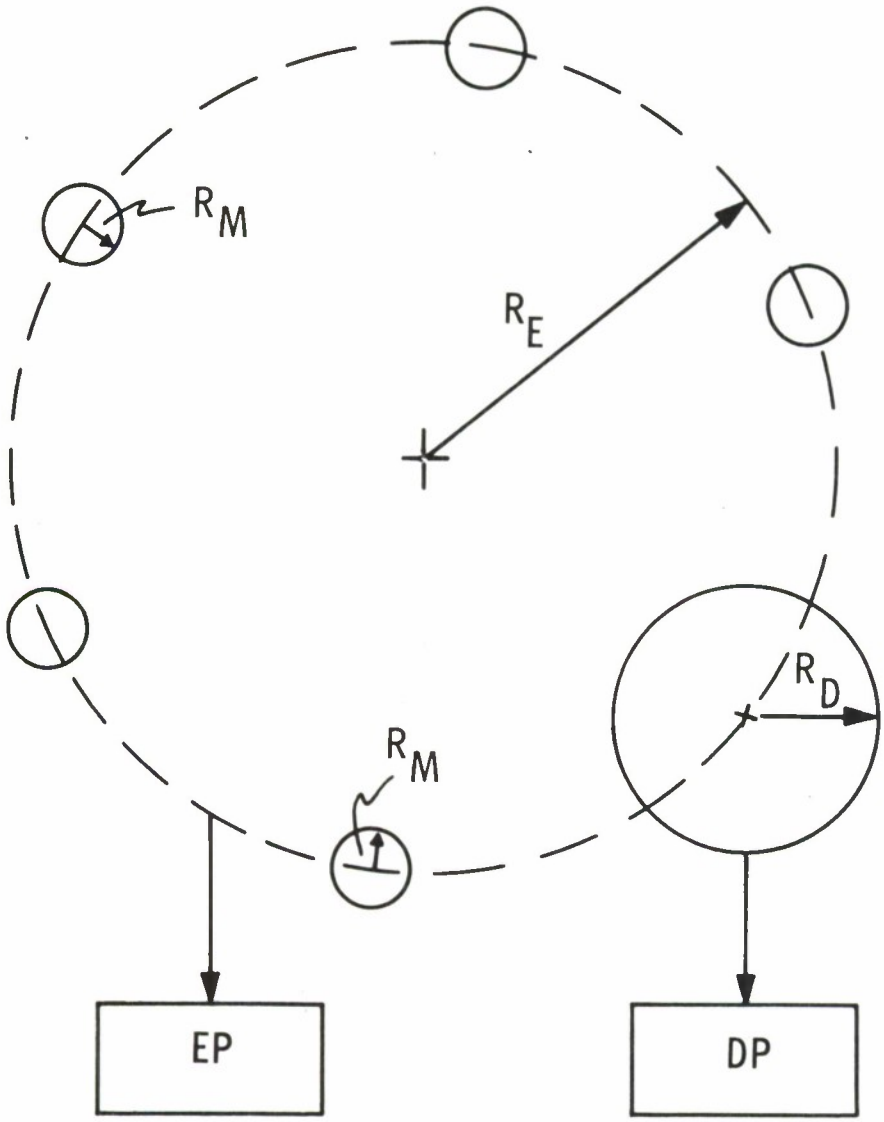

Figure F-10. System Parameters

In the following paragraphs, the system performance requirements will be developed in terms of the array specification parameters.

F.4.1 Subarray Communications

Using the grouping of sensors suggested in Section F.2.1 and F.3.2, consider an equilateral triangular arrangement of instruments as shown in Figure F-11. Denoting the minimum distance between elements as r, the area of the circumscribed circle containing N instruments is represented by its radius. Using r = 6 kilometers [to obtain zero noise correlation (Section F.3.2)], we note from Figure F-12 that the minimum grouping radius (R) for twenty sensors is about 12.5 kilometers. Although crude, we are able to suggest that nineteen sensors, when placed on concentric hexagons (and one in the center) with a minimum element separation of 6 kilometers, will occupy an area of radius 12.5 kilometers, yield a gain of almost 13 dB when processed with conventional beamforming techniques and can be supported by a 2400 baud line. In the following, a subarray aperture ($2R_M$) of 25 kilometers will be employed.

F.4.2 Detection Array-Processing

Assuming a uniform equilateral distribution of sensors, the number of beams required to cover the teleseismic region between 0.04 sec/kilometer and 0.08 sec/kilometer, with a loss of no more than 3 dB, can be related to detection array radius (R_D) and the frequency of the received signal, as exhibited in Figure F-13.

Using Figure F-12, we require the array radius to be about 30 kilometers to achieve 20dB array gain, when the minimum spacing between elements is 6 kilometers. For a 1 Hz signal and an array aperture of 60 kilometers, we note from Figure F-13, that about 100 beams are required to cover the teleseismic region.

The detection processing (DP) is thereby grossly specified. To wit, apply one-step beamforming (BF), filtering (FIL) and rectification-integration and

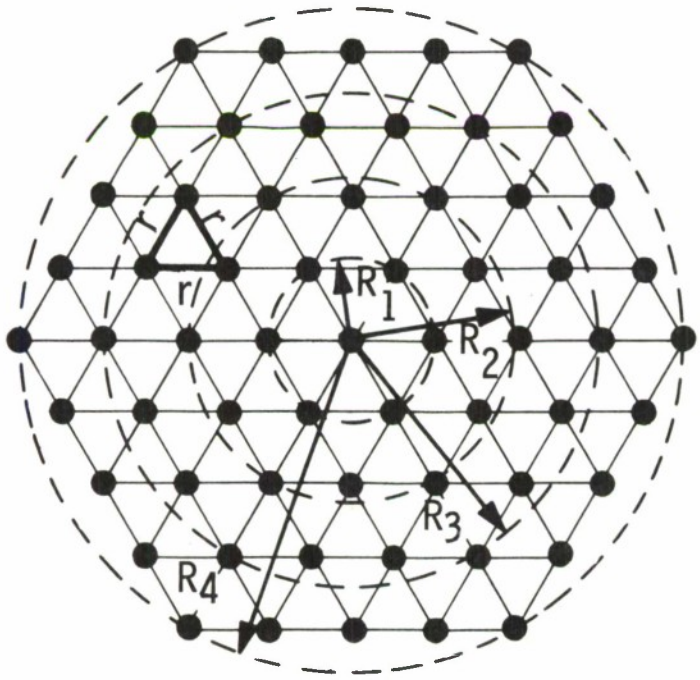

Figure F-11. Equilateral Triangle Distribution

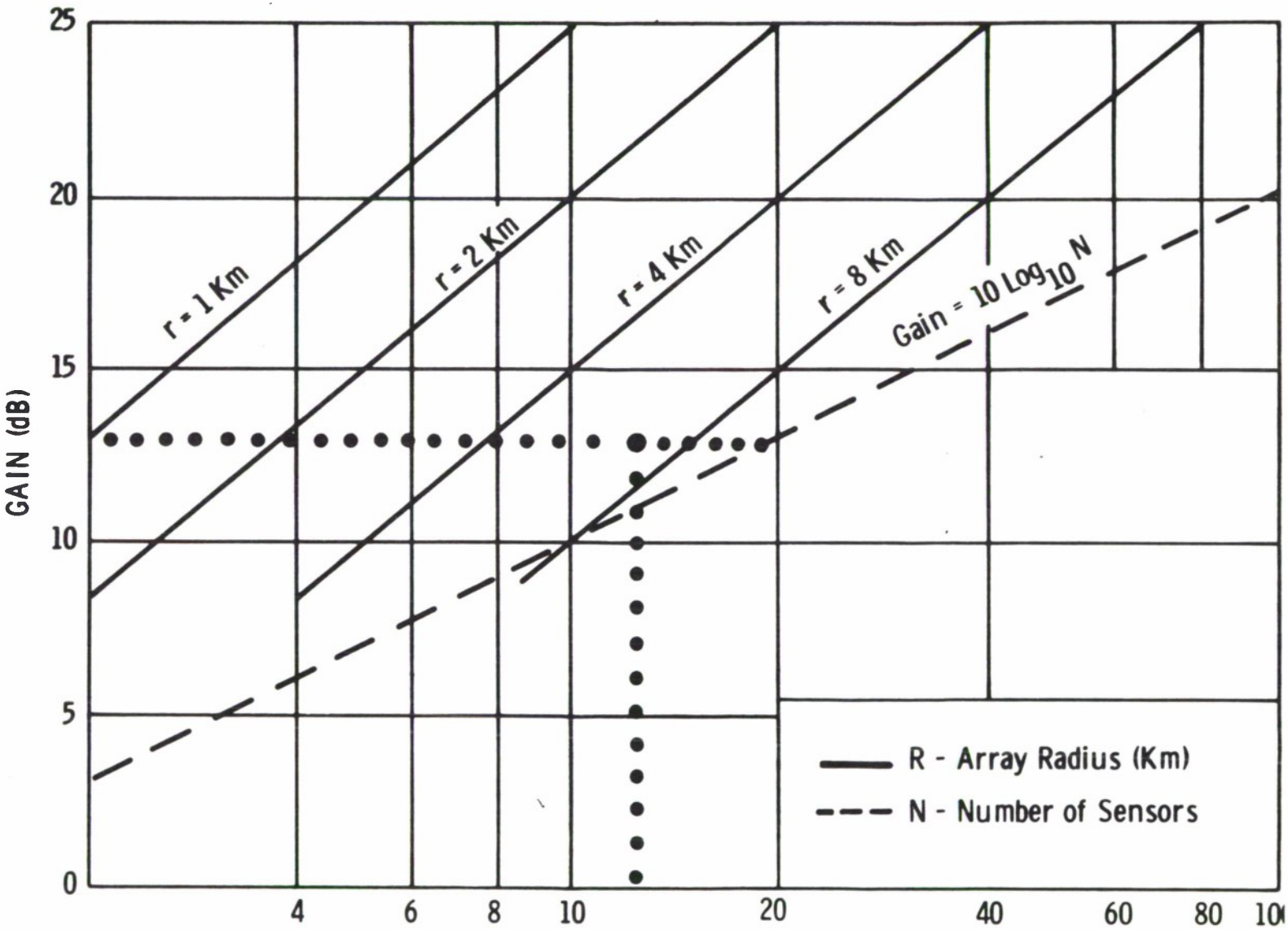

Figure F-12. Detection Array Gain

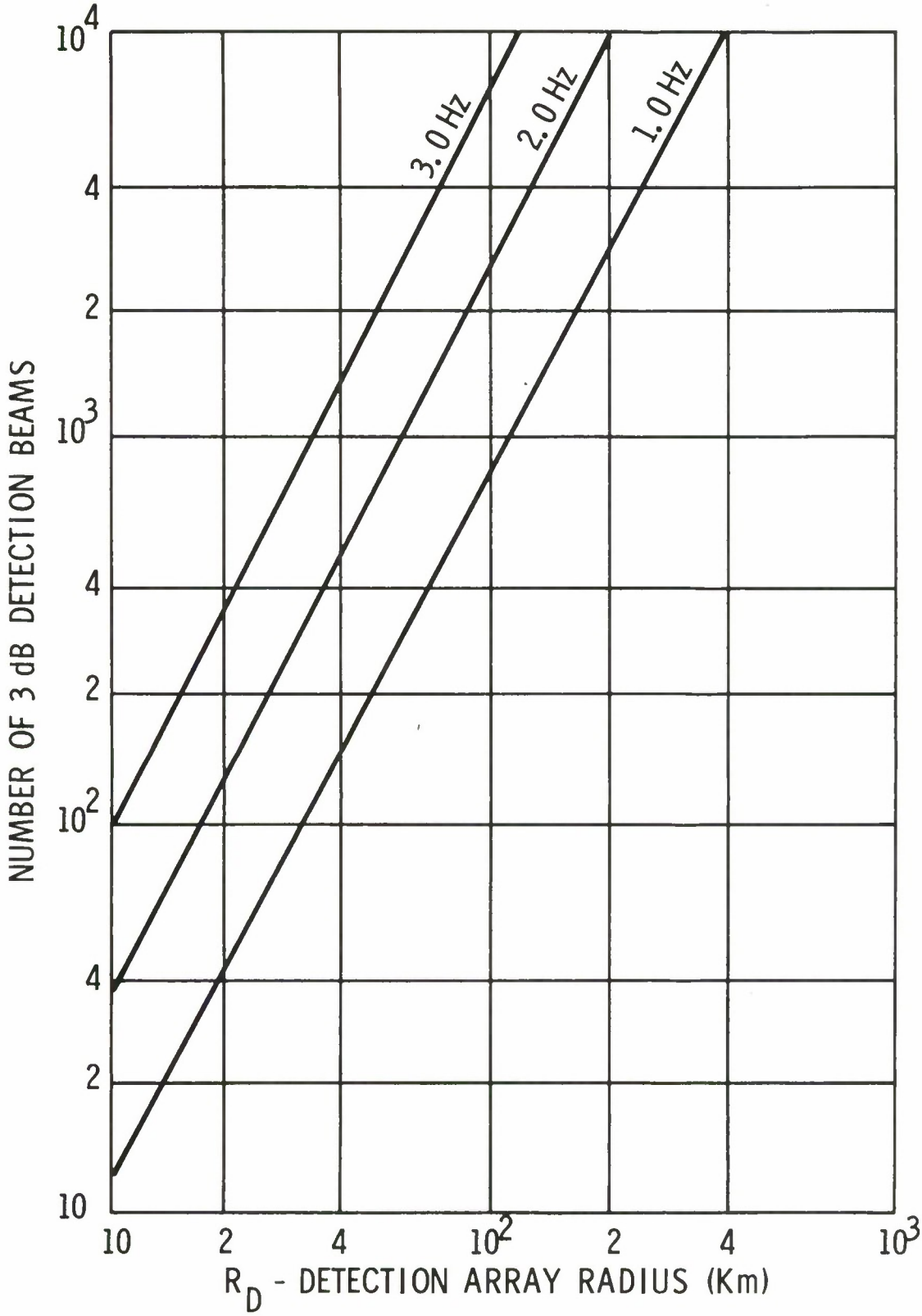

Figure F-13. Teleseismic World Coverage (0.04-0.08 Sec/Km)

thresholding (RIT). Beamforming and filtering (3rd order bandpass) will be executed at 10 Hz and RIT at 2.5 Hz. The output will be a queue of detected arrivals containing identification, the time which the detection criterion was first satisfied and first not satisfied, maximum magnitude per beam satisfying the criterion and the average noise when the arrival was declared.

To assess the requirement relative to existing capability[4], a comparison to the micro-programmed machines was made, and is depicted in Figure F-14. Using 100 sensors uniformly placed over an aperture of 60 kilometers, the speed and memory requirements are plotted as a function of the number of beams formed. When generating 100 detection beams from 100 sensors, the memory requirements are well within that available; and the speed requirement is about 70 percent of present capability.

F.4.3 Event Array-Processing

Application of the theory presented in Section F.2.3 implies that the signal to noise ratio of the fully processed event record depends upon event magnitude. For example, a magnitude 4.0 event will be some 10 dB stronger than a magnitude 3.5 event and one may expect the output record signal to noise ratio (S/N) to reflect this difference. It is, therefore, reasonable to specify the location precision in terms of not only the event array aperture, signal frequency and system gain-bandwidth product, but the event processing output S/N as well.

Equation F-8 is depicted in Figure F-15. For this example, we have taken f = 1 Hz and WT = 1. If one desires an event location error of about 50 kilometers when S/N = 12 dB, a 200 kilometer event array aperture is required.

In order to support this requirement, the event beams are specified in terms of the uncertainty of event location as determined by the detection processing function. In Figure F-16, the number of event beams is presented as a function of the ratio of the event and detection array radii with received signal frequency as a parameter. The 9 dB detection beam contour is a conservative selection. To demonstrate sensitivity, the 3 dB contour is also depicted. Referring to Section F.3.3, there is very little energy beyond 2 Hz.

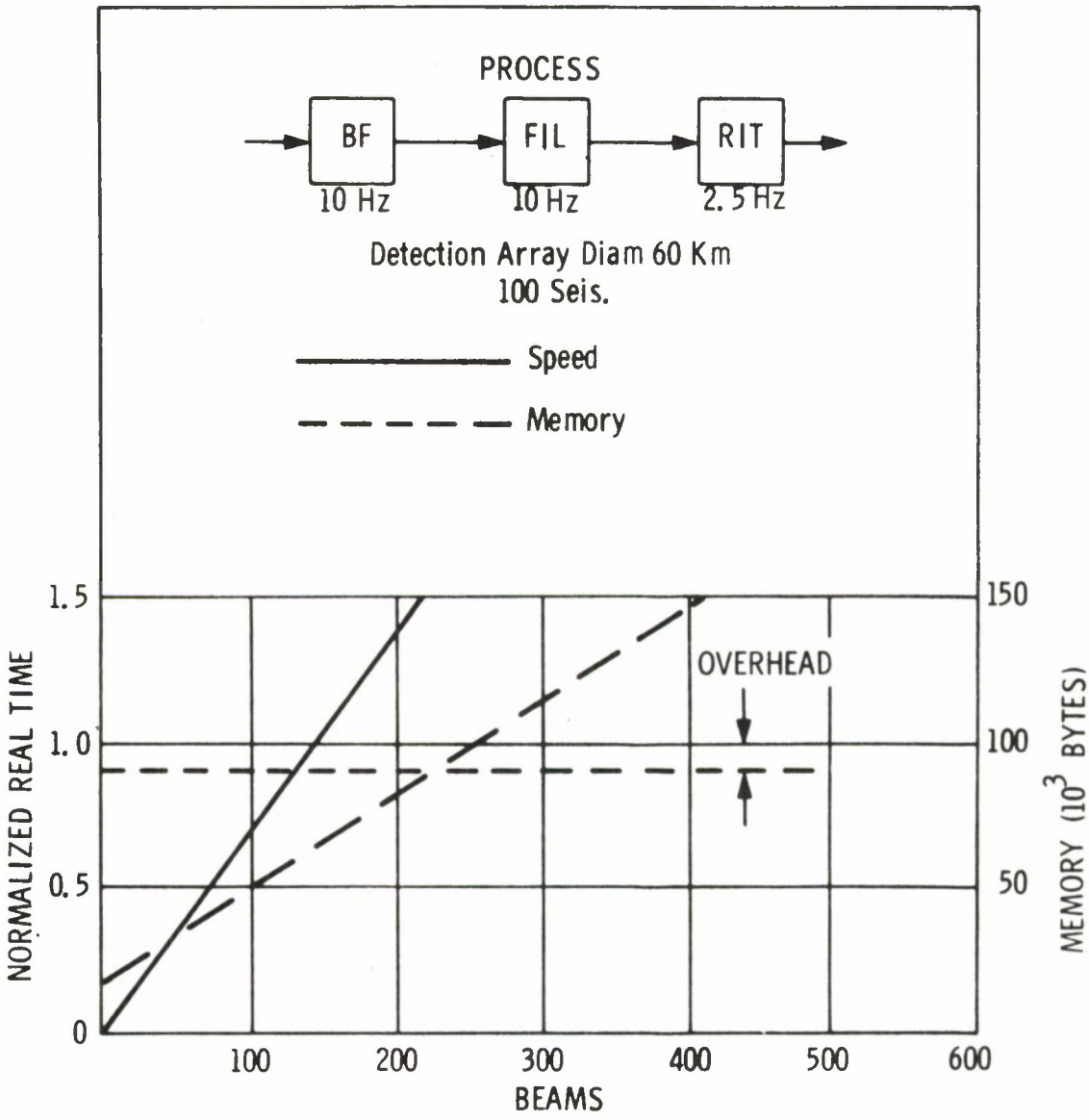

Figure F-14. Detection Processing

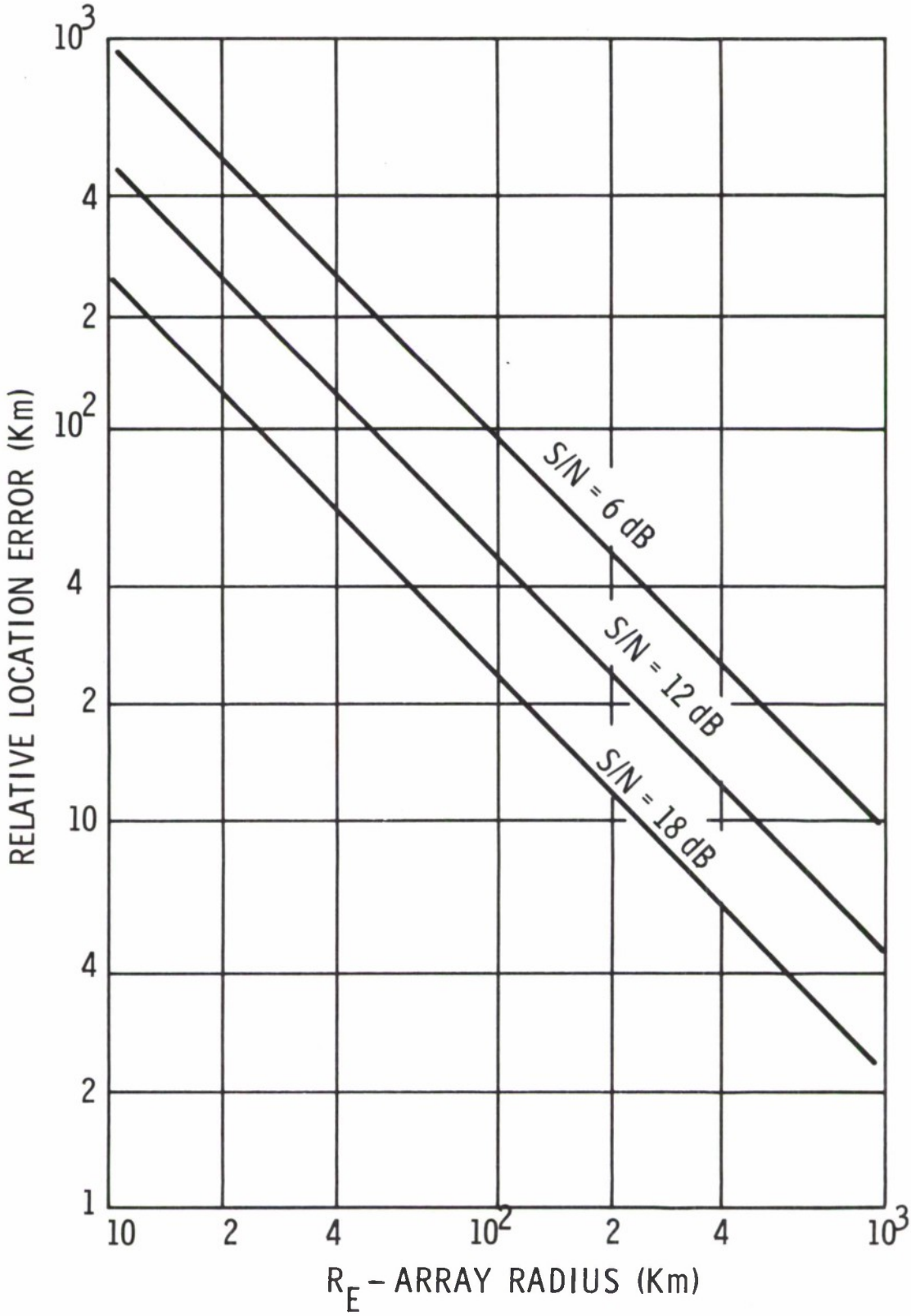

Figure F-15. Relative Location

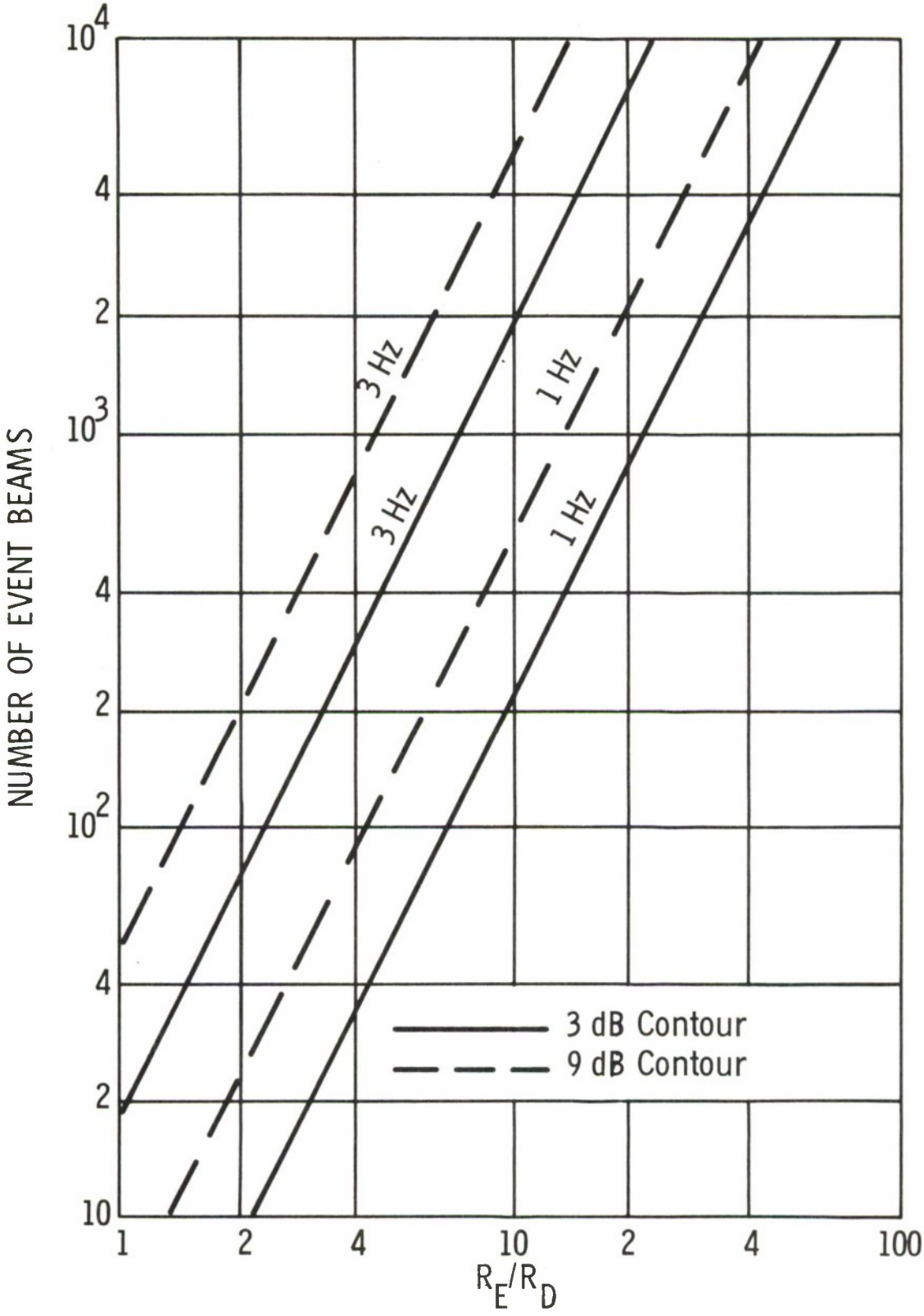

Figure F-16. Event Beam Coverage

At the 3 dB-3 Hz point, we take $R_E/R_D = 3$ and no more than 200 event beams are required.

The remaining parameter needed to specify the event beamforming requirement is the number of sensors (or groups) constituting the event array. For convenience, we will assume that the number of event sensors (N_E) is equal to the number of detection sensors (N_D). The effect of more or less sensors will be examined subsequently.

Defining five subarrays of 19 or 20 sensors each, execute two-step beamforming generating event array beams from one subarray beam per subarray. The subarray beams and filters are assumed to be formed at a rate of 10 Hz with a beamforming resolution of 10 Hz. The array beam resolution is 10 Hz, but is formed at 5 Hz; and RIT is executed at 2.5 Hz. The machine speed and memory requirements are depicted in Figure F-17. At 200 beams, the speed is less than 20 percent of available real-time capacity and the memory is much less than the detection processor.

It would, however, be prudent to use both the detection array and the event array instruments for event processing (EP). In this manner, an additional theoretical gain of 3 dB is potentially available. Here, the processing requirement is about equivalent to available real-time capability, and the memory requirement is essentially the sum of the detection and event processing needs. Since event processing speed capability is related to the rate of event occurrence, overall event beam forming computations are deemed small compared to the arrival and best beam selection process, and the bulletin computations. These are the subject of current study.

F.4.4 Event Location Confidence

The relative location accuracy prediction, presented in Section F.4.3, is a bias free statistic and subject to a probability confidence. The confidence error sensitivity bound is depicted in Figure F-18. If location estimates are to be made with greater than 50 percent confidence, select $\alpha = 1.0$.

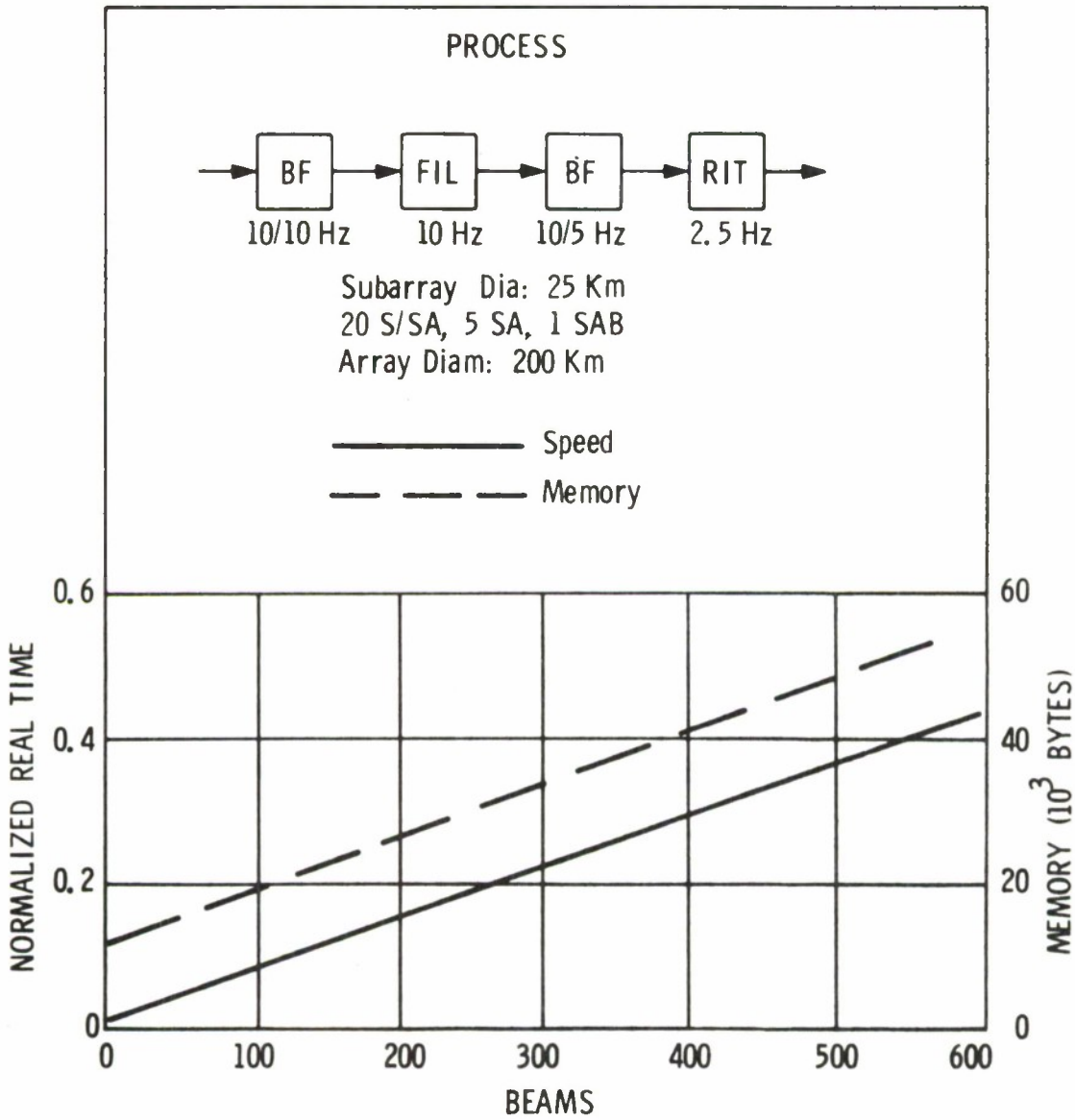

Figure F-17. Event Processing

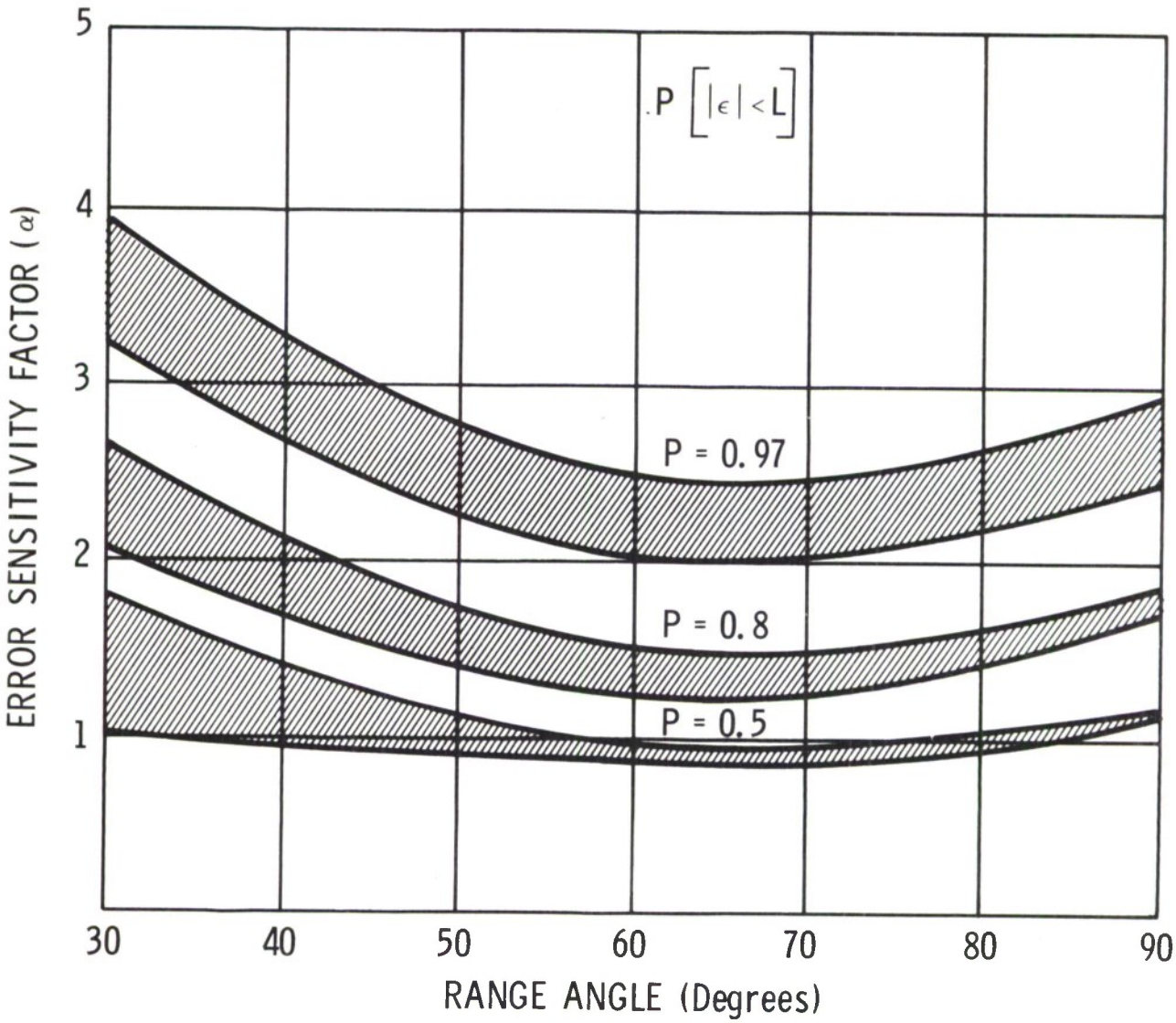

Figure F-18. Minimax Sensitivity Bound

To relate the process to its input, the number of detection and event sensors has also been introduced. In Equation F-8, the product of the circular event array radius and the ratio of the root of the number of event and detection sensors has been modified by the confidence error sensitivity parameter (i.e., $R_E\sqrt{1 + N_E/N_D} / 100\alpha$). Under the assumption there is no signal loss through the process, system performance can be estimated in terms of event magnitude with respect to the input ambient noise conditions as depicted in Figure F-19.

To estimate the number of event sensors required to achieve the event location objective, specification of the input event magnitude is necessary. For example, we will require with 50 percent confidence, a 100 kilometer event location accuracy for events up to one magnitude unit below the ambient noise level. For the previously discussed case ($N_E = N_D$), we note from Figure F-19 that $R_E \approx 160$ kilometers. However, if $N_E/N_D = 3$, the event array radius can only be reduced to about 110 kilometers.

It is reiterated that both the steering delay and geographic coordinate conversion errors have been neglected. Inclusion of the effect of these bias errors in this random variable portrayal will no doubt worsen the location error estimates.

F.4.5 Beam Patterns

The preceding discussion has been without regard to array geometry effect on beam patterns. Depicted in Figure F-20 is the beam pattern of a 21 element quasi uniformly distributed pentagon 25 kilometer aperture subarray. No side lobes greater than about 9.0 dB are noted out to 0.2 sec/kilometer. A 60 kilometer array with a similar distribution and with about 100 elements can be synthesized and when its subarray beam is combined with the subarray beams of the 25 kilometer aperture subarrays, the composite array side lobe performance will be somewhat improved.

Depicted in Figure F-21 is the beam pattern of a regular pentagon event array with one element placed in the center for a total of six elements (subarrays).

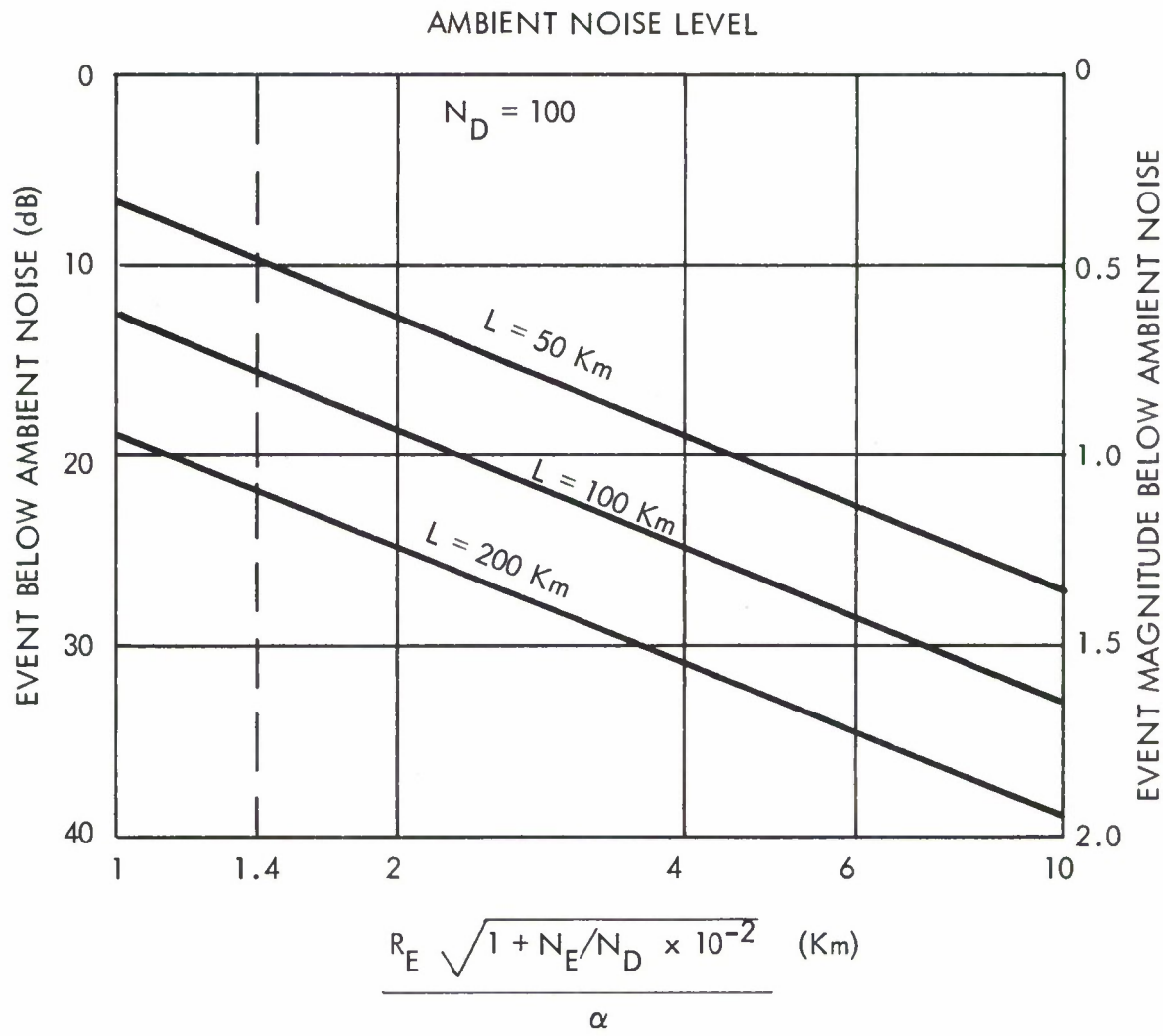

Figure F-19. Event Array Parameter

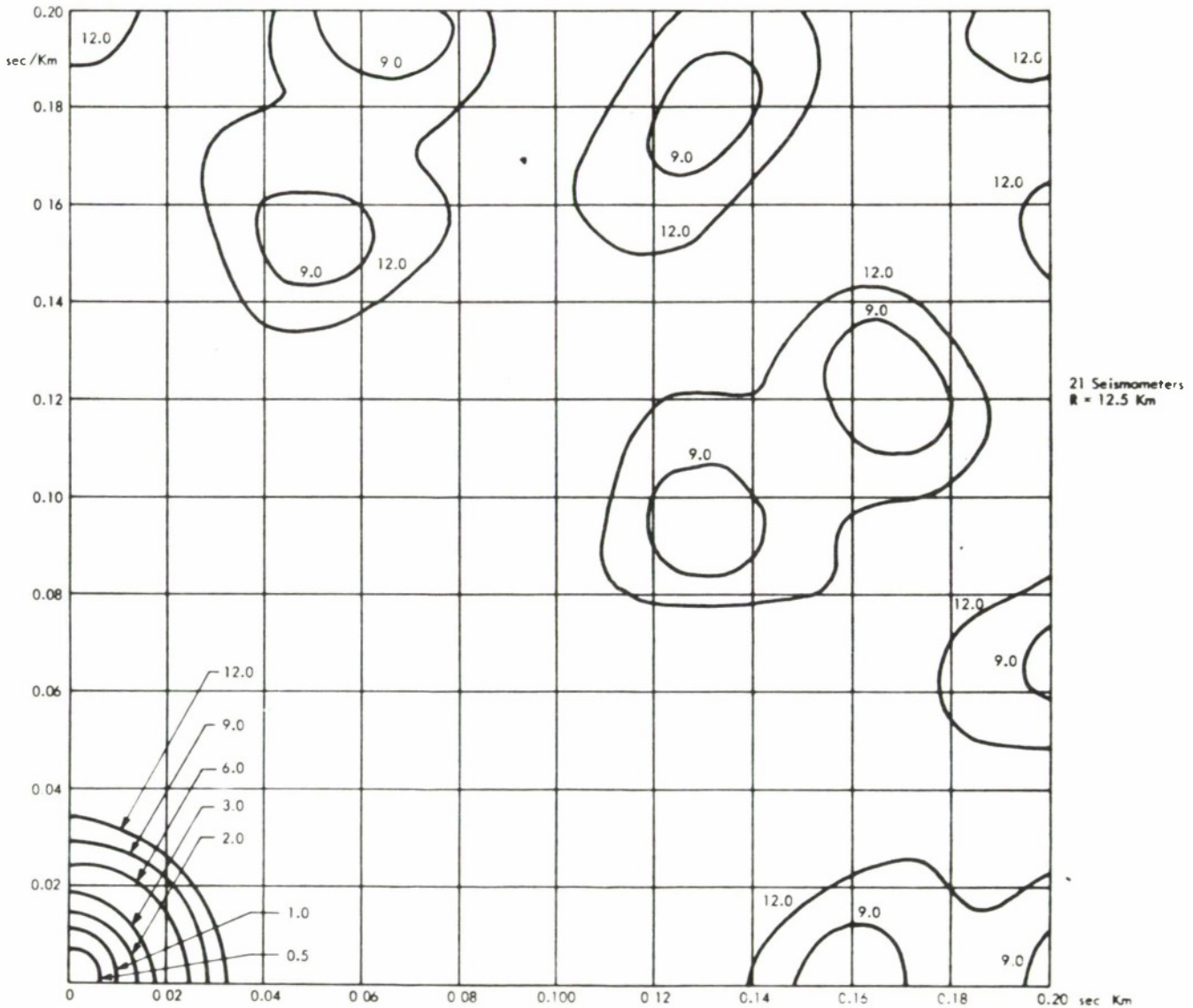

Figure F-20. Quasi Pentagon Subarray Beam Pattern

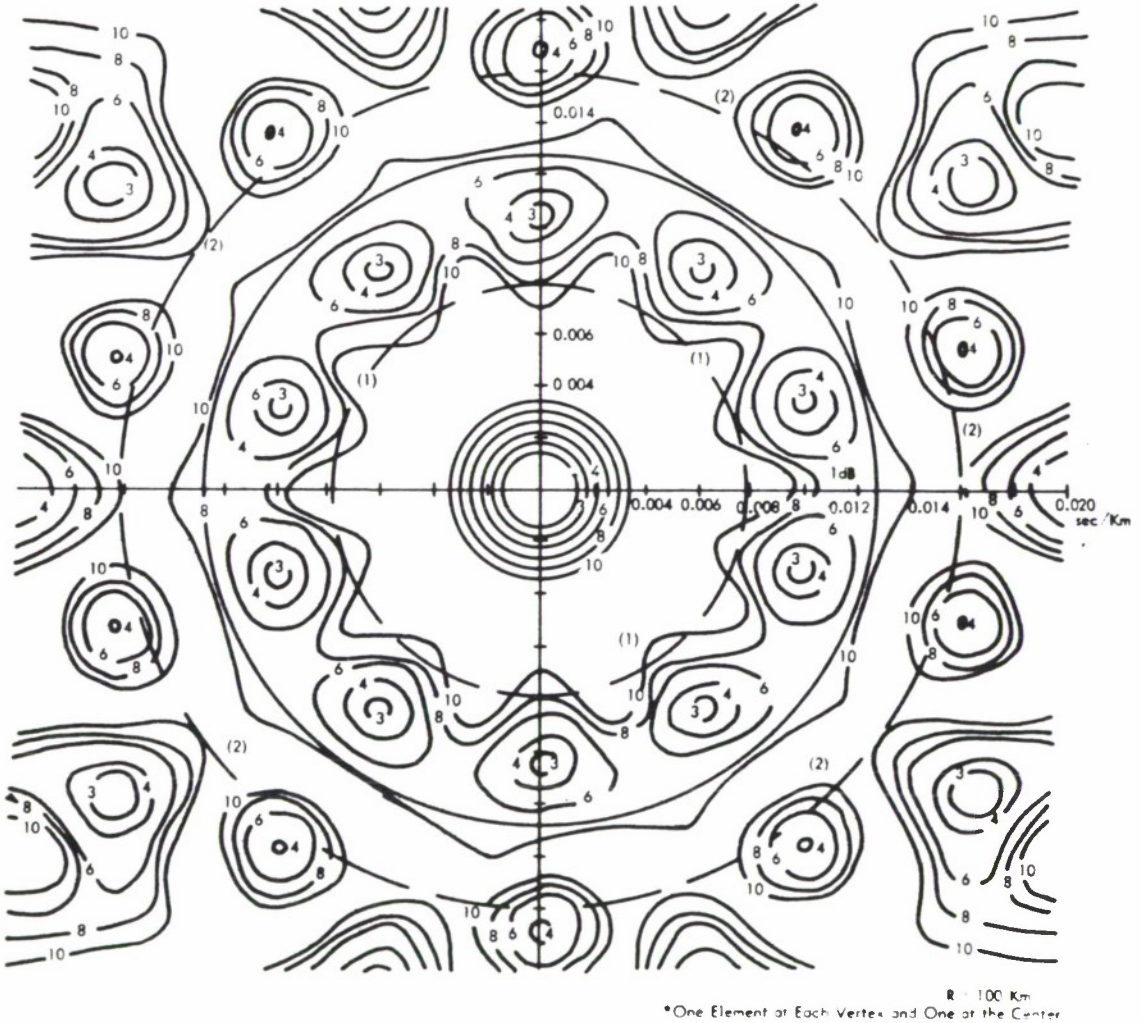

Figure F-21. Regular Pentagon Beam Pattern

The radius is taken as 100 kilometers which results in a leg length of about 85 kilometers. The first side lobes exist at 0.01 sec/kilometer and are only 3 dB down. The dashed concentric circles labeled (1) and (2) are the subarray beam 1 and 2 dB contours respectively. Due to the subarray beams, the event array side lobe will be down at least 4.5 dB at 0.01 sec/kilometer. The technique employed here, using the subarray rejection capability to reduce event array side lobes, can be augmented by additional element placement.

When specifying the lumped detection array and a distributed event array primarily for the location requirement (and for the long-period instrument spacing), it is desirable to obtain maximum utilization of the sensors in both arrays. As suggested in Section F.4, the detection and event array requirements are vastly different and support different specifications. Hence, a compromise is needed.

Consider the case when $N_E = N_D$, and we place the detection array in the center of an event array. In this case, one-half of the total sensors do not materially contribute to event location. However, when the detection array is placed on peripheral of the event array (as shown in Figure F-10), most of the elements contribute to event location. This argument supports an asymmetric array geometry and identifies the as yet to be investigated array azimuthally orientated noise directionality effects.

The asymmetrical array loss, estimated by element weighting, was found to be less than 0.4 dB for values of $N_E/N_D = 2$, and negligible for $N_E/N_D < 2$. The asymmetrical array beam pattern shown in Figure F-22 was computed by weighting the six element case above such that $N_D = N_E$. Here, there appears significant degradation in side lobe structure and further array design study is required before an event array can be hypothesized. However, the effects of array aperture on identification of post-P arrivals and evasion, and the presently envisioned classification procedures support the above suggested gross parametric relations. Array shading can be introduced and/or additional subarrays may be placed contingent upon long period instrument requirements to minimize side lobes and directional noise, and maximize location accuracy

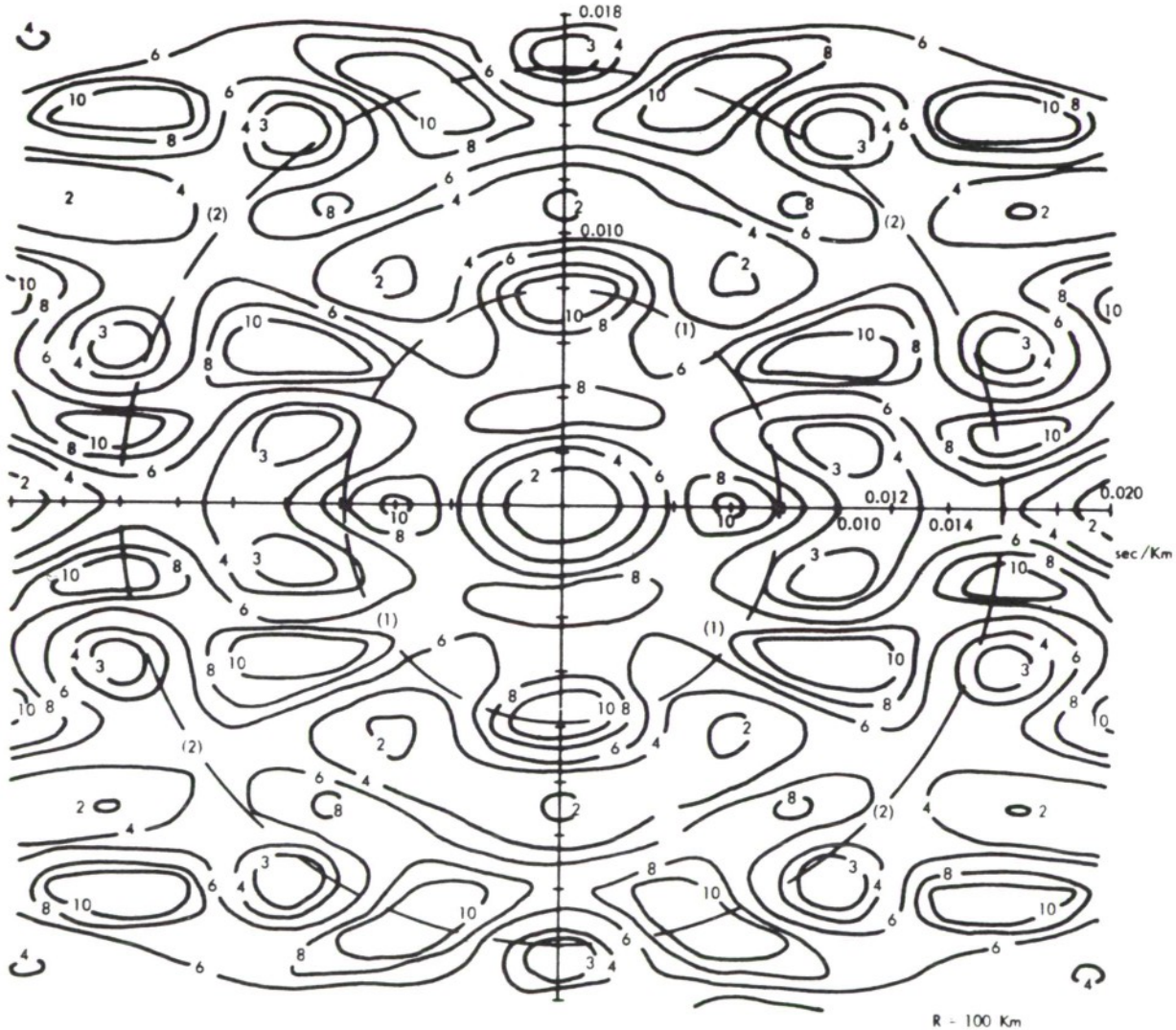

Figure F-22. Asymmetrical Pentagon Beam Pattern

along certain azimuths. The potency and practicality of these suggestions have not been investigated, nor has the effect of time delay errors as a function of array radius been established.

F.5 SUMMARY

The tri-level array processing system hypothesized has been specified in terms of gross system requirements. The pertinent system parameters are summarized in Table F-2.

This analysis has been restricted to consider only a portion of the array-processing design problem in terms of a particular desired product. In order to demonstrate the approach, certain objectives were specified (i.e., 20 dB detection array gain and 50 kilometer relative location accuracy when the output record S/N is greater than 12 dB). Other products may be desirable. For example, integration of the long-period instruments, although provided for in the subarray communication loading and event array geometry, is a glaring omission. It can, however, be readily incorporated with a knowledge of the long-period noise coherence. Further, an isotropic noise field has been assumed, and, for site locations where a strong directional noise source is likely to exist, this conventional processing synthesis procedure may require extension.

Further, the effects of detection threshold margin on false alarm rate, the effects of aperture on steering delay errors, and the effects of the apparently inseparable steering delay and geographical bias errors on location accuracy have, in the interest of expediency, been ignored. When suitably accurate experimental data recorded and processed with sufficient precision, becomes available, it is planned to extend this analysis as needed.

Using the grouping concept hypothesized in Section F.4.1, for both the detection and event arrays, we note that we are able to withstand subarray failures without catastrophic system effects. If the redundant processor concept[2,3] is maintained for detection processing and sensor recording, the event processor may assume the detection function for the case of a detection channel failure. The additional requirement imposed is one of sizing the event processor such that it has a sufficient catch-up capability.

Table F-2

PARAMETER SUMMARY

Case	Objective	Parameter
Subarray	2400 Baud Line	Uniform Distribution: 20 SP 1 LP
	78 dB Range	Subarray Aperture: 25 Km
	1/4 dB Resolution	Sampling: 10 Hz (5 Hz Filter) SP 1 Hz (0.5 Hz Filter) LP
Detection Array	20 dB Detection Gain	Uniform Distribution: 100 SP or 5 SA
	0.04 - 0. 08 sec/Km	Array Aperture: 60 Km or 5 SA
	3 dB Beam at 1.5 Hz	Beams: 100
		Processing: Conventional (One-Step)
Event Array	50 Km Relative Location	Circular Distribution: 5 Subarrays
	0.5 Mag. Event Below Noise	Array Aperture: 200 Km
	Confidence of 50%	Beams: 1 Subarray Beam and 200 Array Beams
	12 dB Processed Record S/N	Processing: Conventional (Two-Step)

With respect to minimizing installation and operating cost, the above delineated synthesis procedure provides a cost function which is strongly dependent on array radius and the total number of sensors. The constraint is related to both system objectives.

Unclassified
Security Classification

DOCUMENT CONTROL DATA - R&D

(Security classification of title, body of abstract and indexing annotation must be entered when the overall report is classified)

1. ORIGINATING ACTIVITY *(Corporate author)*
International Business Machines Corporation
18100 Frederick Pike
Gaithersburg, Maryland 20760

2a. REPORT SECURITY CLASSIFICATION
Unclassified

2b. GROUP
N/A

3. REPORT TITLE

SECOND QUARTERLY TECHNICAL REPORT - LASA EXPERIMENTAL SIGNAL PROCESSING SYSTEM

4. DESCRIPTIVE NOTES *(Type of report and inclusive dates)*

5. AUTHOR(S) *(Last name, first name, initial)*

6. REPORT DATE	7a. TOTAL NO. OF PAGES	7b. NO. OF REFS
May 1967		

8a. CONTRACT OR GRANT NO.	9a. ORIGINATOR'S REPORT NUMBER(S)
AF19 (628)-67-C-0198	ESD-TR-67-602
b. PROJECT NO.	
c.	9b. OTHER REPORT NO(S) *(Any other numbers that may be assigned this report)*
d.	NONE

10. AVAILABILITY/LIMITATION NOTICES

This document has been approved for public release and sale; it's distribution is unlimited.

11. SUPPLEMENTARY NOTES	12. SPONSORING MILITARY ACTIVITY
	Electronic Systems Division L.G. Hanscom Field Bedford, Massachusetts 01730

13. ABSTRACT

This Second Quarterly Technical Report for the LASA Experimental Signal Processing System discusses the effort expended during the second quarter to provide the hardware and software to support research and development directed toward the study of seismic signal processing; and it delineates work tasks planned for the next quarter. This document also presents detailed information related to configurations, array monitor and control, data compression, scaling, display, and array design.

DD FORM 1 JAN 64 1473

Unclassified
Security Classification

14. KEY WORDS	LINK A		LINK B		LINK C	
	ROLE	WT	ROLE	WT	ROLE	WT

INSTRUCTIONS

1. ORIGINATING ACTIVITY: Enter the name and address of the contractor, subcontractor, grantee, Department of Defense activity or other organization *(corporate author)* issuing the report.

2a. REPORT SECURITY CLASSIFICATION: Enter the overall security classification of the report. Indicate whether "Restricted Data" is included. Marking is to be in accordance with appropriate security regulations.

2b. GROUP: Automatic downgrading is specified in DoD Directive 5200.10 and Armed Forces Industrial Manual. Enter the group number. Also, when applicable, show that optional markings have been used for Group 3 and Group 4 as authorized.

3. REPORT TITLE: Enter the complete report title in all capital letters. Titles in all cases should be unclassified. If a meaningful title cannot be selected without classification, show title classification in all capitals in parenthesis immediately following the title.

4. DESCRIPTIVE NOTES: If appropriate, enter the type of report, e.g., interim, progress, summary, annual, or final. Give the inclusive dates when a specific reporting period is covered.

5. AUTHOR(S): Enter the name(s) of author(s) as shown on or in the report. Enter last name, first name, middle initial. If military, show rank and branch of service. The name of the principal author is an absolute minimum requirement.

6. REPORT DATE: Enter the date of the report as day, month, year, or month, year. If more than one date appears on the report, use date of publication.

7a. TOTAL NUMBER OF PAGES: The total page count should follow normal pagination procedures, i.e., enter the number of pages containing information.

7b. NUMBER OF REFERENCES: Enter the total number of references cited in the report.

8a. CONTRACT OR GRANT NUMBER: If appropriate, enter the applicable number of the contract or grant under which the report was written.

8b, 8c, & 8d. PROJECT NUMBER: Enter the appropriate military department identification, such as project number, subproject number, system numbers, task number, etc.

9a. ORIGINATOR'S REPORT NUMBER(S): Enter the official report number by which the document will be identified and controlled by the originating activity. This number must be unique to this report.

9b. OTHER REPORT NUMBER(S): If the report has been assigned any other report numbers *(either by the originator or by the sponsor)*, also enter this number(s).

10. AVAILABILITY/LIMITATION NOTICES: Enter any limitations on further dissemination of the report, other than those imposed by security classification, using standard statements such as:

(1) "Qualified requesters may obtain copies of this report from DDC."

(2) "Foreign announcement and dissemination of this report by DDC is not authorized."

(3) "U. S. Government agencies may obtain copies of this report directly from DDC. Other qualified DDC users shall request through

_____."

(4) "U. S. military agencies may obtain copies of this report directly from DDC. Other qualified users shall request through

_____."

(5) "All distribution of this report is controlled. Qualified DDC users shall request through

_____."

If the report has been furnished to the Office of Technical Services, Department of Commerce, for sale to the public, indicate this fact and enter the price, if known.

11. SUPPLEMENTARY NOTES: Use for additional explanatory notes.

12. SPONSORING MILITARY ACTIVITY: Enter the name of the departmental project office or laboratory sponsoring *(paying for)* the research and development. Include address.

13. ABSTRACT: Enter an abstract giving a brief and factual summary of the document indicative of the report, even though it may also appear elsewhere in the body of the technical report. If additional space is required, a continuation sheet shall be attached.

It is highly desirable that the abstract of classified reports be unclassified. Each paragraph of the abstract shall end with an indication of the military security classification of the information in the paragraph, represented as *(TS), (S), (C), or (U)*.

There is no limitation on the length of the abstract. However, the suggested length is from 150 to 225 words.

14. KEY WORDS: Key words are technically meaningful terms or short phrases that characterize a report and may be used as index entries for cataloging the report. Key words must be selected so that no security classification is required. Identifiers, such as equipment model designation, trade name, military project code name, geographic location, may be used as key words but will be followed by an indication of technical context. The assignment of links, rules, and weights is optional.